CRANFIELD UNIVERSITY

Ahsan Muhammad

Hybrid ion exchange resins for phosphorus removal from wastewater

School of Water, Environment and Energy

EngD
Academic Year: 2016 - 2017

Supervisors: Prof. Bruce Jefferson & Dr Ana Soares
August 2017

CRANFIELD UNIVERSITY

School of Water, Energy and Environment

EngD

Academic Year 2016 - 2017

Ahsan Muhammad

Hybrid ion exchange resins for phosphorus removal from wastewater

Supervisors: Prof. Bruce Jefferson & Dr Ana Soares
August 2017

This thesis is submitted in partial fulfilment of the requirements for the degree of EngD

Abstract

Phosphorus is not only a non-renewable resource but also a major cause of eutrophication in natural environments. Accordingly, legislation aims to control point source discharges from wastewater treatment with new targets likely to be as low as 0.1 mg L^{-1}. Current wastewater treatment options for phosphorus removal, based on either biological or chemical processes, are capable of meeting the new consents. However, challenges exist with both such that alternative approaches are required. One of the most promising is the use of hybrid ion exchange resins where ferric oxide nanoparticles have been embedded within the structure of the base resin. The aim of the current thesis is to understand and critically evaluate the technical and economic challenges associated with using the hybrid resin for phosphorus removal.

Technical assessment demonstrates the efficacy of the resin in meeting the new standard as either a polishing process or as the main treatment unit for phosphorus removal. Elucidation of the impact of background water constituents revealed the importance of the ferric oxide nanoparticles in conjunction with targeted regeneration to enable effective removal in complex matrices. Batch experiments revealed that a combination of pseudo-second order and intra particle diffusion models can be used to model the system. The media capacity was maximum (8.5 mg g_{media}^{-1}) in the first cycle and reduced to a more consistent 2.5 – 3.7 mg g_{media}^{-1} between cycle 3 to 9. Adsorption of nitrate ions from the wastewater effluent was found to cause the most inhibition to the removal of phosphorus, followed by sulphate and then humic acid. Column trials establish the effectiveness of the process even at very low contact times of 0.5 to 1 minute. However, optimum operation was achieved around empty bed contact times of 3-5 minutes as these generate extended serviceable bed life. The media can remove phosphorus down to 0.1 mg P L^{-1} for treating both, full phosphorus load (at sites with no other phosphorus removal mechanism) and for phosphorus polishing (at sites where phosphorus concentration has been to reduced to ~1 mg L^{-1} through existing treatment). Furthermore, the resin also removed COD at a level between 40-50%, making it suitable for sites needing organic polishing.

Economic analysis revealed the process offered a plausible economic alternative to standard solutions to meet low phosphorus consents. For small works (2,000 PE), HAIX fixed bed system was found to be economically competitive below empty bed contact time of 7 minutes. For medium works (20,000 PE), this increased to an empty bed contact time of 10 minutes. A mobile clean-up system for the regenerant (NaOH) has been deemed more economical for small works (2,000 PE), whereas the chemical quantity needed for medium works (20,000 PE) required an on-site clean-up system. The potential to substantially reduce total costs were identified such that confidence can be placed in the economic suitability of the solution. Importantly, the economic plausibility of the process did not require inclusion of the sale of the recovered phosphate product such that the technology is appropriate within both linear and circular economic models.

Keywords: phosphorus, hybrid ion exchange resin, circular economy.

Acknowledgments

I would like to thank ‘Allah’ Almighty, for giving me the opportunity and strength to do my research.

My biggest thanks to Prof. Bruce Jefferson who has pushed me and supported me and without whom I would not have even come close to finishing. As a fellow Chemical Engineer, I aspire to be as knowledgeable and enthusiastic about my work. I would also like to thank Dr. Ana Soares for her support and contribution to the project.

I would like to thank Severn Trent Water, Anglian Water, Thames Water, Yorkshire Water, Wessex Water, Scottish Water and ESPRC for funding the project. I would especially like to thank Pete Vale from Severn Trent Water for his continued involvement in the project. Special thanks to Karen de Groot and Kate Silby at Wessex Water, for being so supportive and helpful while I was writing my thesis.

I am thankful for all the support and guidance from the technical team including Jane Hubble, Alan Nelson, Nigel Janes and Paul Barton. I would especially like to Alan Nelson for all those interesting talks in the lab and for putting up with my last-minute requests for equipment and cell tests. I would also like to thank Nigel Janes for the numerous trips to the pilot hall to collect samples when I could not drive and would have been stuck with out his help.

Within the STREAM programme I would like thank Tania Rice for her support and for making so many things easier and enjoyable. I would like to thank Nicole Jenkins, my fellow cohort 3 researcher, my friend, for hearing me complain about my research and pilot plant and for making it easier by telling me that you are going through the same. A special thanks to Rachel Whitton, for helping me cope with your words of encouragement, for showing me the light at the end of the tunnel when I could not see it myself.

Finally, my parents, without whom I would not be who I am today. Thank you. For sacrificing everything so that your children could have what you never had. For

being gentle and strict. For your support in every aspect imaginable. For all your love. I would also like to thank my brother, Danish, for his love and support and for distracting me with ‘Manga’ suggestions when I was too stressed out. For driving to Cranfield to pick me up when I was too tired to come myself. I would like to thank my supporting wife, Maryam Yasin for all the encouragement, love, yummy food and countless attempts to calm my nerves. You have sacrificed more than I have, you have never complained about me working on the weekends, for not having a proper holiday in a while, for living away from home when I had to. Last but not least, my 1.5-year-old daughter Ismah. I want to thank you for putting up with me being locked away in the study, for not being able to play with you as much I wanted to. The most difficult time during the research was when I used to get to see you once every fortnight, two weeks after you were born. I promise to spend all my time playing with you from now onwards.

Table of Contents

List of Figures

List of Tables

List of Equations

Abbreviations

CAPEX	Capital Expenditure
COD	Chemical Oxygen Demand
DOC	Dissolved Organic Carbon
EBCT	Empty Bed Contact Time
HAIX	Hybrid Anion Exchanger
HRT	Hydraulic Retention Time
IX	Ion Exchanger
LUB	Length of Used Bed
MTZ	Mass Transfer Zone
NP	Nanoparticle
OPEX	Operating Expenditure
P	Phosphorus
PE	Population Equivalent
SF	Sand Filter
UK	United Kingdom
UWWTD	Urban Wastewater Treatment Directive
WFD	Water Framework Directive
WLC	Whole Life Cost
WWTW	Wastewater Treatment Works

.

Chapter 1. Introduction

1.1 Background

Apart from being a non-renewable resource, phosphorus is also the major cause of eutrophication in rivers, lakes and coastal waters (Jellali *et al*., 2011). The major contributors of phosphorus to surface water are agricultural, municipal, industry and background source (Ngatia *et al*., 2017). Wastewater is one of the richest sources of phosphorus containing on average 250,000 tons annually (Jellali *et al*., 2011). A typical concentration of phosphorus in municipal wastewater is around 6-14 mg L^{-1} depending on diet. The other contributors of phosphorus in municipal wastewater include phosphate-based soaps, cleaners and personal care products (Vale, 2017).

North America has some of the most stringent consents with phosphorus concentrations not to be exceeded beyond 10 $\mu g.L^{-1}$ in protected waters (Liu *et al*., 2016). The Water Framework Directive 2000/60/EC along with Council Directive 91/271/EEC has set annual phosphorus averages in wastewater effluents between 1-2 mg P L^{-1}, depending on size of the wastewater treatment works and sensitivity of the receiving waters (Melia *et al*., 2017). These consents are expected to be tightened, down to as low as 0.1 mg P L^{-1} (Vale, 2017).

Current wastewater treatment options for phosphorus removal are based on either enhanced biological reactor configurations and/or the use of metal coagulants (Pratt *et al*., 2012). Both have been shown to be capable of meeting the low final phosphorus discharges required by new legislation such as the Water Framework Directive. However, biological solutions work best with feed waters enriched in COD and have reduced robustness when operated for discharge consents below 0.5 mg L^{-1} (Pratt *et al*., 2012). In the case of chemical solutions, reaching very low P levels is straightforward but requires good mixing of large chemical doses and effective solids separation to avoid the risk of elevated metal residuals in the discharged water. Accordingly, a number of new technologies are being researched to provide alternative options that alter the cost-benefit balance such as the use of microalgae (Whitton *et al.*, 2016;

Gonçalves *et al.,* 2017), reactive media (Barca *et al*., 2013) and sorption media (Acelas *et al*., 20*15*a; Martin *et al*., 2013b). In case of sorption media, a variety of materials have been tested including enriched media where metal species are embedded within the framework of the material such as biochar (de Rozari *et al.,* 2016), activated carbon, zeolites and anion exchangers (Martin *et al*., 2017). The later materials are known under the name hybrid ion exchange resins (HAIX). The materials are commercially available and used for arsenate removal in ground waters in the USA and the sub-continent. The media has previously been shown to be effective for phosphate removal from wastewater to enable compliance with a 0.1 mg P L^{-1} standard (Martin, 2010). The embedded nanoparticles provide a pathway for selective removal and recovery of the phosphate positioning the technology as a resource recovery unit providing a route for added value.

1.2 Aims and Objectives

The overall aim of the project was to understand and critically evaluate the technical and economic challenges with using hybrid anion exchanger (HAIX) media for removing phosphorus from wastewater. To deliver the overall aim the following objectives were set:

Objective 1. To review metal oxide loaded adsorbents and understand the impact of conditions and operational parameters on their performance.

Objective 2. To understand the impact of competing ions on the selectivity of HAIX media.

Objective 3. To understand the impact of operational parameters on the performance of HAIX in fixed bed columns.

Objective 4. To understand the key parameters that influence the overall economic viability for implementing HAIX to remove phosphorus at WWTW.

1.3 Thesis Plan

The thesis is presented as chapters formatted as journal papers. All papers were written by the primary author Ahsan Muhammad and edited by Professor Bruce

Jefferson and Dr Ana Soares. The experimental work was designed and completed by Ahsan Muhammad at Cranfield University or at a selected Severn Trent Water sewage treatment works. The links between the different objectives and chapters are addressed in Table 1.1.

A literature review (Chapter 2, Paper 1) was completed on use of metal oxide media for phosphorus removal. The review shed light on the selectivity of the different sorbents, the mode of testing their performance and the challenges associated with utilizing them for phosphorus removal. The main focus of the literature review was on sorbents loaded with metals oxides as they have shown to be highly selective for phosphorus removal.

The experimental work then assessed the impact of background water constituents on the capacity and selectivity of the resin (Chapter 3, Paper 2). The resins were pre-loaded with nitrate, sulphate and humic acid and tested with a mono component solution as well as wastewater to explore both direct competition for adsorption sites and the long-term impact of accumulation of material onto the base resin. This was followed by looking at the impact of multiple batch cycles to ascertain the role of selective regeneration with the nanoparticle component. The data was fitted to a range of potential dynamic models to further explore the critical mechanisms of operation.

In addition, the impact of empty bed contact time was investigated on the performance of HAIX to remove full phosphorus load and for phosphorus polishing (Chapter 4, Paper 3). The empty bed contact time is one of the most important parameters in sorption plants as it determines the required size of the vessels as well as the amount of media required. The media capacity, length of mass transfer zone and unused bed were calculated to understand the impact of empty bed contact times.

The findings from chapters 3 and 4 along with previous work (Martin *et al*., 2013b) were used to design a fixed-bed system for 2,000 and 20,000 PE WWTW (Chapter 5, Paper 4). A suspended ion-exchange system was also designed to compare against the fixed bed system. The economics of both systems were compared against coagulant dosing followed by tertiary and quaternary filtration

in the form of cloth-filter and depth-filters. The major components were identified and their impact on the economics of HAIX was studied through a sensitivity analysis. Overall the paper commented on the economic plausibility of using the process as an option for P removal.

The technical and economic analysis were then combined to discuss the implication of the work through responding to a number of key questions around what the media can do, what is an appropriate design basis and where are the most suitable application from an economic perspective. The chapter finishes by exploring the role of circular economic thinking on the overall outlook. (Chapter 6 - Implications of the work: Overall perspective on the appropriateness of HAIX media for wastewater treatment in the UK).

Finally, Chapter 7 summarises the key conclusions and recommends additional areas of work to further develop the HAIX technology and improve its economic attractiveness. Table 1 summarises the thesis and the respective papers.

Table 1.1 Thesis structure outlining the objectives addressed.

Chapter	Paper	Title	Objective met
1		Introduction	
2	1	Metal oxide media for phosphorus removal from wastewater: A review	1
3	2	The impact of background wastewater constituent on the selectivity and capacity of a hybrid ion exchange resin for phosphorus removal from wastewater	2
4	3	Laboratory scale column experiments to determine the impact of short empty bed contact times on phosphorus adsorption and removal of organic constituents from a low and high P loaded wastewater using hybrid ion exchange resin.	3
5	4	Hybrid ion exchanger for tertiary phosphorus removal – an economic analysis to ascertain the potential and key development areas.	4
6	--	Implications of the work: Overall perspective on the appropriateness of HAIX media for wastewater treatment in the UK	1, 2, 3, 4
7	--	Conclusions and further work	

1.4 References

Acelas, N. Y., Martin, B. D., López, D. and Jefferson, B. (2015) 'Selective removal of phosphate from wastewater using hydrated metal oxides dispersed within anionic exchange media', *Chemosphere*, 119, pp. 1353–1360.

Barca, C., Troesch, S., Meyer, D., Drissen, P., Andreìs, Y. and Chazarenc, F. (2013) 'Steel slag filters to upgrade phosphorus removal in constructed wetlands: Two years of field experiments', *Environmental Science and Technology*, 47(1), pp. 549–556.

Gonçalves, A. L., Pires, J. C. M. and Simões, M. (2017) 'A review on the use of microalgal consortia for wastewater treatment', *Algal Research*, 24 (Part B), pp. 403–415.

Jellali, S., Wahab, M. A., Hassine, R. B., Hamzaoui, A. H. and Bousselmi, L. (2011) 'Adsorption characteristics of phosphorus from aqueous solutions onto phosphate mine wastes', *Chemical Engineering Journal*, 169(1–3), pp. 157–165.

Liu, Q., Wan, J., Wang, J., Li, S., Dagot, C. and Wang, Y. (2016) 'Recovery of phosphorus via harvesting phosphorus-accumulating granular sludge in sequencing batch airlift reactor', *Bioresource Technology*, 224, pp. 87–93.

Martin, B. D., De Kock, L., Gallot, M., Guery, E., Stanowski, S., MacAdam, J., McAdam, E. J., Parsons, S. A. and Jefferson, B. (2017) 'Quantifying the performance of a hybrid anion exchanger/adsorbent for phosphorus removal using mass spectrometry coupled with batch kinetic trials', *Environmental Technology*, In Press.

Martin, B. D., De Kock, L., Stephenson, T., Parsons, S. A. and Jefferson, B. (2013) 'The impact of contactor scale on a ferric nanoparticle adsorbent process for the removal of phosphorus from municipal wastewater', *Chemical Engineering Journal*, 215–216, pp. 209–215.

Melia, P. M., Cundy, A. B., Sohi, S. P., Hooda, P. S. and Busquets, R. (2017) 'Trends in the recovery of phosphorus in bioavailable forms from wastewater', *Chemosphere*, 186, pp. 381–395.

Ngatia, L. W., Hsieh, Y. P., Nemours, D., Fu, R. and Taylor, R. W. (2017) ‘Potential phosphorus eutrophication mitigation strategy: Biochar carbon composition, thermal stability and pH influence phosphorus sorption’, *Chemosphere*, 180, pp. 201–211.

Pratt, C., Parsons, S. A., Soares, A. and Martin, B. D. (2012) ‘Biologically and chemically mediated adsorption and precipitation of phosphorus from wastewater’, *Current Opinion in Biotechnology*, 23(6), pp. 890–896.

de Rozari, P., Greenway, M. and El Hanandeh, A. (2016) ‘Phosphorus removal from secondary sewage and septage using sand media amended with biochar in constructed wetland mesocosms’, *Science of the Total Environment*, 569–570, pp. 123–133.

Vale, P. (2017) ‘Applying a circular economy model to wastewater treatment’, in *WWT Wastewater*, Birmingham.

Whitton, R., Le Mével, A., Pidou, M., Ometto, F., Villa, R. and Jefferson, B. (2016) ‘Influence of microalgal N and P composition on wastewater nutrient remediation’, *Water Research*, 91, pp. 371–378.

Chapter 2. Metal oxide media for phosphorus removal from wastewater: A review

Ahsan Muhammad, Ana Soares and Bruce Jefferson
Cranfield University, Bedfordshire, MK43 0AL, UK

Abstract

The removal of phosphorus from wastewater to very low levels is becoming a standard requirement for wastewater treatment. New targets go below current standards of 1-2 mg P L^{-1} to require as a low as 0.1 mg P L^{-1} and this puts a strain on existing approaches for phosphorus removal. The use of sorption processes offers the potential to meet such a challenge but existing materials such as activated carbon and ion exchange resin are limited through competition from other constituents. The use of metal oxides transforms this as they provide selectivity through forming stronger bonds with phosphate than with the other components. Accordingly, inclusion of metal oxides into carrier materials such as ion exchange resins provide a novel method for phosphorus removal. Review of the available literature confirms their efficacy and selectivity. However, much of the work has been conducted in batch, treating synthetic solutions raising questions about translation into practical operation and assessment of economic appropriateness.

Keywords: phosphorus, metal oxides, hybrid ion exchange resins

2.1 Introduction

Phosphorous is the 11th most abundant element but is a non-renewable mineral that is an essential nutrient for all living things along with carbon and nitrogen. Carbon and nitrogen are available in the atmosphere, but phosphorus is not, and this make it the limiting environment component for life. Phosphorus is sourced from inorganic phosphate rocks with the largest reserves occurring in a handful of countries such as China, Morocco, Western Sahara and America (Lwin *et al*, 2017; Cho, 2013). Of the current mined phosphorus, 82 % is utilized for agriculture, 7 % for production of animal feed and the remaining 11 % for

pharmaceuticals, oils, detergents and textiles (Cieslik and Konieczka, 2016) Phosphorus demand is predicted to increase by 50-100 % by 2050, whereas, according to some estimates, the phosphorus reserves will be depleted in 50-100 years (Lwin *et al.*, 2017; Cieslik and Konieczka, 2016)

As phosphorus is the main limitation for growth in natural systems, its release is key to eutrophication which can severely impact water quality by causing high turbidity, low dissolved oxygen, unpleasant odour and bad taste (Li *et al.*, 2009). Phosphorus enters water bodies through agricultural and storm water run-off, human waste and industrial discharges. However, a major route linked to eutrophication comings is from point source discharges from wastewater treatment facilities. In response, legislation such as the Water Framework (WFD), Urban Wastewater Treatment (UWWTD) and Habitats Directives seeks to control phosphorus levels coming from sewage effluent discharges. According to UWWTD, the discharge consent is 2 mg L^{-1} for sewage treatment works with population equivalent between 10,000 – 100,000 and 1 mg L^{-1} for population equivalent larger than 100,000 (Tran *et al.*, 2012). It is anticipated, that to achieve good ecological standard, water companies will be expected to achieve stricter consent limits. These new consents will be as low as 0.1 mg P L^{-1} for large treatment works and 0.5 mg L^{-1} for small treatment works (Brockett, 2016)

Phosphorus is present in wastewater as organic phosphate, inorganic phosphate (orthophosphate) and polyphosphate at a concentration between 5-20 mg L^{-1} (Zeng *et al.*, 2004). Currently the two most commonly used techniques for phosphorus removal from wastewater are chemical precipitation and biological removal. However, it has been reported that chemical and biological removal are unable to resiliently achieve the new consents (Acelas *et al.*, 2015).

Standard biological processes remove phosphorus through uptake into the bacterial biomass sufficient to satisfy their metabolic requirements. This equates to around 20-40 % removal (Tchobanoglous *et al.*, 2003) which means processes such as activated sludge can achieve effluent quality between 2-4 mg L^{-1}. This can be improved to 0.5-1 mg L^{-1} if the process can be adapted to encourage the growth of polyphosphate accumulating organisms (PAOs) in processes such as

the Bardenpho process (Zhang *et al*., 2015) Enhanced biological phosphorus removal processes are cost efficient and have no added chemical costs but the performance can be effected by factors such as having sufficient available carbon, alkalinity, available inorganics such as magnesium, temperature, pH, solids retention time, sludge quality and settlement. Importantly there needs to be a high COD:P ratio beyond that normally expected in municipal sewage such that, the process tends to be used where substantial industrial wastewater inputs are included into the treatment. Additionally, good secondary clarification is required to achieve P concentrations below 1 mg L^{-1} with many sites incorporating back up chemical dosing system in case of low performance or failure of the system (Martin, 2010; Su *et al*., 2013).

At sites not suitable for biological P removal, chemical precipitation is used. Metals salts such as ferric sulphate, ferric chloride and aluminium sulphate are dosed into the effluent to precipitate the dissolved phosphate and form flocs which are then settled out by sedimentation, filtration or other clarification processes (Condi and Parker, 2015; Morse *et al*., 1998). The process offers many advantages such as a reduced susceptibility to shock loads, temperature changes and alterations in feed concentration. To meet existing discharge consent for P, a dose ratio of around 2.7:1 by mass is required. However, to reach the new standard, a dose ratio approaching 8:1 is required if single point dosing is utilised (Whitton, 2016). This can be reduced by multiple point dosing with secondary dosing prior to tertiary clarification with technologies such as cloth and depth filters (Ruixia *et al*., 2002; Martin, 2010). However, if the required standard is below 0.3 mg L^{-1} recent demonstration trials have indicated that two stage clarification will be required. The net impact is a significant increase in both capital and operating costs that leads to consideration of alternative approaches. Examples include the use of suspended and immobilised algae (Whitton *et al*., 2015), crystallisation through the inclusion of reactive media and the use of adsorption processes.

Microalgae are ubiquitous in wastewater environments in low concentrations. However, when the concentration is enriched, algae can become an effective way

to remove nutrients including phosphorus. The majority of systems using algae are based on high rate algae ponds (HRAP) with long retention time (4-10 days) and shallow water depths to utilise sunlight. Immobilisation has been suggested as an alternative approach whereby the algae are concentrated into polymer beads enabling much higher removal rates to be achieved and reducing the required retention time to hours (4-12 hours) (Whitton *et al*., 2015). The mechanisms of phosphorus removal have been identified as a combination of biological uptake and chemical precipitation into calcium phosphate. The relative predominance of each pathway depends on pH with precipitation dominating over the pH range 8-10 (Whitton *et al*., 2017). Achievable effluent concentrations below 0.1 mg L^{-1} have been demonstrated and the residual algae can be used for biogas generation offering potential added value. However, challenges remain in regard to the energy demand, chemical use and separation of the resultant algae in HRAP and the regular supply of beads for the immobilised system (Ometto *et al*., 2014; Whitton, 2016).

Crystallization has been shown to remove phosphorus from secondary effluent by accumulation on a seed crystal such as phosphate rock or bone charcoal. Xonlite and powdered converter slag have also been used as seed materials to remove phosphorus from the supernatant of the concentrated sludge and membrane-filtrate wastewater respectively (Menglin *et al*., 2016; Kaneko and Nakajima, 1988; Jang and Kang, 2002). Phosphorus can be removed from secondary effluent in, either, a calcium form such as hydroxyapatite (HAP, $Ca_5(PO_4)_3OH$) or in magnesium form such as struvite (MAP, $MgNH_3PO_4$). This occurs in 3 steps; formation of supersaturation, nucleation (crystal birth) and crystal growth (Dai *et al*., 2016). Struvite and hydroxyapatite can both be used as a fertilizer, but struvite is preferred as essential nutrients (phosphorus, nitrogen and magnesium) are released simultaneously and that too at a slower rate, allowing more uptake time for plants (Korchef *et al*., 2011; Bhuiyan *et al*., 2008). However, HAP is better equipped to remove phosphorus from wastewater with low concentration of phosphorus (Dai *et al*., 2016). The advantages of this method include, reduced chemical use compared to chemical precipitation method and no added sludge handling problems and costs. However, the

performance of this process can be adversely affected by the bicarbonate alkalinity of the secondary effluent (Kaneko and Nakajima, 1988).

Phosphorus removal via sorption onto media can be considered more useful and efficient than chemical precipitation and biological methods, especially when removing down to very low levels. The majority of phosphorus at that stage is in the phosphate form which has a high valency and weight compared to the other ions present suggesting it may be able to be removed selectively if the right media can be utilised. In addition, such processes normally have relatively easy pathways to reverse the uptake offering potential recovery routes. One of the most promising groups of sorption materials are the metal oxides as they potentially offer high capacity and selectivity. Accordingly, the review aims to assess the efficacy and challenges associated with the use of metal oxides for removal of phosphorus from wastewater

2.2 Adsorption

Adsorption as a process has been used for over 4000 years with early reports indicating use of charcoal for the reduction of metal ores such as zinc and copper in Egypt and treatment of a range of infections as well as drinking water in Greece (Inglezakis and Poulopos, 2006). The first quantitative observations of adsorption were made between 1777-1785 and later employed to remove colour from tartaric acid solution. Similarly, the English sugar industry started using charcoal for decolorization in 1794 (Inglezakis and Poulopos, 2006; Dabrowski, 2001). Until the 1950s, industrial application of adsorption was limited to water treatment and purification of industrial vent gases but in more recent times it has extended to use in cosmetics, paints and food as well as the pharmaceutical industry (Dabrowski, 2001).

At its heart, adsorption is a phase transfer process used to remove dissolved substances from fluids. The process of adsorption takes place in four steps (Tchobanoglous *et al*, 2003):

1. *Bulk solution transport* where the material that must be adsorbed moves to the boundary layer of the liquid surrounding the media.

2. *Film diffusion transport* involves the movement of the adsorbate to the entrance of the pores of the adsorbent.
3. *Pore transport* involves the adsorbate being transported through the pores by molecular diffusion through the pore liquid and/or diffusion along the surface of the adsorbent.
4. *Adsorption (or sorption)* involves the adsorbate getting attached to an available adsorbent site.

The adsorbate gets accumulated on the adsorbent by either physical adsorption or chemisorption. Chemisorption is a process where a bond is formed between the adsorbate and adsorbent due to a transfer of electrons between them. The strength of the resultant bond makes regeneration and recovery difficult and so media that operates by physical adsorption tends to be preferred. In such cases, non-specific bonds are formed through forces such as van der Waals and electrostatics through a reversible, exothermic process (Cooney, 1998; Crittenden *et al*., 2012). In such cases the processes tend to be mass transfer limited and are influenced by three interactions,

1. Adsorbate-water interactions are determined by solubility of the adsorbate
2. Adsorbate-surface interactions are determined by surface chemistry
3. Water-surface interactions are determined by solubility of the adsorbate

The strength of adsorbate-surface interactions determines the extent of the adsorption. The pore size and the surface area of the absorbent determines the number of adsorption sites and accessibility to those sites for the adsorbates. Key properties of any media used for adsorption include:

- A high specific surface area
- A high internal porosity
- An appropriate surface chemistry to attract the target adsorbate
- Mechanical strength

Several of these properties relate to pore size with smaller size pores equating to larger surface areas. However, the pore size of the adsorbent limits the adsorbates that can enter the internal structure of the materials. Highly porous

adsorbents are brittle and break easily resulting in significant losses such that the porosity of adsorbents never exceeds 50 % (Worch, 2012). The key operational properties of an adsorption media are the capacity for retention of the target pollutant (mg g_{media}^{-1}) and the duration of operation before the media requires regeneration (BV – bed volumes). The operational properties are determined experimentally through a combination of batch and fixed bed column setups. In batch experiments, a measured dose of the media is added to a flask along with either a synthetic solution or wastewater effluent. The flask is then agitated on an orbital shaker until equilibrium is reached (usually 24 hours). The remaining concentration in the liquid is used to determine the mass of material accumulated and hence its capacity at that given liquid concentration.

$$q_e = \frac{(C_o - C_e)V}{m} \qquad \textbf{Equation 1}$$

Batch experiments are quick and easy and are useful to understand the impact of variables such as pH, background water constituents and temperature. on capacity. However, to understand operationally relevant performance, continuous column experiments are required. In such cases a column of media is fed with the test solution and the resultant effluent measured over time until it reaches the same concentration as the feed. The key outcome is a relationship between the empty bed contact time and the total volume of water that can be treated to either a target breakthrough concentration or exhaustion (Worch, 2012). To reduce the impact of wall effects on the shape of the breakthrough curve, the diameter of the column must be at least 10 times the diameter of the sorbent particle diameter (Worch, 2012). Different bed depths are investigated until the breakthrough curve becomes consistent which can then be used to design large scale adsorption systems (Cooney, 1998).

2.2.1 Adsorption media for phosphorus removal

A range of adsorbents have been trialled for phosphorus removal including clay minerals, furnace slag, fly ash, metal oxides, and modified hybrid materials.

2.2.1.1 Non metal oxides

Adsorbents made from by-products of agricultural and industrial processes have been shown to be inexpensive and effective removers of phosphorus. Examples include by-products from metal refining (slags, ochre, red muds) and energy industries (fly ash, shale) where the media contains relatively high concentrations of iron, aluminium and calcium oxides which have been shown to be effective at removing phosphorus. One of the key influencing parameters is pH through a combination of alteration of the surface charges and change to the speciation of the available phosphorus. For instance, the capacity of iron oxide tailings, a by-product of the mineral processing industry in Canada, decreased from 8.6 mg L^{-1} at pH 3.2 to 4.6 mg L^{-1} at pH 9.5. The media showed poor desorbability (between 13-14 %) because of the strong bonding between phosphorus and the iron tailings (Zheng and Liu, 2004). Fe(III)/Cr(III) hydroxide sludge obtained from Southern Petrochemical Industries Corporation Limited (SPIC) also showed maximum capacity under acidic conditions with a capacity of 6.5 mg g_{media}^{-1} at pH 4.0 in batch experiments that followed second order kinetics (Namasivayam and Prathap, 2005). pH has also been shown to impact the performance of red mud, a by-product of the Bayer process to refine bauxite into alumina. However, removals as high as 99% are reported with the uptake following Pseudo-first-order kinetics and achieving a maximum phosphorus capacity of 0.58 mg g_{media}^{-1} (Li *et al*., 2006; Huang *et al*., 2008).

Phosphorus removal from such materials is complex and thought to occur through a combination of precipitation and adsorption. To illustrate, in the case of fly ash, adsorption was identified to account for about 30-40 % of the measured removal, with the rest of the removal coming from calcium phosphate precipitation (Lu *et al*., 2009). Fly ash has also been used to synthesize other materials which were then tested for phosphorus removal such as lanthanum hydroxide powder with a diameter of 180 μm. The capacity was found to be enhanced compared to commercially available lanthanum hydroxide (Xie *et al*., 2004). In another study, fly ash was converted into a zeolite with performance maximised at pH 3.5-9 (Chen *et al*., 2006). Xie *et al*., (2013) also synthesized zeolite from fly ash using a modified hydrothermal process. This resulted in 2-4 times increase in surface

area and 2-3 times increase in phosphorus capacity compared to either fly ash or zeolite produced using conventional methods.

A wide range of naturally occurring minerals and soils have also been tested such as kaolinite, zeolite, laterites, alunite. The materials have been shown to be effective with for instance, kaolinite removing 99 % of phosphorus from a wastewater effluent (Kamiyango *et al*., 2009). Similarly, Attapulgite, a clay mineral, removed 97.2 % of the phosphorus in the first 5 minutes in a batch setup, achieving an equilibrium capacity of around 3 mg g_{media}^{-1}. Column experiments revealed a serviceable bed life of 1440 bed volumes when removing phosphorus from eutrophic lake water (Yin and Kong, 2014). Modification of the material through acid and thermal treatment increased capacity to 5.1 mg g_{media}^{-1} (Ye *et al*., 2006). However, the material was found to have poor desorbability with only 10-13 % being recovered suggesting that it is only effective in a single use form, potentially as a soil amendment. Kanuma clay (K-clay) is a highly permeable and porous clay consisting of metal oxides such as SiO_2, Al_2O3, Fe_2O_3, MgO and CaO. K-clay was found to have a phosphorus capacity of 4.39 mg g_{media}^{-1} following pseudo second-order kinetics in a batch setup (Yang *et al*., 2013).

2.2.1.2 Metal oxides

Precipitated metal oxides have also been considered due to their large surface area and preferred surface properties. Synthesis involves dissolution of the parent metal salt in deionised water before adjusting the pH to 7-8 where the solubility product of the hydroxide form is at its minimum. The precipitated product is then washed, filtered and ground into a fine powder (Liu *et al*., 2014; Liu *et al*., 2015). Reported trials include oxides of lanthanum, ferric, magnesium, titanium, zirconia, aluminium and copper, in single, binary and tertiary forms (Table 2.1). The resultant media are very small with for instance, zirconium oxide tested with an average particle size of 5 nm achieving a maximum adsorptive capacity of 99.01 mg g_{media}^{-1} treating a synthetic mono component solution (Su *et al*., 2013). Equivalent capacity for activated aluminium and lanthanum oxides were 46.95 mg g_{media}^{-1} and 20.88 mg g_{media}^{-1} respectively. The capacity was observed to decrease significantly when treating wastewater effluents yielding capacities of

44.00 mg g_{media}^{-1} and 3.64 mg g_{media}^{-1}. Importantly, this demonstrates that certain metal oxides provide greater selectivity toward phosphorus such that they are less impacted from competition from the other constituents in the water such as sulphate, nitrate and chloride (Xie *et al*., 2014). This has been attributed to the types of bonding that occurs where the phosphate can form an inner sphere complex and selectivity is maximised (Alcelas *et al*., 2015).

Capacity appears to be enhanced when binary and tertiary metal oxide complexes are used (Table 2.1). For instance, the capacity of lanthanum oxide was reported as 46.9 mg g_{media}^{-1} compared to 85 mg g_{media}^{-1} when used as part of a Ferric-Magnesium-Lanthanum oxide complex (Xie *et al*., 2014; Yu and Chen, 2015). Inclusion of other constituents reduced the capacity of the complex with the greatest reduction seen in relation to addition of humic acid and carbonate where the capacity reduced to 65 and 66 mg g_{media}^{-1} respectively. Regeneration of capacity was seen to be a function of pH with for instance, in the case of zirconium oxide, phosphate recovery increasing from 15 % at pH 7 to 93 % at pH 13 (Table 2.2). However, regeneration over multiple cycle shows a reduction in capacity for metal complexes of Ferric-Magnesium- Lanthanum oxide, Ferric-Copper oxide and Ferric-Titanium oxide (Yu and Chen, 2015; Li *et al*., 2014; Lu *et al*., 2015). The greatest reduction seen represented a loss of 30 % of the initial capacity and indicates that the long-term operability of such materials needs consideration.

2.2.1.3 Metal oxide loaded sorbents

Whilst metal oxides show potential for phosphorus removal, serious issues around operability limit implementation. When used as a powder, the fine particles aggregate in water reducing surface area and generate excessive pressure drops in flow through systems (Pidou *et al*, 2009; Pan *et al*, 2014). To overcome such challenges, the metal oxide particles are commonly dispersed into a range of materials which act as skeleton frameworks such as activated carbon, chitosan, zeolites, silicates and ion exchange resin (Table 2.3). For example, chitosan beads have been used as a framework for zirconium and copper oxides and has been synthesized in many forms including quaternary

amine modified beats, chitosan blended with PVA and glutaraldehyde and functionalised chitosan beads. The virgin beads also exhibit good phosphorus removal behaviour with reported capacities of between 19 – 159.5 mg g_{media}^{-1}, in a batch setup with no competing ions (Sowmya and Meenakshi, 2013; Rajeswari *et al*., 2015; De Sousa *et al*., 2012). Similar experience is reported with ion exchange beads and the other materials. However, such materials offer little selectivity towards phosphorus such that capacity is significantly influenced by the presence of other constituents. To illustrate in the case of chitosan, the capacity reduced from 67 mg g_{media}^{-1} to 17.2 mg g_{media}^{-1} due to the inclusion of an equi-mass of nitrate to phosphate (Sowmya and Meenakshi, 2013). In untreated sewage, concentration of nitrogen species is between 20 - 70 mg L^{-1} compared to 4 - 12 mg L^{-1} for phosphorus species (Tchobanoglous *et al*., 2003). Like with conventional ion exchange resins, phosphate will be outcompeted by nitrate for the synthesized chitosan media. Inclusion of metal oxides into the framework of the parent materials does not increase capacity in synthetic mono-component systems but does increase selectivity in the presence of other constituents. For instance, the capacity of Copper (II) loaded chitosan beads reduced 50 % when sulphate was added to the solution compared to 75 % reduction based on just the chitosan bead (Sowmya and Meenakshi, 2013; Dai *et al*., 2011). The same level of reduction was seen with Zirconium oxides as well where the capacity reduced from 58 mg g_{media}^{-1} to 27 mg g_{media}^{-1} in the presence of 500 mg L^{-1} of sulphate (Liu and Zhang, 2015). In other studies, carbonate has been seen to cause the biggest change in capacity when using a zirconium oxide embedded chitosan system where the removal of phosphate decreased from 97 % with no competing ions compared to 9 % in the presence of carbonate ions. This was attributed to the increase in pH due to carbonate ions (Liu *et al*, 2015).

Table 2.1 Metal oxides

Adsorbent	Water type	Water Composition	Outcomes	Reference
Ferric-Magnesium-Lanthanum oxide	Synthetic	PO_4^{-3} (20-500 mg L^{-1})	Isotherm – Langmuir Kinetic model – Pseudo second order Capacity = 415.2 mg g_{media}^{-1}	Yu and Chen, 2015
		PO_4^{-3} (20 mg L^{-1})	Capacity = 85 mg g_{media}^{-1}	
		PO_4^{-3} (20 mg L^{-1}) SO_4^{2-} (0 – 960.6 mg L^{-1})	Capacity = 82 to 74 mg g_{media}^{-1}	
		PO_4^{-3} (20 mg L^{-1}) F^- (0 – 9.495 mg L^{-1})	Capacity = 82 to 71 mg g_{media}^{-1}	
		PO_4^{-3} (20 mg L^{-1}) HCO_3^- (0 – 600.1 mg L^{-1})	Capacity = 82 to 66 mg g_{media}^{-1}	
		PO_4^{-3} (20 mg L^{-1}) NO^{3-} (0–62 mg L^{-1})	Capacity = 82 to 78 mg g_{media}^{-1}	
		PO_4^{-3} (20 mg L^{-1}) Humic acid (0 – 10 mg L^{-1})	Capacity = 82 to 65 mg g_{media}^{-1}	
		PO_4^{-3} (0.92 mg L^{-1})	Capacity = 66.2 mg g_{media}^{-1}	
Activated Aluminium oxide	Synthetic	PO_4^{-3} (5-200 mg L^{-1})	Isotherm – Langmuir Capacity = 20.88 mg g_{media}^{-1}	Xie *et al*., 2014
		PO_4^{-3} (5 mg L^{-1})	Capacity = 3.8 mg g_{media}^{-1}	

Adsorbent	Water type	Water Composition	Outcomes	Reference
	PO_4^{-3} spiked effluent	PO_4^{-3} (5 mg L^{-1}) SO_4^{2-} - (20 mg L^{-1}) NO^{3-} (5.86 mg L^{-1}) Cl^- (152.3 mg L^{-1})	Capacity = 3.64 mg g_{media}^{-1}	
Lanthanum oxide	Synthetic	PO_4^{-3} (5-500 mg L^{-1})	Isotherm – Langmuir Capacity = 46.95 mg g_{media}^{-1}	Xie *et al*., 2014
		PO_4^{-3} (5 mg L^{-1})	Capacity = 45.42 mg g_{media}^{-1}	
	PO_4^{-3} spiked effluent	PO_4^{-3} (5 mg L^{-1}) SO_4^{2-} (20 mg L^{-1}) NO^{3-} (5.86 mg L^{-1}) Cl^- (152.3 mg L^{-1})	Capacity = 44 mg g_{media}^{-1}	
Ferric-Manganese oxide	Synthetic	PO_4^{-3} (0.5-10 mg L^{-1})	Isotherm – Langmuir Kinetic model – Pseudo second order Capacity = 0.223 mol-P mol-Fe^{-1} Phosphate removal = 49 %	Lu *et al*., 2014
		PO_4^{-3} (0.12 mg L^{-1}) SO_4^{2-} (5 mM)	Phosphate removal = 48 %	
		PO_4^{-3} (0.12 mg L^{-1}) SiO_3^{2-} (5 mM)	Phosphate removal = 46 %	
		PO_4^{-3} (0.12 mg L^{-1}) HCO_3^- (5 mM)	Phosphate removal = 42 %	

Adsorbent	Water type	Water Composition	Outcomes	Reference
		PO_4^{-3} (0.12 mg L^{-1}) DOC (5 mM)	Phosphate removal = 38 %	
Titanium-Ferric oxide	Synthetic	PO_4^{-3} (500 mg L^{-1})	Isotherm – Langmuir Kinetic model – Pseudo second order Capacity = 21 mg g_{media}^{-1}	D'Arcy *et al.*, 2011
Ferric-Aluminium-Manganese oxide	Synthetic	PO_4^{-3} (3000 mg L^{-1})	Isotherm – Freundlich Kinetic model – Pseudo second order Capacity = 48.3 mg g_{media}^{-1} Percentage removal = 66 %	Lu *et al.*, 2013
		PO_4^{-3} (10 mg L^{-1}) SO_4^{2-} (0.01 M)	Percentage removal = 63 %	
		PO_4^{-3} (10 mg L^{-1}) SiO_3^{2-} (0.01 M)	Percentage removal = 41 %	
		PO_4^{-3} (10 mg L^{-1}) HCO_3^{-} (0.01 M)	Percentage removal = 61 %	
Zirconium oxide	Synthetic	PO_4^{-3} (5-50 mg L^{-1})	Isotherm – Langmuir Kinetic model – Pseudo second order Capacity = 99.01 mg g_{media}^{-1}	Su *et al.*, 2013
		PO_4^{-3} (5 mg L^{-1})	Percentage removal = 99 %	
		PO_4^{-3} (5 mg L^{-1})	Percentage removal = 98 %	

Adsorbent	Water type	Water Composition	Outcomes	Reference
		Cl^- (10 mM)		
		PO_4^{-3} (10 mg L^{-1}) SO_4^{2-} (10 mM)	Percentage removal = 96 %	
		PO_4^{-3} (10 mg L^{-1}) HCO_3^- (10 mM)	Percentage removal = 98 %	
Ferric-Titanium oxide	Synthetic	PO_4^{-3} (2.5-5 mg L^{-1})	Isotherm – Langmuir Kinetic model – Pseudo second order Capacity = 35.4 mg g_{media}^{-1} Percentage removal = 69 %	Lu *et al.*, 2015
		PO_4^{-3} (10 mg L^{-1}) SO_4^{2-} (0.01 M)	Percentage removal = 67 %	
		PO_4^{-3} (10 mg L^{-1}) SiO_3^{2-} (0.01 M)	Percentage removal = 15.6 %	
		PO_4^{-3} (10 mg L^{-1}) HCO_3^- (0.01 M)	Percentage removal = 55.2 %	
Ferric-Copper oxide	Synthetic	PO_4^{-3} (7 mg L^{-1})	Isotherm – Langmuir Kinetic model – Pseudo second order Capacity = 39.8 mg g_{media}^{-1}	Li *et al.*, 2014
		PO_4^{-3} (5 mg L^{-1})	Percentage removal = 100 %	
		PO_4^{-3} (5 mg L^{-1}) Cl^- (10 mM)	Percentage removal = 98 %	

Adsorbent	Water type	Water Composition	Outcomes	Reference
		PO_4^{-3} (5 mg L^{-1}) SO_4^{2-} (10 mM)	Percentage removal = 98 %	
		PO_4^{-3} (5 mg L^{-1}) HCO_3^- (10 mM)	Percentage removal = 95 %	
		PO_4^{-3} (5 mg L^{-1}) SiO_3^{2-} (0.01 M)	Percentage removal = 59 %	
Ferric-Manganese oxide	Synthetic	PO_4^{-3} (10 mg L^{-1})	Isotherm – Freundlich Kinetic model – Pseudo second order Capacity = 36 mg g_{media}^{-1}	Zhang *et al*., 2009
		PO_4^{-3} (5 mg L^{-1})	Percentage removal = 100 %	
		PO_4^{-3} (5 mg L^{-1}) Cl^- (10 mM)	Percentage removal = 95 %	
		PO_4^{-3} (5 mg L^{-1}) SO_4^{2-} (10 mM)	Percentage removal = 93 %	
		PO_4^{-3} (5 mg L^{-1}) HCO_3^- (10 mM)	Percentage removal = 94 %	

Table 2.2 Regeneration Metal Oxides

Adsorbent	Regenerant	Number of cycles	Outcomes	Reference
Ferric-Magnesium-Lanthanum oxide	0.5M NaOH solution	5	Capacity virgin media = 82 mg g_{media}^{-1} Capacity 1st regeneration cycle = 74 mg g_{media}^{-1} Capacity 2nd regeneration cycle = 70 mg g_{media}^{-1} Capacity 3rd regeneration cycle = 65 mg g_{media}^{-1} Capacity 4th regeneration cycle = 57 mg g_{media}^{-1}	Yu and Chen, 2015
Ferric-Copper oxide	0.5 mol L^{-1}	6	Capacity virgin media = 39 mg g_{media}^{-1} Capacity 1st regeneration cycle = 36 mg g_{media}^{-1} Capacity 2nd regeneration cycle = 34 mg g_{media}^{-1} Capacity 3rd regeneration cycle = 32 mg g_{media}^{-1} Capacity 4th regeneration cycle = 30 mg g_{media}^{-1} Capacity 5th regeneration cycle = 28 mg g_{media}^{-1}	Li *et al*., 2014
Ferric-Manganese oxide	0.001 M NaOH	1	Phosphate recovered = 28 %	Zhang *et al.*, 2009
	0.01 M NaOH	1	Phosphate recovered = 67 %	
	0.1 M NaOH	1	Phosphate recovered = 94 %	
	0.5 M NaOH	1	Phosphate recovered = 94 %	
Ferric-Titanium oxide	0.1 M NaOH	5	Capacity virgin media = 32 mg g_{media}^{-1} Capacity 1st regeneration cycle = 36 mg g_{media}^{-1} Capacity 2nd regeneration cycle = 28 mg g_{media}^{-1} Capacity 3rd regeneration cycle = 27 mg g_{media}^{-1} Capacity 4th regeneration cycle = 26 mg g_{media}^{-1} Capacity 5th regeneration cycle = 25 mg g_{media}^{-1}	Lu *et al*., 2015

Adsorbent	Regenerant	Number of cycles	Outcomes	Reference
Zirconium oxide	0.1 M NaOH pH - 7	1	Phosphate recovered = 15 %	Su *et al*., 2013
	0.1 M NaOH pH - 11	1	Phosphate recovered = 58 %	
	0.1 M NaOH pH - 12	1	Phosphate recovered = 74 %	
	0.1 M NaOH pH - 13	1	Phosphate recovered = 93 %	
	0.1 M NaOH pH – 13.7	1	Phosphate recovered = 95 %	

Silicates have also received significant attention as they have high surface areas and controlled pore diameters making them good adsorbents for metal removal. Iron, lanthanum, zirconium, aluminium and titanium have all been dispersed in different forms of silicates achieving varying rates of phosphate removal (Table 2.3). The hybrid materials are made through post grafting whereby alcohol is used as a solvent to transport the metal oxide which is then fixed into the structure by maintaining a temperature of between 60-110 °C for up to 24 hours. The residual solvent is then removed, and the embedded media rinsed. The adsorbents were found to deliver a maximum capacity between pH 6 and pH 8, with the sorbents showing the lowest capacity at pH 10 and above. For lanthanum and ferric loaded silicates, the presence of sulphate ions had the biggest impact on the capacity followed by fluoride, nitrate and chloride (Huang *et al*., 2015; Delaney *et al*., 2016; Tang *et al*., 2012; Shin *et al*., 2004; Zhang *et al*., 2010; Zhang *et al*., 2011).

Activated carbon is the most commonly used adsorbent in the water industry as it is a highly porous material that has been used to remove a range of contaminants from water and wastewater including heavy metals, nitrate, dyes, pharmaceuticals. Ferric (III) or lanthanum loaded activated carbon has been synthesized by mixing activated carbon with the metal oxide at pH 9.0. The biggest impact on the performance of the synthesized adsorbent was pH with phosphate removal decreasing with increasing pH with highest removal achieved at pH 2 (Shi *et al*, 2011). This indicates that the phosphorous removal was predominately occurring onto the base carbon as metal oxides are expected to perform poorly in very acidic waters. This is due to the speciation of phosphorous which can occur in four forms H_3PO_4, $H_2PO_4^-$, HPO_4^{2-}, and PO_4^{3-} depending on pH. Below pH of 3, the predominant form is H_3PO_4, which binds weakly with metal oxides. As the pH increases (between 3 and 8), $H_2PO_4^-$ and HPO_4^{2-} become the dominant species which are electrostatically adsorbed by the metal oxides. However, a further increase in pH was seen to reduce the adsorption capacity of the metal oxide loaded adsorbents. This is because in alkaline conditions the extent of the positive charge of the metal oxide adsorbents decreases, resulting in weak electrostatic interaction between phosphate and the metal oxide. The

capacity at high pH is further reduced due to competitive adsorption of excessive hydroxyl ions (Lu *et al*., 2013; Pan *et al*., 2009; Liu *et al*., 2015). In fact, the change in species is utilised during regeneration where raising the pH above pH13 is used to recover the captured phosphorus (Martin *et al*., 2013).

The most commonly considered systems are based on using ion exchange resins as they provide high physical and chemical stability, are easy to operate and can be reused multiple times through regeneration. In their parent form, the resins suffer the same challenges concerning selectivity as other medias especially from sulphate due to its higher concentration and higher charge (bivalency), making uptake considerably more favourable than for phosphate with an affinity sequence of (An *et al*., 2014; Sowmya and Meenaksji, 2014; Sowmya and Meenaksji, 2014b):

$$SO_4^{2-} > PO_4^{3-} > NO_3^- > Cl^-$$

Inclusion of metal oxides such as ferric, copper and zirconium adjust this selectivity as phosphate is a strong ligand towards these materials and forms inner-sphere complexes through Lewis-acid base and electrostatic interaction. In contrast, sulphate is a weak ligand and primarily forms outer-sphere complexes with the metal oxide through electrostatic interaction. This results in the metal oxide loaded sorbents having the following affinity sequence (An *et al*., 2014; Pan *et al*., 2009):

$$PO_4^{3-} > SO_4^{2-} > NO_3^- > Cl^-$$

Despite the selectivity of metal oxide loaded sorbents for phosphate ions, it has been reported that accumulation of sulphate ions on the surface of the sorbent weakens the electrostatic attraction between phosphate ions and the metal oxide, resulting in a decrease in capacity (Liu *et al*., 2015). The most common embedded metal oxide is that of Ferric which is commercially available and used for arsenate removal from groundwater in the USA and India. The adsorbent is synthesized by first preparing a $Fe(NO_3)_3$/NaCl/HCl mixture (molar ratio of 1:3:1) which is then run through a fixed bed column where the ferric species exchange onto the resin. The pH is then raised precipitating the sorbed ferric into its

hydroxide form. The resultant nanoparticles are chemically bonded to the resin making them stable such that they only release if the resins are soaked in strong acids. The ferric loaded resin is then thermally treated to obtain the final form (the media shall be called HAIX henceforth) (Li *et al*., 2013; Pan *et al*., 2009).

The performance of ferric loaded ion exchange resins has been tested in both batch and column setups using synthetic single and multicomponent solutions, wastewater effluents and urine. Sendrowski *et al*., (2013) tested commercially available resin PhosX^{np} or LayneRT for phosphate removal from synthetic urine and synthetic hydrolysed urine. Selectivity of the media was tested by doubling the concentration of sulphate in urine resulting in a 10 % decrease in phosphate removal. Pan *et al*., (2009) studied the impact of pH and competing ion on phosphate adsorption by HAIX in a batch setup using synthetic solutions. The media performed best at pH 7, achieving a media capacity of 19 mg g_{media}^{-1}. In the presence of competing sulphate ions, the media capacity dropped by 68 %. Pan *et al*., (2009) observed that in a column setup (synthetic solution with 2 mg L^{-1}), that it took 700 bed volumes to reach a phosphate breakthrough of 0.1 mg L^{-1} at an EBCT of 4 minutes compared to 800 bed volumes for pesticide effluent (3.8 mg P L^{-1}) at an EBCT of 6 minutes. In another study, iron loaded ion exchange resin exhausted with synthetic phosphate solution, had a capacity of 48 mg g_{media}^{-1} (Table 2.4). The impact of bed depth was studied at the same flow rate at 7 different bed heights. By keeping a constant flowrate, the author essentially increased the EBCT. The experiments showed that by increasing the EBCT, the bed volumes to breakthrough and exhaustion increased. Martin *et al*., (2013) conducted a study to assess the impact of the vessel diameter on the performance of iron loaded ion exchange resins. At a fixed EBCT of 4 minutes, the media capacity was seen to increase from 3.4 to 6.3 mg g_{media}^{-1} by increasing the vessel diameter from 15 mm to 500 mm due to the reduction in axial dispersion at the larger column diameters.

The metal oxide loaded media has been shown to be effective at removing phosphorus to below 0.1 mg P L^{-1}, in synthetic water and wastewater effluents. The application of these types of media have the same limitation as other sorption

medias and these include, excessive pressure drops in the vessels due to build-up of solids. This means the metal oxide medias will be best suited as tertiary treatment, following the final settlement tanks. This applies to both scenarios, treating full phosphorus load at sewage treatment works with no existing phosphorus treatment as well as sewage treatment which use coagulant dosing and/or biological phosphorus removal (Figure 1.1).

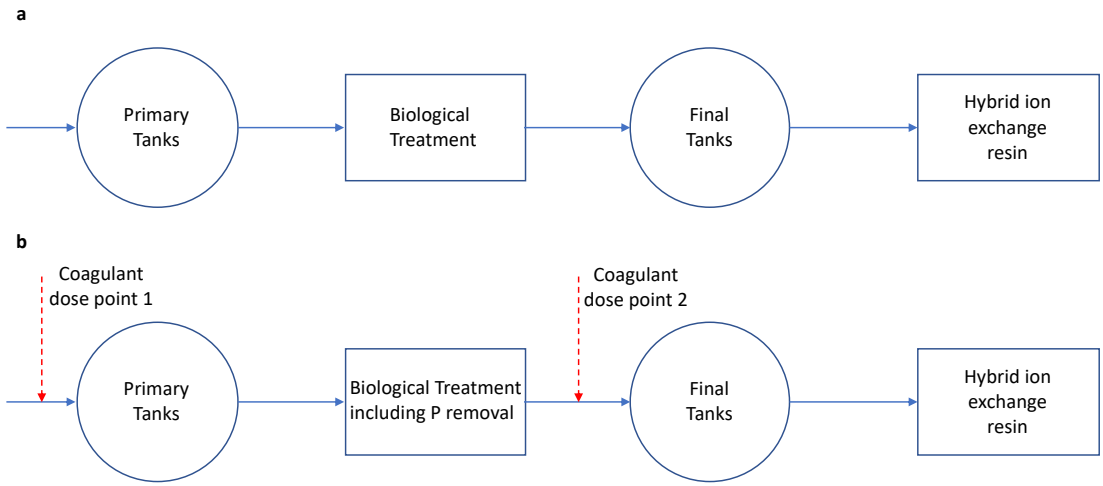

Figure 1.1 Possible application of hybrid ion exchange resin at a) Sewage treatment works with no existing phosphorus removal and, b) Sewage treatment works that utilize coagulant dosing and /or biological phosphorus removal.

Table 2.3 Metal oxide loaded sorbents – batch

Adsorbent	Media size	Water type	Water Composition	Outcomes	Reference
Zr(IV) loaded chitosan beads (ZCB)	20 – 60 μm	Synthetic	PO_4^{-3} (30 mg L^{-1})	Isotherm – Langmuir Kinetic model – Pseudo second order Capacity = 61.7 mg g_{media}^{-1}	Liu and Zhang, 2015
			PO_4^{-3} (10 mg L^{-1})	Kinetic model – Pseudo second order Capacity = 49 mg g_{media}^{-1}	
			PO_4^{-3} (20 mg L^{-1})	Capacity = 58.35 mg g_{media}^{-1}	
			PO_4^{-3} (20 mg L^{-1}) SO_4^{2-} (200 - 500 mg L^{-1})	Capacity = 39 – 28.15 mg g_{media}^{-1}	
			PO_4^{-3} (20 mg L^{-1}) NO^{3-} (200 - 500 mg L^{-1})	Capacity = 57.7 - 57.5 mg g_{media}^{-1}	
			PO_4^{-3} (20 mg L^{-1}) Cl^- (200 - 500 mg L^{-1})	Capacity = 57.8 - 58 mg g_{media}^{-1}	
Zirconium(IV) loaded chitosan particles	100 mesh size	Synthetic	PO_4^{-3} (10 - 300 mg L^{-1})	Isotherm – Langmuir Kinetic model – Pseudo second order Capacity = 71.68 mg g_{media}^{-1} Percentage removed = 98 %	Liu *et al*., 2015
			PO_4^{-3} (5 mg L^{-1}) Cl^- (0.1 M)	Percentage removed = 88 %	
			PO_4^{-3} (5 mg L^{-1}) SO_4^{2-} (0.1 M)	Percentage removed = 80 %	

Adsorbent	Media size	Water type	Water Composition	Outcomes	Reference
			PO_4^{-3} (5 mg L^{-1}) HCO_3^- (0.1 M)	Percentage removed = 8 %	
Copper loaded chitosan beads	3.1 mm	Synthetic	PO_4^{-3} (50 mg L^{-1})	Isotherm – Langmuir Kinetic model – Pseudo-first order and Pseudo-second order Capacity = 70 mg g_{media}^{-1}	An *et al*., 2014
			PO_4^{-3} (50 mg L^{-1}) SO_4^{2-} (50 mg L^{-1})	Capacity = 35 mg g_{media}^{-1}	
Copper loaded chitosan hydrogel beads	2.5 mm	Synthetic	PO_4^{-3} (10-180 mg L^{-1})	Isotherm – Langmuir Kinetic model – Pseudo-first order and Pseudo-second order Capacity = 28.86 mg g_{media}^{-1}	Dai *et al*., 2011
Lanthanum loaded silica spheres	Not given	Synthetic	PO_4^{-3} (2-50 mg L^{-1})	Isotherm – Langmuir Kinetic model – Pseudo second order Capacity = 42.76 mg g_{media}^{-1}	Huang *et al*., 2015
			PO_4^{-3} (50 mg L^{-1})	Capacity = 40 mg g_{media}^{-1}	
			PO_4^{-3} (50 mg L^{-1}) Cl^- (0.01 M)	Capacity = 39 mg g_{media}^{-1}	
			PO_4^{-3} (50 mg L^{-1}) NO^{3-} (0.01 M)	Capacity = 38 mg g_{media}^{-1}	
			PO_4^{-3} (50 mg L^{-1}) SO_4^{2-} (0.01 M)	Capacity = 38 mg g_{media}^{-1}	
			PO_4^{-3} (50 mg L^{-1}) HCO_3^- (0.01 M)	Capacity = 29 mg g_{media}^{-1}	

Adsorbent	Media size	Water type	Water Composition	Outcomes	Reference
Zirconium loaded mesoporous silicate	Not given	Synthetic	PO_4^{-3} (5-30 mg L^{-1})	Isotherm – Freundlich Kinetic model – Pseudo second order Capacity = 319.7 mg g_{media}^{-1}	Tang *et al*., 2012
Aluminium loaded mesoporous silicate	Not given	Synthetic	PO_4^{-3} (10 mg L^{-1})	Isotherm – Langmuir Kinetic model – Pseudo second order Capacity = 619 μmol g_{media}^{-1}	Shin *et al*., 2004
Lanthanum loaded mesoporous silicate	Not given	Synthetic	PO_4^{-3} (50 mg L^{-1})	Isotherm – Langmuir Kinetic model – Pseudo second order Capacity = 20 mg g_{media}^{-1}	Zhang *et al*., 2010
			PO_4^{-3} (50 mg L^{-1}) SO_4^{2-} (400 mg L^{-1})	Capacity = 18 mg g_{media}^{-1}	
Ferric loaded mesoporous silicate	Powder	Synthetic	PO_4^{-3} (30-100 mg L^{-1})	Isotherm – Langmuir Kinetic model – Pseudo second order Capacity = 51.8 mg g_{media}^{-1}	Zhang *et al*., 2011
			PO_4^{-3} (50 mg L^{-1})	Capacity = 33 mg g_{media}^{-1}	
			PO_4^{-3} (50 mg L^{-1}) Cl^- (100 - 900 mg L^{-1})	Capacity = 30 – 27.5 mg g_{media}^{-1}	
			PO_4^{-3} (50 mg L^{-1}) NO^{3-} (100 - 900 mg L^{-1})	Capacity = 24 - 15 mg g_{media}^{-1}	
			PO_4^{-3} (50 mg L^{-1})	Capacity = 18 - 10 mg g_{media}^{-1}	

Adsorbent	Media size	Water type	Water Composition	Outcomes	Reference
			SO_4^{2-} (100 - 900 mg L^{-1})		
Lanthanum loaded activated carbon fibre	0.4-0.6 cm	Synthetic	PO_4^{-3} (10-70 mg L^{-1})	Isotherm – Langmuir Kinetic model – Pseudo second order Capacity = 10.5 mg g_{media}^{-1}	Zhang *et al.*, 2012
			PO_4^{-3} (5-30 mg L^{-1})	Isotherm – Langmuir Kinetic model – Pseudo second order Capacity = 11 mg g_{media}^{-1}	Liu *et al.*, 2011
Ferric loaded activated carbon	Not given	Synthetic	PO_4^{-3} (2-1200 mg L^{-1})	Isotherm – Freundlich Kinetic model – Pseudo second order Capacity = 98.39 mg g_{media}^{-1}	Shi *et al.*, 2011
Ferric loaded anion exchanger D-201	0.6 – 1 mm	Synthetic	PO_4^{-3} (10-1000 mg L^{-1})	Kinetic model – Pseudo first order Capacity = 17.8 mg g_{media}^{-1}	Pan *et al.*, 2009
			PO_4^{-3} (10-1000 mg L^{-1}) SO_4^{2-} (100 - 900 mg L^{-1})	Capacity = 5.8 mg g_{media}^{-1}	
PhosXnp or LayneRT – commercially available ferric loaded anion exchange resin	Not given	Synthetic urine	PO_4^{-3} (20 mmol L^{-1}) SO_4^{2-} (10 - 900 mmol L^{-1})	Isotherm – Langmuir Capacity = 10.1 mg g_{media}^{-1}	O'Neal and Boyer, 2013
		Synthetic hydrolyzed urine	PO_4^{-3} (13.6 mmol L^{-1}) SO_4^{2-} (10 - 15 mmol L^{-1}) HCO_3^- (250 - 267 mmol L^{-1})	Isotherm – Freundlich Capacity = 6.90 mg g_{media}^{-1}	
		Synthetic Anaerobic supernatant	PO_4^{-3} (0.72 - 2.58 mmol L^{-1}) HCO_3^- (149 mmol L^{-1})	Isotherm – Freundlich Capacity = 5.15 mg g_{media}^{-1}	

Adsorbent	Media size	Water type	Water Composition	Outcomes	Reference
		Synthetic household greywater	PO_4^{-3} (0.18 mmol L^{-1}) SO_4^{2-} (0.25 mmol L^{-1}) HCO_3^- (0.30 mmol L^{-1})	Isotherm – Freundlich Capacity = 4.58 mg g_{media}^{-1}	
		Secondary wastewater effluent	PO_4^{-3} (0.051 mmol L^{-1}) SO_4^{2-} (0.058 mmol L^{-1}) HCO_3^- (0.23 mmol L^{-1})	Isotherm – Langmuir and Freundlich Capacity = 1.49 mg g_{media}^{-1}	
PhosXnp or LayneRT – commercially available ferric loaded anion exchange resin	300 – 1200 μm	Synthetic urine	PO_4^{-3} (20 mmol L^{-1}) SO_4^{2-} (15 - 30 mmol L^{-1})	Isotherm – Freundlich Kinetic model – Pseudo first order and Pseudo second order Capacity = 9.54 mg g_{media}^{-1}	Sendrowski and Boyer, 2013
		Synthetic hydrolyzed urine	PO_4^{-3} (5 mmol L^{-1}) SO_4^{2-} (15 - 30 mmol L^{-1})	Isotherm – Freundlich Kinetic model – Pseudo second order Capacity = 7.17 mg g_{media}^{-1}	
Purolite FerrIX A33E – commercially available iron oxide loaded anion exchange resin	0.3 – 1.2 mm	Synthetic	PO_4^{-3} (5 – 30 mg L^{-1})	Isotherm – Langmuir Capacity = 48 mg g_{media}^{-1}	Nut *et al*., 2014
Ferric oxide loaded IRA-400 (Amberlite)	20 – 25 mesh size	Synthetic	PO_4^{-3} (5 mg L^{-1})	Isotherm – Freundlich Kinetic model – Pseudo second order Capacity = 111.1 mg g_{media}^{-1}	Acelas *et al*., 2015
			PO_4^{-3} (5 mg L^{-1}) SO_4^{2-} (100 mg L^{-1})	Isotherm – Langmuir Capacity = 18.52 mg g_{media}^{-1}	

Adsorbent	Media size	Water type	Water Composition	Outcomes	Reference
		Small plant wastewater	PO_4^{-3} (6.8 mg L^{-1}) SO_4^{2-} (60 mg L^{-1})	Isotherm – Langmuir Capacity = 26.74 mg g_{media}^{-1}	
		Large plant wastewater	PO_4^{-3} (0.98 mg L^{-1}) SO_4^{2-} (155 mg L^{-1})	Isotherm – Freundlich Capacity = 14.14 mg g_{media}^{-1}	
Zirconium oxide loaded IRA-400 (Amberlite)	20 – 25 mesh size	Synthetic	PO_4^{-3} (5 mg L^{-1})	Isotherm – Freundlich Kinetic model – Pseudo second order Capacity = 91.74 mg g_{media}^{-1}	
			PO_4^{-3} (5 mg L^{-1}) SO_4^{2-} (100 mg L^{-1})	Isotherm – Langmuir Capacity = 18.97 mg g_{media}^{-1}	
		Small plant wastewater	PO_4^{-3} (6.8 mg L^{-1}) SO_4^{2-} (60 mg L^{-1})	Isotherm – Langmuir Capacity = 29.85 mg g_{media}^{-1}	
Copper oxide loaded IRA-400 (Amberlite)	20 – 25 mesh size	Synthetic	PO_4^{-3} (5 mg L^{-1})	Isotherm – Freundlich Kinetic model – Pseudo second order Capacity = 74.07 mg g_{media}^{-1}	
			PO_4^{-3} (5 mg L^{-1}) SO_4^{2-} (100 mg L^{-1})	Isotherm – Langmuir Capacity = 3.12 mg g_{media}^{-1}	

Table 2.4 Metal loaded sorbents - column

Adsorbent	Adsorption conditions	Regeneration conditions	Water type and Composition	Cycle	Breakthrough (Bed volumes)				Other outcomes/ conditions	Reference
					0.1	0.5	1	Saturation		
Zirconium loaded macro porous strongly basic anion exchanger (HZO-201)	EBCT = 6 minutes Flow rate = 0.83 mL min^{-1}	4 regeneration cycles using 5 % NaOH and 5 % NaCl at an EBCT of 30 minutes and flow rate of 0.2 mL min^{-1}	<u>Synthetic</u> PO_4^{-3} (2 mg L^{-1}) SO_4^{2-} (100 mg L^{-1}) NO_3^- (10 mg L^{-1}) Cl^- (80 mg L^{-1}) HCO_3^- (100 mg L^{-1}) SiO_3^{2-} (5 mg L^{-1})	1	10 -30	1600	1920			Chen *et al*., 2015
				2	10-30	1300	1600			
				5	10-30	1300	1600			
			<u>Wastewater effluent</u> PO_4^{-3} (1.33 mg L^{-1}) SO_4^{2-} (48.6 mg L^{-1}) NO_3^- (29.3 mg L^{-1}) Cl^- (73.5 mg L^{-1}) COD (20.1 mg L^{-1})	1	10-30	1800	2250	2300		
				3	10-30	1120	1560	1625		
				5	10-30	1120	1560			

Adsorbent	Adsorption conditions	Regeneration conditions	Water type and Composition	Cycle	Breakthrough (Bed volumes)				Other outcomes/ conditions	Reference
					0.1	0.5	1	Saturation		
			NH_3-N 0.52 mg L^{-1})							
0.15- Hydrous iron oxide modified diatomite (HIOMD)	EBCT =14.5 minutes Flow rate = 0.54 mL min^{-1}		<u>Synthetic</u> PO_4^{-3} (5 mg L^{-1})	1	160	250	380	1300		Wang *et al*., 2016
Zr(IV)-loaded mono-phosphonic acid resin (Zr-MPR)	EBCT = 2 minutes Flow rate =1 mL min^{-1}	1 regeneration cycle using 0.1 M NaOH at EBCT of 20 minutes and flow rate of 0.1 mL min^{-1}.	<u>Synthetic</u> PO_4^{-3}(1.344 mg L^{-1}) SO_4^{2-} (20 mg L^{-1}) Cl^- (10 mg L^{-1}) HCO_3^- (15 mg L^{-1})	1	210	260	330	550 (based on predicting from graph 1.		Awual *et al*., 2011
				2	Paper states that adsorbent kept the same capability.					
Copper loaded chitosan beads	EBCT = 35 minutes Flow rate = 1 mL min^{-1}		<u>Synthetic</u> PO_4^{-3} (4.9 mg L^{-1}) SO_4^{2-} (52.4 mg L^{-1}) NO_3^- (49.1 mg L^{-1}) HCO_3^- (100 mg L^{-1})	1	Could not be determined from graph	50	80	230		An et al, 2014

Adsorbent	Adsorption conditions	Regeneration conditions	Water type and Composition	Cycle	Breakthrough (Bed volumes)				Other outcomes/ conditions	Reference
					0.1	0.5	1	Saturation		
Ferric loaded anion exchanger D-201	EBCT = 4 minute	5 cycles using 5 % NaOH-NaCl solution at EBCT of 15 minutes.	Synthetic PO_4^{-3} (2 mg L^{-1})	1	660	875	970	Not given		Pan *et al*., 2009
			SO_4^{2-} (120 mg L^{-1}) Cl^- (100 mg L^{-1}) HCO_3^- (100 mg L^{-1})	5	660	875	950	Not given		
	EBCT = 6 minute	1 cycle	Pesticide manufacturing effluent PO_4^{-3} (3.8 mg L^{-1}) COD (150 mg L^{-1})	1	780	940	1000	Not given		
Purolite FerrIX A33E – commercially available iron oxide loaded anion exchange resin	Flow rate = 2.5 m h^{-1} Bed depth = 3 – 19 cm EBCT = 072 – 4.6 minutes		Synthetic PO_4^{-3} (20 mg L^{-1})	1	Could not be determined from graphs			3 – 28 hours		Nur *et al*., 2014
	Bed height = 12 cm		Synthetic	1	Could not be determined from graphs			13 – 30 hours		

Adsorbent	Adsorption conditions	Regeneration conditions	Water type and Composition	Cycle	Breakthrough (Bed volumes)				Other outcomes/ conditions	Reference
					0.1	0.5	1	Saturation		
	Flow rate = 2.5 m h^{-1} EBCT = 2.88 minutes		PO_4^{-3}(5 - 30 mg L^{-1})							
	Bed height = 12 cm Flow rate = 2.5 m h^{-1} EBCT = 2.88 minutes	1 M NaOH	Synthetic PO_4^{-3} (30 mg L^{-1})	4	Similar performance for the first 3 cycles with slight reduction in the 4th cycle.			13 hours		
Ferric loaded anion exchange resin	Bed height = 10 cm EBCT = 0.7 minutes		Synthetic PO_4^{-3} (20 mg L^{-1})	1	Could not be determined from graphs		382	1815	EBCT = 0.5 minutes	Li *et al*., 2013
							636	1910	EBCT = 0.7 minutes	
							764	1910	EBCT = 1.5 minutes	
							466	2037	Bed height = 5 cm	
							573	2165	Bed height = 10 cm	

Adsorbent	Adsorption conditions	Regeneration conditions	Water type and Composition	Cycle	Breakthrough (Bed volumes)				Other outcomes/ conditions	Reference
					0.1	0.5	1	Saturation		
	Flow rate = 10 mL min^{-1}						580	2000	Bed height = 20 cm	
Ferric loaded anion exchange IRA-900	EBCT = 2.2 minutes	2% NaOH-NaCl	Synthetic PO_4^{-3} (0.260 μg L^{-1}) SO_4^{2-} (120 mg L^{-1}) Cl^- (90 mg L^{-1}) HCO_3^- (100 mg L^{-1})	1	10200	N/A	N/A	16000	Doubling the sulphate concentration had no impact on performance.	Blaney *et al*., 2007
			Secondary effluent PO_4^{-3} (0.260 mg L^{-1}) SO_4^{2-} (120 mg L^{-1}) Cl^- (90 mg L^{-1}) HCO_3^- (100 mg L^{-1})	1	10400	N/A	N/A	17000	No impact on performance after	
				2	10400	N/A	N/A	16000		
LayneRT – commercially available iron oxide loaded anion exchange resin	EBCT = 4 minutes		Groundwater (dosed) PO_4^{-3} (4 mg L^{-1}) SO_4^{2-} (204 mg L^{-1})	1	0	420	580	830	Column diameter = 15 mm	Martin *et al*., 2013
					60	555	715	>1020	Column diameter = 25 mm	

Adsorbent	Adsorption conditions	Regeneration conditions	Water type and Composition	Cycle	Breakthrough (Bed volumes)				Other outcomes/ conditions	Reference
					0.1	0.5	1	Saturation		
			Cl^- (28 mg L^{-1}) NO_3^- (0.3 mg L^{-1})		320	425	490	>1020	Column diameter = 100 mm	
					650	740	760	>1020	Column diameter = 250 mm	
					675	690	720	>1020	Column diameter = 500 mm	

2.3 Conclusions

A review of metal oxide media for phosphorous removal from wastewater indicates the material has great potential providing high capacities and selectivity. Operational challenges associated with using metal oxide powdered is overcome through the use of hybrid media where the metal oxides are doped into the framework of the base material. A number of options exist such as chitosan, silicates, activated carbon and ion exchange resins. Phosphate form a strong bond with metal oxides such as ferric enabling it to outcompete with higher concentrations of sulphate and other constituents. Looking forward there are a number of areas that will enrich the current knowledge base and help accelerate the implementation of the media. Consequently, the key knowledge gaps that need addressing are;

- Much of the existing work on metal oxide medias is based on synthetic waters in a batch setup. Whilst such approaches provide critical insight, a shift towards real wastewaters and column experiments will greatly accelerate development toward implementation with emphasis on the role of empty bed contact time (Chapter 4) and the background water chemistry (Chapter 3) on media performance.
- The long-term impact of regeneration on the media's performance in a fixed bed system. This will also help establish the number of cycles before the media needs replacement. Understanding organic removal over multiple cycles also needs to be investigated if the media is to be utilized for organic polishing (outside the scope of this thesis).
- To establish the conditions under which the media will be economically attractive against other solutions at small (2,000 PE) and medium sewage treatment works (20,000 PE). The economics of the media in a fixed-bed system should be compared against a suspended system to determine the most economical set-up (Chapter 5).

2.4 Acknowledgements

The authors gratefully acknowledge financial support from the Engineering and

Physical Sciences Research Council (EPSRC) through their funding of the STREAM Industrial Doctorate Centre, and from the project sponsors Anglian Water, Severn Trent Water. Scottish Water, Thames Water, Yorkshire Water and Wessex Water for their financial and technical support throughout the project.

2.5 References

Acelas, N. Y., Martin, B. D., López, D. and Jefferson, B. (2015) 'Selective removal of phosphate from wastewater using hydrated metal oxides dispersed within anionic exchange media', *Chemosphere*, 119, pp. 1353–1360.

An, B., Jung, K.-Y., Zhao, D., Lee, S.-H. and Choi, J.-W. (2014) 'Preparation and characterization of polymeric ligand exchanger based on chitosan hydrogel for selective removal of phosphate', *Reactive and Functional Polymers*, 85, pp. 45–53.

Awual, M. R., El-Safty, S. a. and Jyo, A. (2011) 'Removal of trace arsenic(V) and phosphate from water by a highly selective ligand exchange adsorbent', *Journal of Environmental Sciences*, 23(12), pp. 1947–1954.

Bhuiyan, M. I. H., Mavinic, D. S. and Kochl, F. A. (2008) 'Phosphorus recovery from wastewater through struvite formation in fluidized bed reactors: A sustainable approach', *Water Science and Technology*, 57(2), pp. 175–181.

Blaney, L. M., Cinar, S. and SenGupta, A. K. (2007) 'Hybrid anion exchanger for trace phosphate removal from water and wastewater', *Water Research*, 41(7), pp. 1603–1613.

Brockett, J. (2016) *Putting the focus on phosphorus*. Available at: http://utilityweek.co.uk/news/putting-the-focus-on-phosphorus/1220872#.WKeJNbaLSV4 (Accessed: 17 February 2017).

Chen, J., Kong, H., Wu, D., Hu, Z., Wang, Z. and Wang, Y. (2006) 'Removal of phosphate from aqueous solution by zeolite synthesized from fly ash', *Journal of Colloid and Interface Science*, 300(2), pp. 491–497.

Chen, L., Zhao, X., Pan, B., Zhang, W., Hua, M., Lv, L. and Zhang, W. (2015) 'Preferable removal of phosphate from water using hydrous zirconium oxide-based nanocomposite of high stability', *Journal of Hazardous Materials*, 284, pp. 35–42.

Chen, S., Shi, Y., Wang, W., Li, Z., Gao, J., Bao, K., Han, R. and Zhang, R. (2014) 'Phosphorus removal from continuous phosphate-contaminated water by electrocoagulation using aluminum and iron plates alternately as electrodes', *Separation Science and Technology*, 49(6), pp. 939–945.

Cho, R. (2013) *Phosphorus: Essential to Life—Are We Running Out?*, *State of the Planet*. Available at: http://blogs.ei.columbia.edu/2013/04/01/phosphorus-essential-to-life-are-we-running-out/ (Accessed: 18 February 2017).

Cieślik, B. and Konieczka, P. (2016) 'A review of phosphorus recovery methods at various steps of wastewater treatment and sewage sludge management. The concept of "no solid waste generation" and analytical methods', *Journal of Cleaner Production*, 142, pp. 1–13.

Conidi, D. and Parker, W. J. (2015) 'The effect of solids residence time on phosphorus adsorption to hydrous ferric oxide floc', *Water Research*, 84, pp. 323–332.

Cooney, D. O. (1998) *Adsorption Design for Wastewater Treatment*. Taylor & Francis (Environmental engineering).

Cordell, D., Drangert, J. O. and White, S. (2009) 'The story of phosphorus: Global food security and food for thought', *Global Environmental Change*, 19(2), pp. 292–305.

Crittenden, J. C., M. W. H., Trussell, R. R., Hand, D. W. and Howe, K. J. (2012) *MWH's Water Treatment: Principles and Design*. Wiley.

D'Arcy, M., Weiss, D., Bluck, M. and Vilar, R. (2011) 'Adsorption kinetics, capacity and mechanism of arsenate and phosphate on a bifunctional TiO 2-Fe 2O 3 bi-composite', *Journal of Colloid and Interface Science*, 364(1), pp. 205–212.

Dabrowski, A. (2001) ‘Adsorption--from theory to practice.’, *Advances in colloid and interface science*, 93(1–3), pp. 135–224.

Dai, H., Lu, X., Peng, Y., Zou, H. and Shi, J. (2016) ‘An efficient approach for phosphorus recovery from wastewater using series-coupled air-agitated crystallization reactors’, *Chemosphere*, 165, pp. 211–220.

Dai, J., Yang, H., Yan, H., Shangguan, Y., Zheng, Q. and Cheng, R. (2011) ‘Phosphate adsorption from aqueous solutions by disused adsorbents: Chitosan hydrogel beads after the removal of copper(II)’, *Chemical Engineering Journal*, 166(3), pp. 970–977.

Delaney, P., McManamon, C., Hanrahan, J. P., Copley, M. P., Holmes, J. D. and Morris, M. A. (2011) ‘Development of chemically engineered porous metal oxides for phosphate removal’, *Journal of Hazardous Materials*, 185(1), pp. 382–391.

Huang, W., Wang, S., Zhu, Z., Li, L., Yao, X., Rudolph, V. and Haghseresht, F. (2008) ‘Phosphate removal from wastewater using red mud’, *Journal of Hazardous Materials*, 158(1), pp. 35–42.

Huang, W., Yu, X., Tang, J., Zhu, Y., Zhang, Y. and Li, D. (2015a) ‘Enhanced adsorption of phosphate by flower-like mesoporous silica spheres loaded with lanthanum’, *Microporous and Mesoporous Materials*, 217, pp. 225–232.

Huang, W., Yu, X., Tang, J., Zhu, Y., Zhang, Y. and Li, D. (2015b) ‘Enhanced adsorption of phosphate by flower-like mesoporous silica spheres loaded with lanthanum’, *Microporous and Mesoporous Materials*, 217, pp. 225–232.

Inglezakis, V. and Poulopoulos, S. (2006) *Adsorption, Ion Exchange and Catalysis: Design of Operations and Environmental Applications*. First. Amsterdam: Elsevier Science.

Irdemez, Ş., Demircioğlu, N., Yildiz, Y. S. and Bingül, Z. (2006) ‘The effects of current density and phosphate concentration on phosphate removal from wastewater by electrocoagulation using aluminum and iron plate electrodes’, *Separation and Purification Technology*, 52(2), pp. 218–223.

Irdemez, Ş., Yildiz, Y. S. and Tosunoğlu, V. (2006) 'Optimization of phosphate removal from wastewater by electrocoagulation with aluminum plate electrodes', *Separation and Purification Technology*, 52(2), pp. 394–401.

Jang, H. and Kang, S. H. (2002) 'Phosphorus removal using cow bone in hydroxyapatite crystallization', *Water Research*, 36(5), pp. 1324–1330.

Kamiyango, M. W., Masamba, W. R. L., Sajidu, S. M. I. and Fabiano, E. (2009) 'Phosphate removal from aqueous solutions using kaolinite obtained from Linthipe, Malawi', *Physics and Chemistry of the Earth, Parts A/B/C*, 34(13–16), pp. 850–856.

Kammerer, J., Carle, R. and Kammerer, D. R. (2011) 'Adsorption and ion exchange: Basic principles and their application in food processing', *Journal of Agricultural and Food Chemistry*, 59(1), pp. 22–42.

Kaneko, S. and Nakajima, K. (1988) 'Phosphorus Removal by Crystallization Using a Granular Activated Magnesia Clinker', *Journal (Water Pollution Control Federation)*. Water Environment Federation, 60(7), pp. 1239–1244.

Korchef, A., Saidou, H. and Amor, M. Ben (2011) 'Phosphate recovery through struvite precipitation by CO2 removal: Effect of magnesium, phosphate and ammonium concentrations', *Journal of Hazardous Materials*, 186(1), pp. 602–613.

Lenntech (2000) *Phosphorous removal from wastewater*. Available at: http://www.lenntech.com/phosphorous-removal.htm (Accessed: 19 February 2017).

Li, C., Ma, J., Shen, J. and Wang, P. (2009) 'Removal of phosphate from secondary effluent with Fe2+ enhanced by H2O2 at nature pH/neutral pH', *Journal of Hazardous Materials*, 166(2–3), pp. 891–896.

Li, G., Gao, S., Zhang, G. and Zhang, X. (2014) 'Enhanced adsorption of phosphate from aqueous solution by nanostructured iron(III)-copper(II) binary oxides', *Chemical Engineering Journal*. Elsevier B.V., 235, pp. 124–131.

Li, N., Ren, J., Zhao, L. and Wang, Z. (2013) 'Removal of Cr(VI) ions from wastewater using nanosized ferric oxyhydroxide loaded anion exchanger on a fixedbed column', *Desalination and Water Treatment*, 52(19–21), pp. 3572–3578.

Li, N., Ren, J., Zhao, L. and Wang, Z. L. (2013) 'Fixed bed adsorption study on phosphate removal using nanosized FeOOH-modified anion resin', *Journal of Nanomaterials*, 2013, pp. 1–6.

Li, Y., Liu, C., Luan, Z., Peng, X., Zhu, C., Chen, Z., Zhang, Z., Fan, J. and Jia, Z. (2006) 'Phosphate removal from aqueous solutions using raw and activated red mud and fly ash', *Journal of Hazardous Materials*, 137(1), pp. 374–383.

Liu, J., Wan, L., Zhang, L. and Zhou, Q. (2011) 'Effect of pH, ionic strength, and temperature on the phosphate adsorption onto lanthanum-doped activated carbon fiber', *Journal of Colloid and Interface Science*, 364(2), pp. 490–496.

Liu, Q., Hu, P., Wang, J., Zhang, L. and Huang, R. (2015) 'Phosphate adsorption from aqueous solutions by Zirconium (IV) loaded cross-linked chitosan particles', *Journal of the Taiwan Institute of Chemical Engineers*, pp. 1–9.

Liu, Q., Hu, P., Wang, J., Zhang, L. and Huang, R. (2016) 'Phosphate adsorption from aqueous solutions by Zirconium (IV) loaded cross-linked chitosan particles', *Journal of the Taiwan Institute of Chemical Engineers*, 59, pp. 311–319.

Liu, X. and Zhang, L. (2015) 'Removal of phosphate anions using the modified chitosan beads: Adsorption kinetic, isotherm and mechanism studies', *Powder Technology*, 277, pp. 112–119.

Lu, J., Liu, D., Hao, J., Zhang, G. and Lu, B. (2015a) 'Phosphate removal from aqueous solutions by a nano-structured Fe-Ti bimetal oxide sorbent', *Chemical Engineering Research and Design*. Institution of Chemical Engineers, 93(May), pp. 652–661.

Lǔ, J., Liu, H., Liu, R., Zhao, X., Sun, L. and Qu, J. (2013) 'Adsorptive removal of phosphate by a nanostructured Fe-Al-Mn trimetal oxide adsorbent', *Powder Technology*, 233, pp. 146–154.

Lu, J., Liu, H., Zhao, X., Jefferson, W., Cheng, F. and Qu, J. (2014) 'Phosphate removal from water using freshly formed Fe-Mn binary oxide: Adsorption behaviors and mechanisms', *Colloids and Surfaces A: Physicochemical and Engineering Aspects*, 455(1), pp. 11–18.

Lu, S. G., Bai, S. Q., Zhu, L. and Shan, H. D. (2009) 'Removal mechanism of phosphate from aqueous solution by fly ash', *Journal of Hazardous Materials*, 161(1), pp. 95–101.

Lwin, C. M., Murakami, M. and Hashimoto, S. (2017) 'The implications of allocation scenarios for global phosphorus flow from agriculture and wastewater', *Resources, Conservation and Recycling*, 122, pp. 94–105.

Martin, B. D. (2010) *Removal and Recovery of Phosphorus from Municipal Wastewaters using a Ferric Nanoparticle Adsorbent*. Cranfield University.

Martin, B. D., De Kock, L., Stephenson, T., Parsons, S. a. and Jefferson, B. (2013) 'The impact of contactor scale on a ferric nanoparticle adsorbent process for the removal of phosphorus from municipal wastewater', *Chemical Engineering Journal*, 215–216, pp. 209–215.

Menglin, Y., Danyang, Y., Jeng, S., Duanmei, S. and Zhengwen, X. (2016) 'Phosphorus removal and recovery from High Phosphorus wastewater by HAP crystallization Process', *Oriental Journal of Chemistry*, 21(1), pp. 235–241.

Morse, G. K., Brett, S. W., Guy, J. A. and Lester, J. N. (1998) 'Review: Phosphorus removal and recovery technologies', *Science of the Total Environment*, 212(1), pp. 69–81.

Namasivayam, C. and Prathap, K. (2005) 'Recycling Fe(III)/Cr(III) hydroxide, an industrial solid waste for the removal of phosphate from water.', *Journal of hazardous materials*, 123(1–3), pp. 127–34.

Nguyen, D. D., Ngo, H. H., Guo, W., Nguyen, T. T., Chang, S. W., Jang, A. and Yoon, Y. S. (2016) 'Can electrocoagulation process be an appropriate technology for phosphorus removal from municipal wastewater?', *Science of the Total Environment*, 563–564, pp. 549–556.

Nur, T., Johir, M. A. H., Loganathan, P., Nguyen, T., Vigneswaran, S. and Kandasamy, J. (2014) 'Phosphate removal from water using an iron oxide impregnated strong base anion exchange resin', *Journal of Industrial and Engineering Chemistry*. The Korean Society of Industrial and Engineering Chemistry, 20(4), pp. 1301–1307.

Ometto, F. Whitton, R., Coulon, F., Jefferson, B. and Villa, R. (2014) Improving the energy balance of an integrated microalagl wastewater treatment process. *Waste and Biomass Valorization*, **5**, 245-253

O'Neal, J. A. and Boyer, T. H. (2013) 'Phosphate recovery using hybrid anion exchange: Applications to source-separated urine and combined wastewater streams', *Water Research*, 47(14), pp. 5003–5017.

Pan, B., Han, F., Nie, G., Wu, B., He, K. and Lu, L. (2014) 'New Strategy To Enhance Phosphate Removal from Water by Hydrous Manganese Oxide'.

Pan, B., Wu, J., Pan, B., Lv, L., Zhang, W., Xiao, L., Wang, X., Tao, X. and Zheng, S. (2009) 'Development of polymer-based nanosized hydrated ferric oxides (HFOs) for enhanced phosphate removal from waste effluents', *Water Research*, 43(17), pp. 4421–4429.

Pidou, M., Parsons, S. A., Raymond, G., Jeffrey, P., Stephenson, T. and Jefferson, B. (2009) Fouling control of a membrane coupled photo catalytic process treating greywater. *Water Research*., 43, 3932-3939

Rajeswari, A., Amalraj, A. and Pius, A. (2015) 'Removal of phosphate using chitosan-polymer composites', *Journal of Environmental Chemical Engineering*, 3(4, Part A), pp. 2331–2341.

Rousseau, R. W. (1987) *Handbook of Separation Process Technology*. Wiley (A Wiley-Interscience publication).

Ruixia, L., Jinlong, G. and Hongxiao, T. (2002) 'Adsorption of fluoride, phosphate, and arsenate ions on a new type of ion exchange fiber.', *Journal of colloid and interface science*, 248(2), pp. 268–74.

Sendrowski, A. and Boyer, T. H. (2013) ‘Phosphate removal from urine using hybrid anion exchange resin’, *Desalination*, 322, pp. 1–9.

Shalaby, A., Nassef, E., Mubark, A. and Hussein, M. (2014) ‘Phosphate removal from wastewater by electrocoagulation using aluminium electrodes’, *American Journal of Environmental Engineering and Science*, 1(5), pp. 90–98.

Shi, Z. L., Liu, F. M. and Yao, S. H. (2011) ‘Adsorptive removal of phosphate from aqueous solutions using activated carbon loaded with Fe(III) oxide’, *Xinxing Tan Cailiao/New Carbon Materials*. Institute of Coal Chemistry, Chinese Academy of Sciences, 26(4), pp. 299–306.

Shin, E. W., Han, J. S., Jang, M., Min, S. H., Park, J. K. and Rowell, R. M. (2004) ‘Phosphate Adsorption on Aluminum-Impregnated Mesoporous Silicates: Surface Structure and Behavior of Adsorbents’, *Environmental Science and Technology*, 38(3), pp. 912–917.

Sousa, A. F. De, Braga, T. P., Gomes, E. C. C., Valentini, A. and Longhinotti, E. (2012) ‘Adsorption of phosphate using mesoporous spheres containing iron and aluminum oxide’, *Chemical Engineering Journal*, 210, pp. 143–149.

Sowmya, A. and Meenakshi, S. (2013) ‘An efficient and regenerable quaternary amine modified chitosan beads for the removal of nitrate and phosphate anions’, *Journal of Environmental Chemical Engineering*, 1(4), pp. 906–915.

Sowmya, A. and Meenakshi, S. (2014a) ‘A novel quaternized chitosan-melamine-glutaraldehyde resin for the removal of nitrate and phosphate anions’, *International Journal of Biological Macromolecules*, 64, pp. 224–232.

Sowmya, A. and Meenakshi, S. (2014b) ‘A novel quaternized resin with acrylonitrile/divinylbenzene/vinylbenzyl chloride skeleton for the removal of nitrate and phosphate’, *Chemical Engineering Journal*, 257, pp. 45–55.

Sowmya, A. and Meenakshi, S. (2014c) ‘A novel quaternized resin with acrylonitrile/divinylbenzene/vinylbenzyl chloride skeleton for the removal of nitrate and phosphate’, *Chemical Engineering Journal*, 257, pp. 45–55.

Su, Y., Cui, H., Li, Q., Gao, S. and Shang, J. K. (2013a) 'Strong adsorption of phosphate by amorphous zirconium oxide nanoparticles', *Water Research*, 47(14), pp. 5018–5026.

Su, Y., Cui, H., Li, Q., Gao, S. and Shang, J. K. (2013b) 'Strong adsorption of phosphate by amorphous zirconium oxide nanoparticles', *Water Research*, 47(14), pp. 5018–5026.

Tang, Y., Zong, E., Wan, H., Xu, Z., Zheng, S. and Zhu, D. (2012) 'Zirconia functionalized SBA-15 as effective adsorbent for phosphate removal', *Microporous and Mesoporous Materials*, 155, pp. 192–200.

Tchobanoglous, G., Burton, F. L., Stensel, H. D. and Eddy, M. & (2003) *Wastewater Engineering: Treatment and Reuse*. McGraw-Hill Education (McGraw-Hill higher education).

Thomas, W. J. and Crittenden, B. D. (1998) *Adsorption Technology and Design*. Butterworth-Heinemann.

Tran, N., Drogui, P., Blais, J. F. and Mercier, G. (2012) 'Phosphorus removal from spiked municipal wastewater using either electrochemical coagulation or chemical coagulation as tertiary treatment', *Separation and Purification Technology*, 95, pp. 16–25.

Wang, Z., Lin, Y., Wu, D. and Kong, H. (2016) 'Hydrous iron oxide modified diatomite as an active filtration medium for phosphate capture', *Chemosphere*, 144, pp. 1290–1298.

Whitton, R., Ometto, F., Pidou, M., Jarvis, P., Villa, R. and Jefferson, B. (2015) Microalgae for municipal wastewater nutrients remediation: mechanisms, reactors and outlook for tertiary treatment. *Environ Technol Reviews*, 4, 133-148.

Whitton, R., Le Mevel, A., Pidou, M., Ometto, F., Villa, R. and Jefferson, B. (2016) Influence of microalgal N and P composition on wastewater nutrient remediation. *Water Res.,* 91, 371-378.

Whitton, R. (2016) Algae reactors for wastewater treatment. EngD thesis Cranfield University.

Worch, E. (2012) *Adsorption Technology in Water Treatment: Fundamentals, Processes, and Modeling*. De Gruyter.

Xie, J., Lin, Y., Li, C., Wu, D. and Kong, H. (2014) 'Removal and recovery of phosphate from water by activated aluminum oxide and lanthanum oxide', *Powder Technology*, 269, pp. 351–357.

Xie, J., Wang, Z., Lu, S., Wu, D., Zhang, Z. and Kong, H. (2014) 'Removal and recovery of phosphate from water by lanthanum hydroxide materials', *Chemical Engineering Journal*, 254, pp. 163–170.

Xie, J., Wang, Z., Wu, D., Zhang, Z. and Kong, H. (2013) 'Synthesis of zeolite/aluminum oxide hydrate from coal fly ash: A new type of adsorbent for simultaneous removal of cationic and anionic pollutants', *Industrial and Engineering Chemistry Research*, 52(42), pp. 14890–14897.

Xu, X., Gao, B. Y., Tan, X., Yue, Q. Y., Zhong, Q. Q. and Li, Q. (2011) 'Characteristics of amine-crosslinked wheat straw and its adsorption mechanisms for phosphate and chromium (VI) removal from aqueous solution', *Carbohydrate Polymers*, 84(3), pp. 1054–1060.

Yang, S., Zhao, Y., Chen, R., Feng, C., Zhang, Z., Lei, Z. and Yang, Y. (2013) 'A novel tablet porous material developed as adsorbent for phosphate removal and recycling', *Journal of Colloid and Interface Science*, 396, pp. 197–204.

Ye, H., Chen, F., Sheng, Y., Sheng, G. and Fu, J. (2006) 'Adsorption of phosphate from aqueous solution onto modified palygorskites', *Separation and Purification Technology*, 50(3), pp. 283–290.

Yin, H. and Kong, M. (2014) 'Simultaneous removal of ammonium and phosphate from eutrophic waters using natural calcium-rich attapulgite-based versatile adsorbent', *Desalination*, 351, pp. 128–137.

Yu, Y. and Paul Chen, J. (2015) ‘Key factors for optimum performance in phosphate removal from contaminated water by a Fe–Mg–La tri-metal composite sorbent’, *Journal of Colloid and Interface Science*, 445, pp. 303–311.

Zeng, L., Li, X. and Liu, J. (2004) ‘Adsorptive removal of phosphate from aqueous solutions using iron oxide tailings’, *Water Research*, 38(5), pp. 1318–1326.

Zhang, G., Liu, H., Liu, R. and Qu, J. (2009) ‘Removal of phosphate from water by a Fe–Mn binary oxide adsorbent’, *Journal of Colloid and Interface Science*, 335(2), pp. 168–174.

Zhang, J., Shen, Z., Mei, Z., Li, S. and Wang, W. (2011) ‘Removal of phosphate by Fe-coordinated amino-functionalized 3D mesoporous silicates hybrid materials’, *Journal of Environmental Sciences*. The Research Centre for Eco-Environmental Sciences, Chinese Academy of Sciences, 23(2), pp. 199–205.

Zhang, J., Shen, Z., Shan, W., Chen, Z., Mei, Z., Lei, Y. and Wang, W. (2010) ‘Adsorption behavior of phosphate on Lanthanum(III) doped mesoporous silicates material’, *Journal of Environmental Sciences*. The Research Centre for Eco-Environmental Sciences, Chinese Academy of Sciences, 22(4), pp. 507–511.

Zhang, J., Shen, Z., Shan, W., Mei, Z. and Wang, W. (2011) ‘Adsorption behavior of phosphate on lanthanum(III)-coordinated diamino-functionalized 3D hybrid mesoporous silicates material’, *Journal of Hazardous Materials*, 186(1), pp. 76–83.

Zhang, L., Zhou, Q., Liu, J., Chang, N., Wan, L. and Chen, J. (2012) ‘Phosphate adsorption on lanthanum hydroxide-doped activated carbon fiber’, *Chemical Engineering Journal*, 185–186, pp. 160–167.

Zhang, Z., Wang, Y., Leslie, G. L. and Waite, T. D. (2015) ‘Effect of ferric and ferrous iron addition on phosphorus removal and fouling in submerged membrane bioreactors’, *Water Research*, 69, pp. 210–222.

Chapter 3. The impact of background wastewater constituent on the selectivity and capacity of a hybrid ion exchange resin for phosphorus removal from wastewater

Ahsan Muhammad, Ana Soares and Bruce Jefferson
Cranfield University, Bedfordshire, MK43 0AL, UK

Abstract

Conventional sorption media is inefficient for phosphorus removal due to preference for competing species such as sulphate, nitrate and organics. This work investigates the performance and selectivity of the hybrid anion exchange (HAIX) media over multiple regenerations and if the competing ions inhibit the uptake of phosphorus. Embedding ferric nanoparticles into the resin structure enhances selectivity. The current work aimed to explore how other constituents within wastewater impact performance. Two impacts were observed: (1) direct competition for adsorption sites and (2) retardation of the mass transfer of phosphate within the internal structure of the resin. The combination of nanoparticles and regeneration with sodium hydroxide effectively stabilised performance enabling the efficacy of the media to remain even in complex water matrices. Modelling confirmed the importance of both impacts the resin such that a combination of pseudo-second order and intra-particle diffusion models were shown to be relevant. The media capacity dropped from 8.5 mg g_{media}^{-1} in cycle 1 to 2.6 mg g_{media}^{-1} in cycle 3. The capacity became consistent in the following cycles ranking between 2.5 – 3.7 mg g_{media}^{-1}. Among the competing ions, sulphate had the highest removal; over 56 % in the first cycle. The removal dropped with each regeneration and was below 10 % in cycle 9. Sorption of nitrate ions was to show the most inhibition to the removal of phosphorus, followed by sulphate and then humic acid.

Keywords: Donnan membrane, nanoparticles, adsorption kinetics, regeneration.

3.1 Introduction

Sorption processes have been used for over 4000 years to purify water (Inglezakis and Poulopoulos, 2006). They work by providing favourable partitioning surfaces for pollutants to attach on to thereby removing them from water. A wide range of materials have been tried including activated carbon, clay minerals, biomaterials, metal nanoparticles and zeolites. The different materials provide difference in contact surface area, surface chemistry and porosity enabling different components to be targeted (Wang and Peng, 2010). A common challenge across all applications is related to selectivity whereby the removal of the target pollutant is reduced through competition for sites on the media from other constituents. This normally restricts applications to the back end of process treatment trains to remove micro-pollutants such as pesticides, hazardous chemicals and metals (Shon *et al*., 2006).

Transitional metal oxides such as Fe(III), Cu(III) and Zr(IV) have recently been shown to be able to provide selective adsorption of anionic pollutants such as arsenate and phosphate (Acelas *et al*., 2015b; Cumbal and Sengupta, 2005; Padungthon *et al*., 2015). These metal oxides, are highly selective for phosphate but mechanically weak and cause excessive pressure drops in fixed beds or flow through systems (Qingjian *et al*., 2008). By dispersing these metal oxide nanoparticles on to support materials like activated carbon, chitosan and anion exchangers, their mechanical strength along with capacity has been shown to enhance. One example gaining increasing attention is the use of hybrid ion exchange resins for the removal of phosphorus from wastewater. The resins are functionalised by having ferric nanoparticles embedded within their polymer matrix to provide selectivity and ease of regeneration. Previous research has shown that 90 % of the media's capacity for phosphorus removal comes from the ferric nanoparticles with the other 10 % coming from the ion exchange component (Martin *et al*., 2013b). Phosphate exists as strong bidentate ligands and can form inner sphere complexes with transition metals such as ferric iron (Xie *et al*., 2014). Competing ions such sulphate and nitrate are weak ligands and can only form outer sphere complexes. This result in sulphate and nitrate only competing with phosphate for the ion exchange sites while the metal oxide component remains

selective for phosphate. The selectivity of the metal oxide loaded resins allows them to have high phosphate removal percentage (>99%) which allows them to remove phosphate to sub 0.1 mg P L^{-1} levels (Martin, 2010). Regeneration of the nanoparticles is different from that of the background ion exchange resin whereby the media is soaked in high pH water to electrostatically release the adsorbed P (De Kock, 2015) whereas the exchanged ion onto the resin require brine regeneration as with common IEX processes. Consequently, use of the ferric nanoparticle component can be decoupled from the base resin by only regenerating with high pH waters (De Kock, 2015). As such the process becomes more akin to a mono component adsorption process enabling it to work effectively in water types where traditional ion exchange systems would not be able to be effective, such as with wastewater.

Previous work has shown that competition in wastewater is likely to come from sulphate, chloride and bicarbonate (Blaney *et al*., 2007; Martin, 2010; Martin *et al.*, 2017). For instance, a 50 mg SO_4 L^{-1} concentration added into a synthetic phosphate solution reduced the capacity of HAIX from 17.8 mg P g^{-1} to 5.6 mg P g^{-1} (Pan et al., 2009). However, the retardation of capacity does not continue as the sulphate concentration goes beyond 100 mg SO_4 L^{-1} (Zhao and Sengupta, 1998). It is thought the sulphate competes for both the anion exchange sites and the ferric nanoparticles although sulphate is known to only form outer sphere complexes with iron (Wijnja and Schulthess, 2000) as opposed to phosphate which can form inner sphere complexes (Acelas *et al*., 2015b). The result is that phosphate can continue to compete with sulphate even though it is normally at a much lower concentration. The resins are known to also remove organics with recent work suggesting a 50 % reduction in COD across the bed (0) with similar finding reported when the resin was used post an anaerobic membrane bioreactor. Potentially the organics can occupy both resin and nanoparticle, forming ligand exchange complexes with the latter (Korshin *et al*.,1997) which is why the resins are so good at organics removals. As with most sorption resin, mass transfer within the structure limits the overall rate of uptake. The material is drawn within the structure due to a Donnan membrane effect whereby the positive charge of the quaternary ammonium groups draws in the anions. Thus, the role

of the other constituents is twofold, direct completion of the sorption sites and retardation of mass transfer through coating the channels reducing the Donnan membrane impact. As the media can be selectively regenerated with respect to the nanoparticle component the impact of long term accumulation of other constituents requires consideration. Therefore, the aim of the current paper is to determine if the adsorption of competing ions can inhibit phosphorus adsorption. This will be assessed by pre-loading the media with sulphate, nitrate and humic acid and comparing it with non-loaded media. Multiple regeneration of the media will also be completed to determine if the performance is consistent or not.

3.2 Materials and Methods

3.2.1 Experimental set up

Secondary wastewater effluent was collected from the University's sewage works. The works treats a population equivalent of 6500-8000 with no existing technology used for P removal. The effluent concentration used throughout the trials varied between 1.76 and 4.8 mg P L^{-1}, 61-70 mg SO_4 L^{-1}, 32 – 46 mg NO_3 L^{-1} with a TOC of between 6.7 and 10.8 mg L^{-1}. Potassium nitrate, potassium phosphate, potassium sulphate, humic acid and sodium chloride were acquired from Sigma-Aldrich (Dorset, United Kingdom). Hydrochloric acid and sodium hydroxide were sourced from Fisher Scientific (Loughborough, United Kingdom).

The hybrid anion exchanger (HAIX) media was acquired from Layne Christensen Company (Texas, United States). The size of the media varied between 0.18 and 1.0 mm with a mean size of 0.69 mm. The media was regenerated in fixed bed columns with an internal diameter of 2.5 cm (obtained from Bio-Rad). A steel mesh was placed at the bottom of the column with a mesh size of 0.1 mm. The media was first backwashed for 30 minutes to remove any fine iron particle left over from manufacturing. 10 bed volumes of 4% sodium chloride were passed through the column at an empty bed contact time of 1 hour. The media was backwashed with deionised water for 1 hour at the end of the regeneration cycle. Iron (III) oxide nanoparticles (<30 nm average particle size) were purchased from Sigma-Aldrich (Dorset, United Kingdom).

To remove the ferric nanoparticle (NP) from HAIX, the media was agitated in an Erlenmeyer flask on an orbital shaker containing 1 gram of media and 20 mL of 2 M hydrochloric acid. The media went through a total of five 24-hour cycles where fresh acid was used for each cycle before being washed in deionised water. This media shall be referred to as ion exchange (IX) henceforth. Commercial iron nanoparticles were purchased as Iron (III) oxide nanoparticles (<30 nm average particle size) from Sigma-Aldrich (Dorset, United Kingdom).

3.2.2 Selectivity and long-term performance of the media

To assess HAIX's selectivity for phosphate, HAIX and IX were exhausted using wastewater effluent and a phosphorus (100 mg L^{-1}) only solution. Both HAIX and IX were regenerated using 4 % sodium hydroxide. 0.3 grams of HAIX and IX were weighed into Erlenmeyer flask and 1 litre of the relevant solution was added. The flasks were agitated on an orbital shaker at 200 rpm. 50 mL samples were taken at 1, 5, 10, 20, 30, 60, 120 minutes and 24 hours. The remaining solution in the flasks was decanted off and 4 % sodium hydroxide was introduced into the flasks. The flasks were agitated for 30 minutes at 200 rpm on an orbital shaker. The media was then rinsed with DI-water. The whole process was repeated nine times.

3.2.3 HAIX vs IX vs ferric nanoparticle

The experiment comparing HAIX, IX and the nanoparticle were carried out with media quantities so that the mass of ferric nanoparticle + ion exchanger was equal to the mass of HAIX. One litre of synthetic water (100 mg P L^{-1}) and wastewater effluent was added to the flasks and samples were taken at 1, 5, 10, 20, 30, 60, 120 minutes and 24 hours.

3.2.4 Preloading the media with competing ions

The experiments involved first pre-loading HAIX with humic acid (100 mg L^{-1}), sulphate (100 mg L^{-1}) and nitrate (100 mg L^{-1}). After equilibrium was reached, the solutions were removed, synthetic water (100 mg P L^{-1}) and wastewater effluent were separately added to the flasks. To understand the impact on adsorption

kinetics and capacity, samples were taken at 1, 5, 10, 20, 30, 60, 120 minutes and 24 hours.

3.2.5 Data Analysis

The media capacity for each species was calculated using Equation 2 (Deng and Shi, 2015):

$$q_e = \frac{(C_0 - C_e) * V}{m} \qquad \textbf{Equation 2}$$

Where q_e is media capacity (mg P g_{media}^{-1}), C_0 is Influent concentration (mg L^{-1}), C is effluent concentration (mg L^{-1}), and m is mass of media in column (g). The dynamic uptake was analysed according to five commonly used models (Table 3.1). The intra-particle diffusion model has been used to understand the mechanisms and rate controlling steps that control the kinetics of adsorption. If adsorption only follows the intra-particle diffusion mechanism, a plot of q versus $t^{1/2}$ will pass through the origin (Dizge *et al.*, 2008; Hameed *et al.*, 2008). In contrast, the external film diffusion model assumes that at time of initial contact, intra-particle diffusion is negligible, external diffusion resistance is principal and the concentration at the surface tends to be zero (Dizge *et al.*, 2008; Ponnusami *et al.*, 2010). Where A_s/V is expressed as (Equation 3), comparison of the two models enable the relative importance of film to intra-particle diffusion to be considered through calculation of the Biot number (Equation 4).

$$\frac{A_s}{\mathrm{V}} = \frac{3\mathrm{m}}{\rho \mathrm{d}} \qquad \textbf{Equation 3}$$

$$B_N = k_f \frac{d}{D} \qquad \textbf{Equation 4}$$

If the Biot number is greater than 100, internal diffusion is the rate limiting mechanism, but if the Biot number is less than 100, the adsorption process is controlled by film transfer (Girish and Murty, 2016).

Table 3.1 Summary of models used to analyse the dynamic data.

Model	Equation	Reference
Pseudo first order	$\ln(q_e - q_t) = lnq_e - k_1 t$	(Lǔ *et al.*, 2013)
Pseudo second order	$\frac{t}{q_t} = \frac{1}{k_2 q_e^2} + \frac{t}{q_e}$	(Vasiliu *et al.*, 2011)
Intra-particle diffusion	$q_t = k_{id} * t^{1/2} + C_i$	(Ponnusami, Rajan and Srivastava, 2010)
External film diffusion	$\ln\left(\frac{C_t}{C_e}\right) = -k_f \frac{A_s}{V} t$	(Ponnusami, Rajan and Srivastava, 2010)
Pore and surface diffusion	$-\log\left(1 - \left(\frac{q_t}{q_e}\right)^2\right) = \left(\frac{4\pi^2 D}{2.3\, d^2}\right) t$	(Dizge *et al.*, 2008)

Where As is the total interfacial area of the particles (cm^2), d is the mean particle diameter (μm), D is the pore and surface mass diffusion coefficient ($cm^2\ s^{-1}$), k_1 is the equilibrium rate constant of pseudo-first-order model ($1\ min^{-1}$), k_2 is the equilibrium rate constant of pseudo-second-order model ($g\ mg^{-1}\ min$), k_i is the intra-particle diffusion coefficient ($mg\ g^{-1}\ min^{0.5}$), k_f is the initial external mass coefficient ($mg\ s^{-1}$), ρ is the density of the adsorbent ($g\ cm^{-3}$), $q_{e,cal}$ is the calculated adsorbed capacity at equilibrium ($mg\ g_{media}^{-1}$), $q_{e,exp}$ is the experimental adsorbed capacity at equilibrium ($mg\ g_{media}^{-1}$), q_t is the adsorbed capacity at time t ($mg\ g_{media}^{-1}$), t is time (minutes) and V is volume of solution (L).

3.2.6 Analytical Methods

Determination of phosphate, sulphate and nitrate was conducted using Spectroquant cell tests supplied by VWR International (Leicestershire, United Kingdom). The methods are analogous to EPA 365.2+3, EPA 375.4 and EPA 352.1 respectively. Humic acid analysis was completed using a Shimadzu TOC-5000A (Milton Keynes, UK).

3.3 Results and Discussion

3.3.1 Impact of inhibition due to competing ions

The capacity of the HAIX media for phosphorus in a mono component system decreased from 114 mg P g media^{-1} with fresh resin to 112, 101 and 73 mg P g_{media}^{-1} when the media was preloaded with humic acid, sulphate and nitrate respectively (Figure 3.1). This represented a loss of 1.5 %, 11.9 % and 36.1 % which compares to capacity reductions of 8.6 %, 4.6 %, and 27.9 % during the equivalent experiment with secondary wastewater (Figure 3.1). In this case, the capacity was substantially reduced compared to the synthetic case at 9.7, 8.9, 9.3 and 7.0 mg P g_{media}^{-1} for the fresh and humic acid, sulphate and nitrate pre-loaded resins respectively. The overall capacity is expected to be lower due to the lower initial P concentrations: 100 mg P L^{-1} in the synthetic compared to 1.76-4.8 mg P L^{-1} in the secondary wastewater. The difference in change between the synthetic and the real wastewater reflect the combination of pre-loading and simultaneous competition which occurs in the real wastewater compared to just preloading which occurs with the synthetic. In both cases the impact of nitrate preloading was observed to have the most significant impact in contrast to previous studies where sulphate had been reported to generate the greatest impact on capacity (Martin, 2010; Martin *et al.*, 2017). Interestingly, humic acid had no significant impact on capacity yet has been attributed to resin blinding in drinking water applications (Mergen *et al.*, 2008).

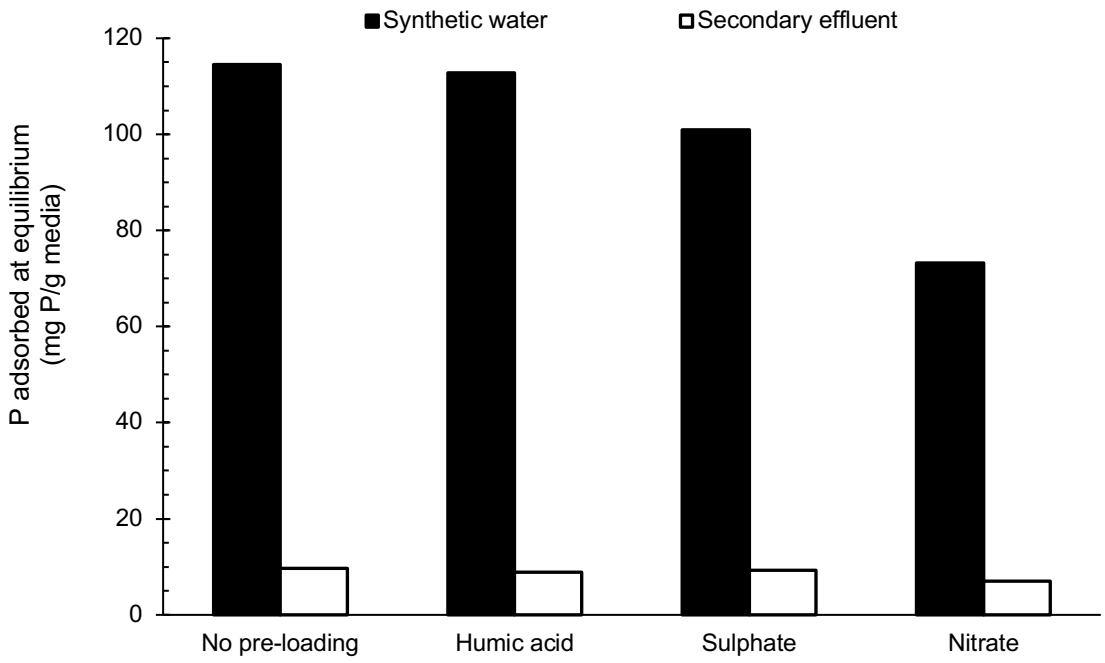

Figure 3.1 Impact of preloading humic acid, sulphate and nitrate against no pre-loading on the media capacity of HAIX at equilibrium.

In contrast to the capacity data, the uptake kinetics of the preloaded resins all had a similar impact. To illustrate, removal levels within the first 5 minutes of the cycle were 33.5 % for the fresh resin and 23.6 %, 27.5 % and 24.3 % when the media was pre-loaded with humic acid, nitrate and sulphate respectively (Figure 3.2A). However, in the case of real wastewater, no significant difference could be observed between the resin that had undergone no pre-loading compared to all three preloaded sets of resin (Figure 3.2B). However, the initial uptake was slightly higher for the preloaded cases with removals levels after 10 minutes of 49, 51 and 54 % of the phosphate for resins preloaded with humic acid, sulphate and nitrate respectively. In comparison, the non pre-loaded resin removed 39 % of the available phosphate after 10 minutes. This continued until the end of the experiment with final removal levels after 250 minutes of 78%, 85 %, 91 % and 93 % for the sulphate pre-loaded, fresh, nitrate preloaded and humic acid preloaded resins respectively.

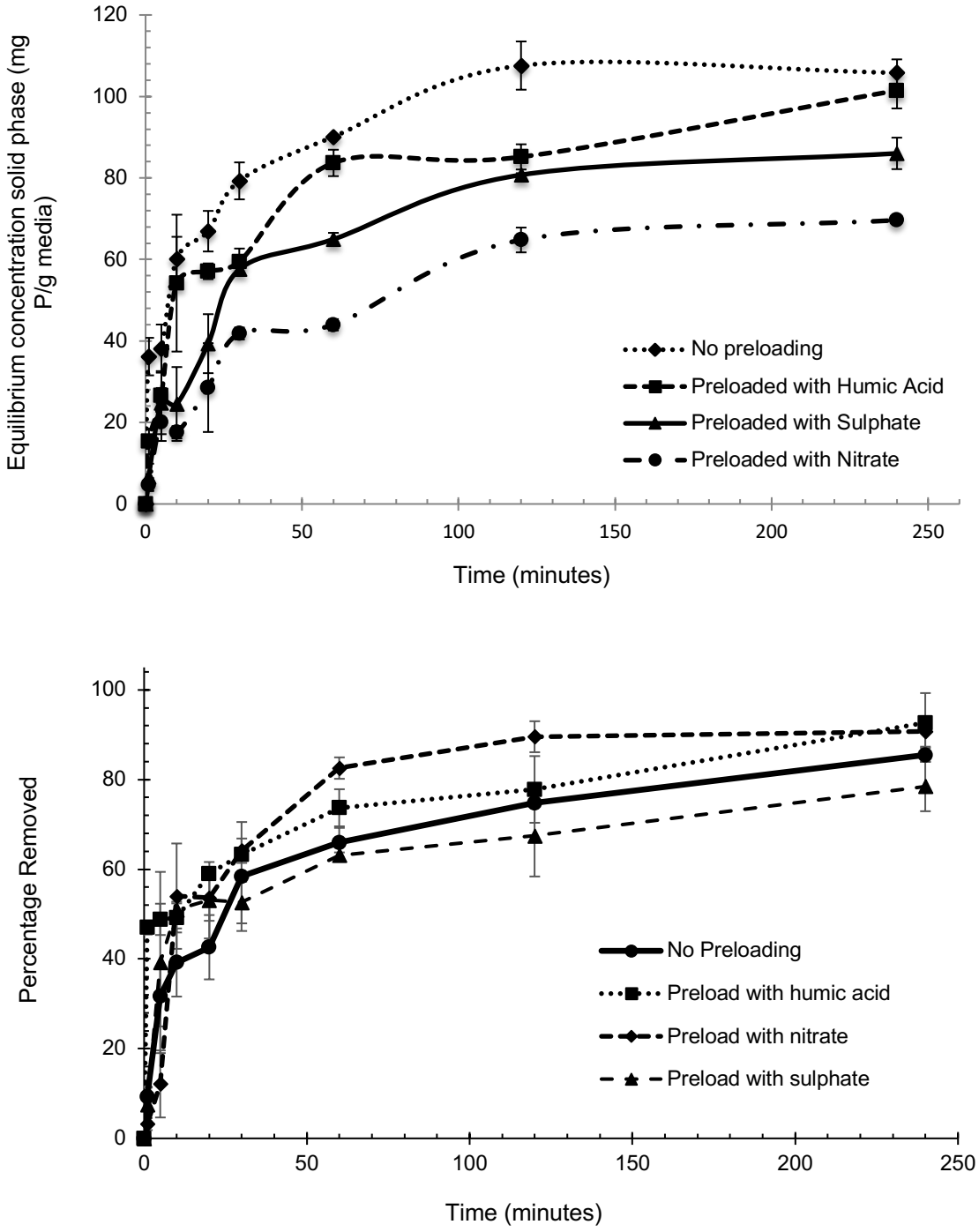

Figure 3.2 Impact of preloading on (A) the rate of uptake of phosphorus using synthetic water and (B) removal efficiency of HAIX media with secondary effluent

3.3.2 Assessing performance of HAIX over multiple batch cycles

The removal of phosphorus increased after the first run from a value of 61 % to 73 % and then remained stable for the successive runs until the ninth cycle when

the removal level decreased to 63 % (Figure 3.3). In comparison, the removal of sulphate was similar to phosphate in the first cycle at 56 % but then decreased progressively through the cycles stabilising between 4-9% between cycles 7 and 9. Nitrate followed a similar trend but with much lower removals starting at 13 % and reduced to between 2-3 %. In contrast, humic acid removal was less consistent but remained within a range of 8-25 % across the cycles. Analysis of the phosphorus levels recovered from the media revealed the greatest quantity during the first regeneration cycle at 0.965 mg. This equates to 90 % of the phosphorous sorbed during the batch removal cycle. Phosphorus recovered in the rest of the cycles ranged between 0.58 – 0.75 mg with a gradual decrease across the cycles equating to a reduction of 40 % between cycle 1 and cycle 9. However, the majority of that reduction occurred across the first three cycles which accounted 70 % of the overall 23 % reduction. This shows that even though the ferric nanoparticle will selectively remove phosphorus, there will be inhibition to phosphorus uptake by the media. This can be attributed to the ion exchange mechanism of the media not being regenerated resulting in an accumulation of charged components reducing the overall positive charge of the resin structure. This will impact on the influence of the Donnan membrane effect in drawing in phosphate into the inner structure of the resin. In addition, the accumulated negative charges will exert a repulsive impact on the phosphate ions (Liu and Zhang, 2015). Previous work on multiple cycle impacts have focussed on using synthetic mono component fluids with media such as activated aluminium oxide, Fe-Mg-La sorbent and Zr(IV)-chitosan. In such cases reductions in media capacity have ranged from 2 % to 20 % (Yu & Chen 2015; Xie *et al*. 2014; Liu & Zhang 2015).

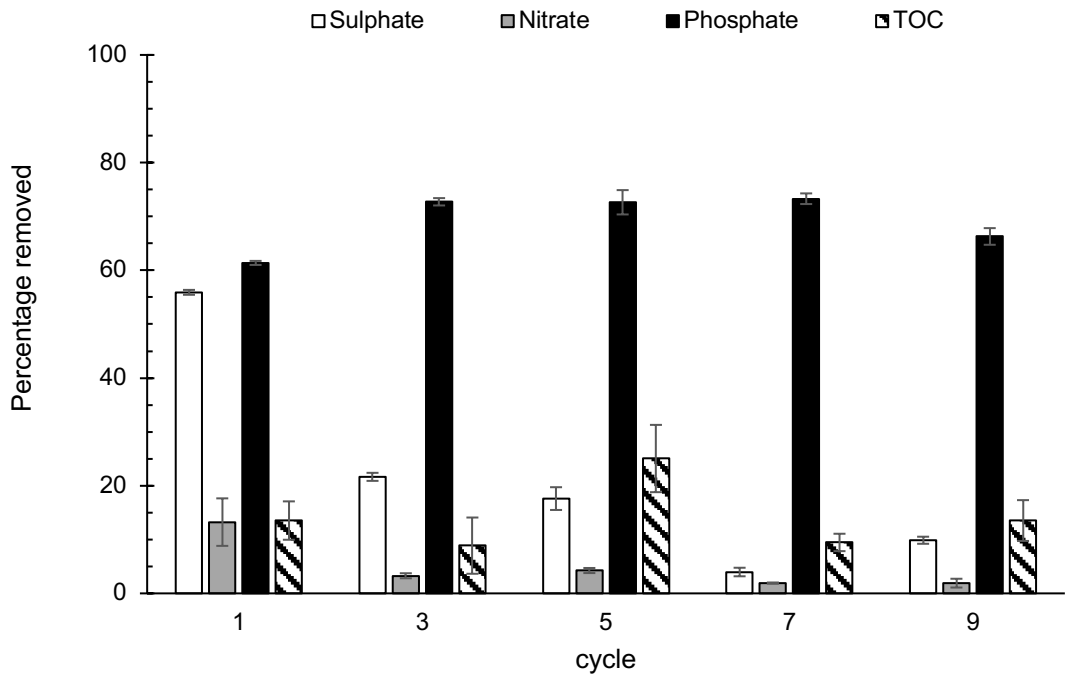

Figure 3.3 Percentage phosphorus, sulphate, nitrate and TOC removed over cycle 1 – 9, at equilibrium using HAIX media and secondary wastewater effluent.

The rate of removal and measured capacity for run 1 was substantially different from all other cycles demonstrating that data using fresh resin should always be used carefully. Both the kinetics and the eventual capacity at 240 minutes were similar for all subsequent runs and did not show signs of gradual deterioration (Figure 3.4). Final capacities varied between 2.5 and 3.7 mg P g_{media}^{-1}. To illustrate the differential performance of the run with the fresh resin to removal after 10 minutes was 40 % with fresh resins compared to 16 %, 14 % and 12 % during run 3, 5 and 7 respectively. The relative consistency of the removal and kinetics of the multiple cycles post the first one reflects a stabilisation of the system. This is seen not just in phosphate removal but in terms of sulphate, nitrate and humic acid. Ultimately it shows the benefit of regenerating with only sodium hydroxide as opposed to a combination with sodium chloride. The latter combination would regenerate both nanoparticle and resin and enable greater impact of the other constituent over the long term. Additionally, it would contaminate the regeneration fluid making phosphorus recovery more difficult (De Kock, 2015).

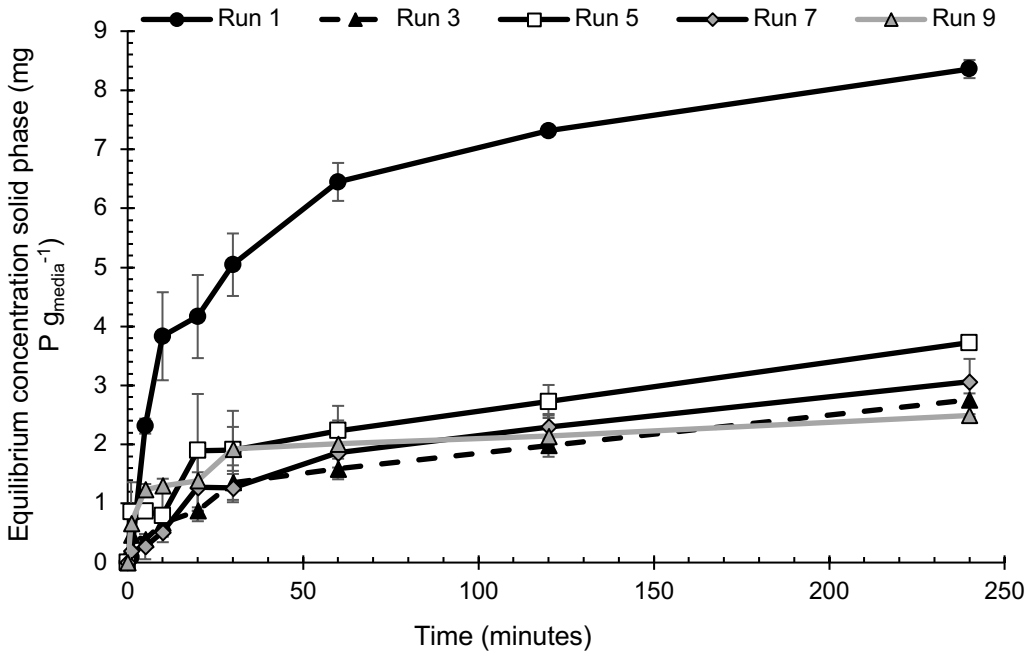

Figure 3.4 Impact of regeneration over 9 runs, on the rate of uptake of phosphorus during the first 4 hours using HAIX media and synthetic water.

3.3.3 Hybrid anion exchanger (HAIX) vs Ion exchanger (IX) vs Nano-particle (NP)

Comparison between the hybrid resin, the resin with the nanoparticles removed and commercial nanoparticles revealed similar removal for the HAIX and IX in the case of the synthetic water (Figure 3.5). For instance, at the end of the 240-minute batch experiment the HAIX resin had removed 34 mg of phosphate representing a removal effectiveness of 61.8 %. In comparison, the IX and the nanoparticles removed 28.9 mg and 22.2 mg respectively. This represented a reduction in removal compared to the HAIX media of 10 and 21 % respectively. In all cases the rate of uptake was rapid during the first 60 minutes and then slowed. The relative proportion of the total uptake that occurred within the first 60 minutes was relatively similar with 74 %, 77 % and 65 % of the total uptake occurring for the HAIX, IX and nanoparticle systems. The reduced performance of the nanoparticle system is congruent with known issues surrounding aggregation of such particles, thereby reducing the available surface area for adsorption (Pidou *et al*., 2009). In part, this is why the nanoparticles are embedded in the resin so that they can remain discrete and maximise their

contact area for uptake as it achieved on a variety of supports including resins, fibres, activated carbon and chitosan (Padungthon *et al*., 2015). In addition, specific advantage is ascribed to the ion exchange resins as they provide an enhancement of transport towards the nanoparticles through the Donnan membrane effect which is exerted by the fixed positive charges of anion exchanger (Blaney, Cinar and SenGupta, 2007).

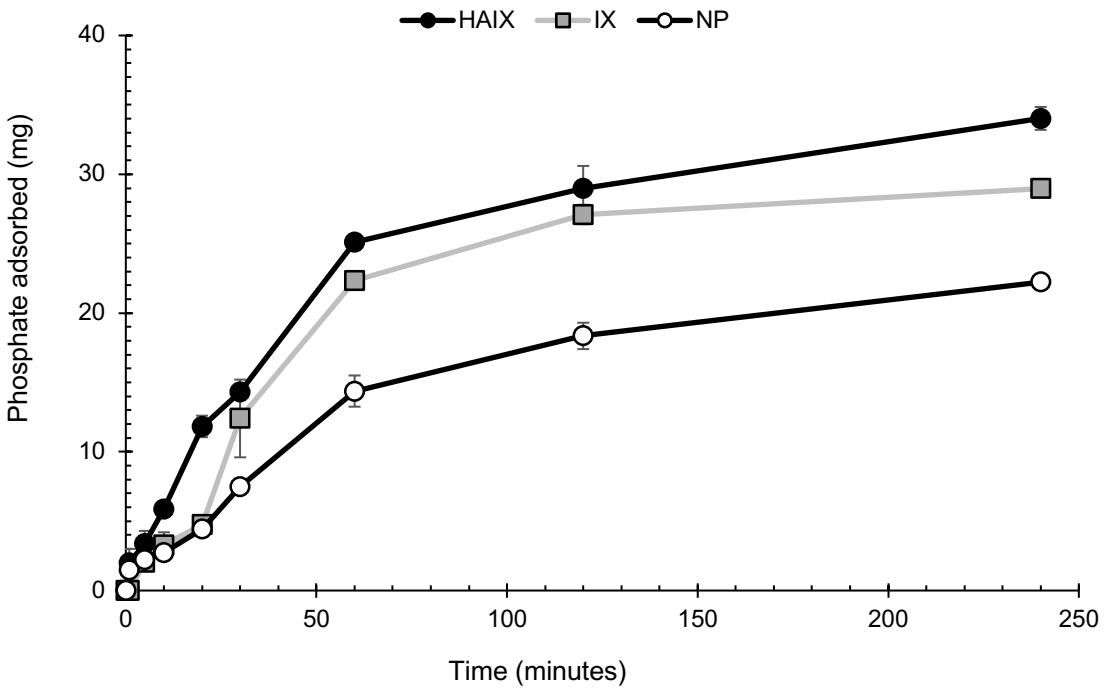

Figure 3.5 Phosphorus adsorbed in the first 4 hours from synthetic water by i) hybrid anion exchange (HAIX), ii) ion exchange (IX) and ferric nanoparticles.

In the case of the secondary effluent trials, a different set of responses were observed whereby the nanoparticles performed similarly to the HAIX resin. This is congruent with previous findings that have suggested only around 10 % of the total removal occurs through the base resin and this only occurs in the initial cycles (Martin *et al*., 2017). To illustrate, at the end of the cycle the HAIX resin had removed 2.5 mg P compared to 2.4 mg P by the nanoparticles (Figure 3.6). Further no significant difference could be observed in relation to the dynamics of uptake in contrast to the IX resin. In that case both the dynamics and the ultimate removal were lower; consistent with inhibition from competing species. Additionally, the IX resin showed variation through batch experiment where

phosphorus appeared to desorb. For instance, the amount of phosphate removed decreased from minute 1 at 1.02 mg to 0.86 mg at minute 5 before increasing again to 1.4 mg after 20 minutes and then decreasing again to 1.15 mg after 60 minutes. This is indicative of competitive displacement with adsorbed phosphate being displaced due to the weak bound that it forms with the resin. In contrast, the HAIX resin showed consistent removal reflecting the inner sphere complexes the phosphate forms with the ferric nanoparticles which cannot be displaced by the other constituents in the water (An *et al*., 2014; You *et al*., 2016).

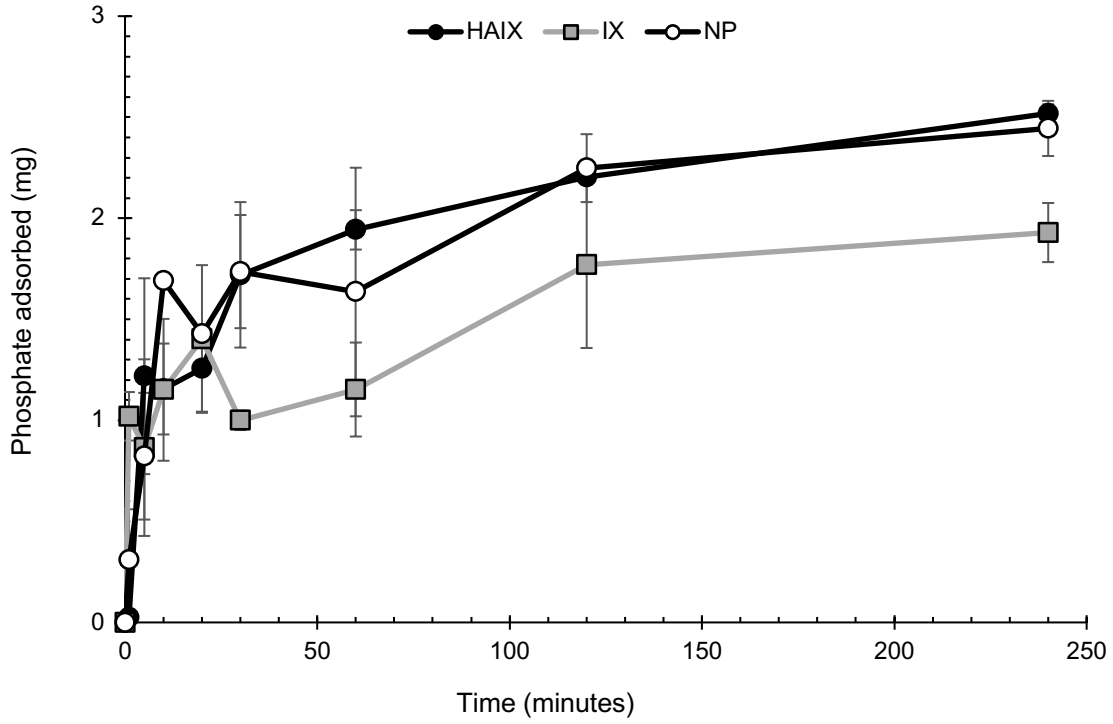

Figure 3.6 Phosphorus adsorbed in the first 4 hours from secondary effluent by i) hybrid anion exchange (HAIX), ii) ion exchange (IX) and ferric nanoparticles.

3.3.4 Adsorption Kinetics

Analysis of the dynamic batch data through established models revealed that the systems was most appropriately described by the pseudo-second-order model for both the synthetic and real wastewater trials across fresh and pre-loaded resins (Table 3.1 and Table 3.2). This was most apparent in the case of sulphate pre-loading and the runs with secondary wastewater indicating that the pseudo-second-order model is the most appropriate modelling form to conduct further

research with. This infers that chemisorption is the rate limiting step instead of mass transfer (Acelas *et al*., 2015b) which is consistent with similar analysis conducted for PVA hydrogel beads, iron(II)-copper(II) oxides and lanthanum doped activated carbon (Hui, Zhang and Ye, 2014; Li *et al*., 2014; Liu *et al*., 2011). The pore and surface diffusion model better described the data compared to the external mass transfer model. This is further indicated by the fact that the plot for intra-particle diffusion model did not go through the origin suggesting that both, intra-particle diffusion and film diffusion influence the rate of adsorption (Khan *et al*., 2015). The data plots present multiple stages and hence the rate constant was calculated for each of the stage; k_{1d} for the first region and k_{2d} for the second region. The first region is the external adsorption stage, which is primarily driven by initial phosphorus concentration with the second region representing gradual adsorption in which the adsorption is controlled by the intraparticle diffusion. As the resin adsorbs more phosphorus, the concentration in the solution decreases and the resistance to phosphorus uptake increases. This results in the rate constant for stage 1 being greater than stage 2 (Acelas *et al*., 2015a). The resultant Biot numbers are between 422 and 2733 beyond the threshold to suggest film diffusion controls but not at the levels typically seen for activated carbon systems (Sulak and Demirbas, 2007). Typical biot number for adsorption on to activated carbon have been found to be less than 100 (Cho *et al*., 2006; Kim *et al*., 2006; Sulaymon, Abid and Al-Najar, 2009) indicating the HAIX media is even more strongly influenced by intraparticle diffusion than is common with activated carbon.

In the case of the multiple cycle experiments, the Biot number increased from 2672 in the first run to between 5345 and 7423 thereafter. The greater Biot number observed was consistent with a better alignment to the intra-particle diffusion model which provides a similar level fit to that of the pseudo-second-order model. The increased fit to the intra-particle diffusion model reflects the impact of progressive loading onto the base resin structure, reducing the impacts of the Donnan membrane effect and so slowing down the diffusion through the internal structure. However, ultimately uptake is onto the nanoparticles through inner sphere complexes which aligns to the pseudo-second-order model.

Table 3.2 Kinetic study for the adsorption of phosphate by hybrid anion exchanger in synthetic water and secondary wastewater effluent.

	Water type	$q_{e,exp}$	Pseudo 1st order			Pseudo 2nd order			External mass transfer		Pore and surface Diffusion		Biot number
			k_1	$q_{e,cal}$	R^2	k_2	$q_{e,cal}$	R^2	k_f	R^2	D_e	R^2	
No preloading	Synthetic	114.59	0.0106	63.47	0.7591	0.0842	114.94	0.9999	0.0799	0.9057	2.025E-06	0.9898	2723.2
Humic acid		112.82	0.0055	81.42	0.7576	0.0469	113.64	0.9995	0.0266	0.7526	1.526E-06	0.9547	1204.8
Nitrate		73.19	0.0126	58.83	0.9996	0.0413	74.63	0.9996	0.0205	0.4584	1.464E-06	0.9898	966.5
Sulphate		100.92	0.0079	74.93	0.9548	0.0426	103.09	0.9995	0.0321	0.9278	1.026E-06	0.9799	2160.9
No preloading	Secondary Effluent	9.72	0.0072	6.69	0.8477	0.0398	9.86	0.9993	0.0214	0.7693	8.321E-07	0.9266	1772.0
Humic acid		8.89	0.0064	4.31	0.9554	0.0591	8.97	0.9994	0.0213	0.6284	1.304E-06	0.8897	1127.9
Nitrate		7.00	0.0100	4.37	0.7461	0.0471	7.11	0.9996	0.0104	0.1110	1.692E-06	0.9515	422.2
Sulphate		9.28	0.0051	6.02	0.7148	0.0336	9.41	0.9976	0.0053	0.7393	4.161E-07	0.8499	879.0

Intra-particle diffusion model

	Water type	k_{1d}	C_1	R_1^2	k_{2d}	C_2	R_2^2
No preloading	Synthetic	14.006	9.834	0.8818	5.1847	50.540	0.9987
Humic acid		13.619	1.046	0.9386	3.6781	45.983	0.8526
Nitrate		6.363	0.363	0.9220	3.077	24.537	0.8859
Sulphate		8.769	0.005	0.9572	2.9444	43.131	0.9246
No preloading	Secondary Effluent	1.005	0.207	0.9242	0.2603	4.338	0.9947
Humic acid		1.179	0.584	0.8812	0.2124	4.633	0.9611
Nitrate		0.899	0.489	0.9560	0.0348	5.725	0.8915
Sulphate		1.596	0.311	0.9690	0.2196	3.864	0.9647

Table 3.3 Kinetic study for the impact on regeneration on the performance of HAIX for phosphorus removal.

	$q_{e,exp}$	Pseudo 1st order			Pseudo 2nd order			External mass transfer		Pore and surface Diffusion		Biot number
		k_1	$q_{e,cal}$	R^2	k_2	$q_{e,cal}$	R^2	k_f	R^2	D_e	R^2	
Run 1	9.778	0.0076	7.194	0.8749	0.0236	10.060	0.9955	0.0322	0.8299	8.321E-07	0.9561	2672.6
Run 3	4.248	0.0038	3.622	0.9602	0.0123	4.439	0.9905	0.0269	0.9808	3.051E-07	0.9478	6074.1
Run 5	5.762	0.0038	4.821	0.9007	0.0138	5.977	0.9894	0.0269	0.9655	2.496E-07	0.9063	7423.8
Run 7	4.487	0.0044	3.897	0.9116	0.0122	4.708	0.9951	0.0322	0.9676	3.051E-07	0.9679	7288.9
Run 9	4.268	0.0024	2.973	0.7577	0.0169	4.369	0.9848	0.0215	0.8614	2.774E-07	0.8596	5345.2

Intra-particle diffusion model

	k_{1d}	C_1	R_1^2	k_{2d}	C_2	R_2^2
Run 1	1.0843	-0.2788	0.9205	0.3143	3.6739	0.9475
Run 3	0.1745	0.101	0.8677	0.1409	0.5232	0.9880
Run 5	0.3898	-0.0724	0.8923	0.1819	0.8439	0.9892
Run 7	0.2601	-0.1141	0.8546	0.1737	0.3985	0.9874
Run 9	0.3052	0.2544	0.8366	0.0565	1.5808	0.9679

3.4 Conclusions

Constituents present within the water impact the performance of HAIX resin in relation to competition for sorption sites and loading of the background resin reducing the rate of intraparticle mass transfer through a reduction in the Donnan membrane effect. Operation over multiple cycle reveals a consistency of performance after an initial drop across the first cycle. Comparison of the individual components of the HAIX resin confirmed the importance of the nanoparticles and the use of selective regeneration with sodium hydroxide. This enables the systems to stabilise and operate effectively within complex competing water matrices. Modelling of the systems is best accomplished through a combination of the intra-particle diffusion model and the pseudo-second-order model to reflect the combined impact of the base resin and the embedded nanoparticles.

3.5 Acknowledgements

The authors gratefully acknowledge financial support from the Engineering and Physical Sciences Research Council (EPSRC) through their funding of the STREAM Industrial Doctorate Centre, and from the project sponsors Anglian Water, Severn Trent Water. Scottish Water, Thames Water, Yorkshire Water and Wessex Water for their financial and technical support throughout the project.

3.6 References

Acelas, N. Y., Martin, B. D., López, D. and Jefferson, B. (2015) 'Selective removal of phosphate from wastewater using hydrated metal oxides dispersed within anionic exchange media', *Chemosphere*, 119, pp. 1353–1360.

An, B., Jung, K.-Y., Zhao, D., Lee, S.-H. and Choi, J.-W. (2014) 'Preparation and characterization of polymeric ligand exchanger based on chitosan hydrogel for selective removal of phosphate', *Reactive and Functional Polymers*, 85, pp. 45–53.

Blaney, L. M., Cinar, S. and SenGupta, A. K. (2007) ‘Hybrid anion exchanger for trace phosphate removal from water and wastewater’, *Water Research*, 41(7), pp. 1603–1613.

Cho, S. Y., Park, S. S., Kim, S. J. and Kim, T. Y. (2006) ‘Adsorption and desorption characteristics of 2-methyl-4-chlorophenoxyacetic acid onto activated carbon’, *Korean Journal of Chemical Engineering*, 23(4), pp. 638–644.

Cumbal, L. and Sengupta, A. K. (2005) ‘Arsenic removal using polymer-supported hydrated iron(III) oxide nanoparticles: Role of Donnan membrane effect’, *Environmental Science and Technology*, 39(17), pp. 6508–6515.

De Kock, L.-A. (2015) *Hybrid ion exchanger supported metal hydroxides for the removal of phosphate from wastewater*' (PhD thesis), University of Johannesburg.

Deng, L. and Shi, Z. (2015) ‘Synthesis and characterization of a novel Mg–Al hydrotalcite-loaded kaolin clay and its adsorption properties for phosphate in aqueous solution’, *Journal of Alloys and Compounds*, 637, pp. 188–196.

Dizge, N., Aydiner, C., Demirbas, E., Kobya, M. and Kara, S. (2008) ‘Adsorption of reactive dyes from aqueous solutions by fly ash : Kinetic and equilibrium studies’, *Journal of Hazardous Materials,* 150, pp. 737–746.

Dizge, N., Demirbas, E. and Kobya, M. (2009) ‘Removal of thiocyanate from aqueous solutions by ion exchange’, *Journal of Hazardous Materials,* 166, pp. 1367–1376.

Girish, C. R. and Murty, V. R. (2016) ‘Mass Transfer Studies on Adsorption of Phenol from Wastewater Using Lantana camara, Forest Waste', *International Journal of Chemical Engineering, volume 2016*.

Hameed, B. H., Mahmoud, D. K. and Ahmad, A. L. (2008) ‘Equilibrium modeling and kinetic studies on the adsorption of basic dye by a low-cost adsorbent : Coconut (Cocos nucifera) bunch waste’, *Journal of Hazardous Materials*, 158, pp. 65–72.

Hui, B., Zhang, Y. and Ye, L. (2014) ‘Preparation of PVA hydrogel beads and adsorption mechanism for advanced phosphate removal’, *Chemical Engineering Journal*, 235, pp. 207–214.

Inglezakis, V. and Poulopoulos, S. (2006) *Adsorption, Ion Exchange and Catalysis: Design of Operations and Environmental Applications*. First Edition. Amsterdam: Elsevier Science.

Kim, T.-Y., CHO, S.-Y., KIM, S.-J., OH, Y.-S. and SUH, S.-H. (2006) ‘ADSORPTION AND DESORPTION CHARACTERISTICS OF CLORINATED PHENOXYACETIC ACIDS ONTO THE ACTIVATED CARBON’, *Revue Roumaine de Chimie*, 51(11), pp. 1109–1120.

Khan, T. A., Chaudhry, S. A. and Ali, I. (2015) ‘Equilibrium uptake, isotherm and kinetic studies of Cd(II) adsorption onto iron oxide activated red mud from aqueous solution’, *Journal of Molecular Liquids*, 202, pp. 165–175.

Korshin, G. V., Benjamin, M. M. and Sletten, R. S. (1997) ‘Adsorption of natural organic matter (NOM) on iron oxide: Effects on NOM composition and formation of organo-halide compounds during chlorination’, *Water Research*, 31(7), pp. 1643–1650.

Li, G., Gao, S., Zhang, G. and Zhang, X. (2014) ‘Enhanced adsorption of phosphate from aqueous solution by nanostructured iron(III)–copper(II) binary oxides’, *Chemical Engineering Journal*, 235, pp. 124–131.

Liu, J., Wan, L., Zhang, L. and Zhou, Q. (2011) ‘Effect of pH, ionic strength, and temperature on the phosphate adsorption onto lanthanum-doped activated carbon fiber’, *Journal of Colloid and Interface Science*, 364(2), pp. 490–496.

Liu, X. and Zhang, L. (2015) ‘Removal of phosphate anions using the modified chitosan beads: Adsorption kinetic, isotherm and mechanism studies’, *Powder Technology*, 277, pp. 112–119.

Lǔ, J., Liu, H., Liu, R., Zhao, X., Sun, L. and Qu, J. (2013) ‘Adsorptive removal of phosphate by a nanostructured Fe-Al-Mn trimetal oxide adsorbent’, *Powder Technology*, 233, pp. 146–154.

Martin, B. D. (2010) '*Removal and Recovery of Phosphorus from Municipal Wastewaters using a Ferric Nanoparticle Adsorbent*' (PhD thesis), Cranfield University.

Martin, B. D., De Kock, L., Gallot, M., Guery, E., Stanowski, S., MacAdam, J., McAdam, E. J., Parsons, S. A. and Jefferson, B. (2017) 'Quantifying the performance of a hybrid anion exchanger/adsorbent for phosphorus removal using mass spectrometry coupled with batch kinetic trials', *Environmental Technology*. In Press.

Martin, B. D., De Kock, L., Stephenson, T., Parsons, S. a. and Jefferson, B. (2013) 'The impact of contactor scale on a ferric nanoparticle adsorbent process for the removal of phosphorus from municipal wastewater', *Chemical Engineering Journal*, 215–216, pp. 209–215.

Mergen, M. R. D., Jefferson, B., Parsons, S. A. and Jarvis, P. (2008) 'Magnetic ion-exchange resin treatment: Impact of water type and resin use', *Water Research*, 42(8–9), pp. 1977–1988.

Padungthon, S., German, M., Wiriyathamcharoen, S. and Sengupta, A. K. (2015) 'Polymeric anion exchanger supported hydrated Zr (IV) oxide nanoparticles : A reusable hybrid sorbent for selective trace arsenic removal', *REACT*, 93, pp. 84–94.

Pan, B., Wu, J., Pan, B., Lv, L., Zhang, W., Xiao, L., Wang, X., Tao, X. and Zheng, S. (2009) 'Development of polymer-based nanosized hydrated ferric oxides (HFOs) for enhanced phosphate removal from waste effluents', *Water Research*, 43(17), pp. 4421–4429.

Pidou, M., Parsons, S. A., Raymond, G., Jeffrey, P., Stephenson, T. and Jefferson, B. (2009) Fouling control of a membrane coupled photo catalytic process treating greywater. *Water Res*., 43, 3932-3939

Ponnusami, V., Rajan, K. S. and Srivastava, S. N. (2010) 'Application of film-pore diffusion model for methylene blue adsorption onto plant leaf powders', *Chemical Engineering Journal*, 163(3), pp. 236–242.

Qingjian, Z., Bingcai, P. A. N., Xinqing, C., Weiming, Z. and Bingjun, P. A. N. (2008) 'Preparation of polymer-supported hydrated ferric oxide based on Donnan membrane effect and its application for arsenic removal', *Science in China Series B: Chemistry,* 51, pp. 379–385.

Shon, H. K., Vigneswaran, S. and Snyder, S. A. (2006) 'Effluent Organic Matter (EfOM) in Wastewater: Constituents, Effects, and Treatment', *Critical Reviews in Environmental Science and Technology*, 36(4), pp. 327–374.

Sulak, M. T. and Demirbas, E. (2007) 'Removal of Astrazon Yellow 7GL from aqueous solutions by adsorption onto wheat bran', *Bioresouce Technology,* 98, pp. 2590–2598.

Sulaymon, A. H., Abid, B. A. and Al-Najar, J. A. (2009) 'Removal of lead copper chromium and cobalt ions onto granular activated carbon in batch and fixed-bed adsorbers', *Eng. & Tech. Journal*, 12, pp. 2336–2351.

Vasiliu, S., Bunia, I., Racovita, S. and Neagu, V. (2011) 'Adsorption of cefotaxime sodium salt on polymer coated ion exchange resin microparticles: Kinetics, equilibrium and thermodynamic studies', *Carbohydrate Polymers*, 85(2), pp. 376–387.

Wang, S. and Peng, Y. (2010) 'Natural zeolites as effective adsorbents in water and wastewater treatment', *Chemical Engineering Journal*, 156(1), pp. 11–24.

Wang, Z., Xing, M., Fang, W. and Wu, D. (2016) 'One-step synthesis of magnetite core/zirconia shell nanocomposite for high efficiency removal of phosphate from water', *Applied Surface Science*. Elsevier B.V., 366, pp. 67–77.

Wijnja, H. and Schulthess, C. P. (2000) 'Vibrational Spectroscopy Study of Selenate and Sulfate Adsorption Mechanisms on Fe and Al (Hydr)oxide Surfaces', *Journal of Colloid and Interface Science*, 229(1), pp. 286–297.

Xie, J., Wang, Z., Lu, S., Wu, D., Zhang, Z. and Kong, H. (2014) 'Removal and recovery of phosphate from water by lanthanum hydroxide materials', *Chemical Engineering Journal*, 254, pp. 163–170.

You, X., Farran, A., Guaya, D., Valderrama, C., Soldatov, V. and Luis, J. (2016) ‘Phosphate removal from aqueous solutions using a hybrid fi brous exchanger containing hydrated ferric oxide nanoparticles’, *Journal of Environmental Chemical Engineering*, 4, pp. 388–397.

Yu, Y. and Paul Chen, J. (2015) ‘Key factors for optimum performance in phosphate removal from contaminated water by a Fe–Mg–La tri-metal composite sorbent’, *Journal of Colloid and Interface Science*, 445, pp. 303–311.

Zhao, D. and Sengupta, A. K. (1998) ‘Ultimate removal of phosphate from wastewater using a new class of polymeric ion exchangers’, *Water Research*, 32(5), pp. 1613–1625.

Chapter 4. Laboratory scale column experiments to determine the impact of short empty bed contact times on phosphorus adsorption and removal of organic constituents from a low and high P loaded wastewater using hybrid ion exchange resin.

Ahsan Muhammad, Ana Soares and Bruce Jefferson
Cranfield University, Bedfordshire, MK43 0AL, UK

Abstract

The use of ferric embedded ion exchange resins has been shown to offer potential to meet low P discharge consents from wastewater. The current work extends previous findings to assess the impact of full load of phosphorus (concentration > 3 mg L^{-1}) and tertiary polishing (concentration ~ 1 mg L^{-1}) applications. The system was shown to deliver effective treatment at very low EBCTs of 0.5 – 3 minutes. However, optimum mass transfer profiles occurred once the EBCT was at least 5 minutes to ensure appropriate serviceable bed lives are achieved. In addition, the resin was observed to remove around 40 – 50 % of COD suggesting its suitability for sites needing both P and organic polishing.

Keywords: hybrid ion exchange, empty bed contact time.

4.1 Introduction

Wastewater treatment options for phosphorus removal are based on either enhanced biological reactor configurations and/or the use of meta salt coagulants (Pratt *et al*., 2012). Both have been shown to be capable of meeting the low final phosphorus discharges required by new legislation such as the Water Framework Directive. However, biological solutions work best with feed waters enriched in COD (Pratt *et al*., 2012) and have reduced robustness when operated for discharge consents below 0.5 mg L^{-1}. In the case of chemical solutions, reaching very low P levels is straightforward but requires good mixing of large chemical doses and effective solids separation to avoid the risk of elevated metal residuals in the discharged water. Accordingly, a number of new technologies are being

researched to provide alternative options that alter the cost-benefit balance such as the use of microalgae (Gonçalves *et al.*, 2017; Whitton *et al*, 2017), reactive media (Barca *et al*., 2013) and sorption media (Martin *et al*., 2017). In case of sorption media, a variety of materials have been tested including enriched media where metal species are embedded within the framework of the material such as biochar (de Rozari, Greenway and El Hanandeh, 2016), activated carbon, zeolites and anion exchangers (Martin *et al*., 2017).

Sorption processes have an established history as water and wastewater treatment processes such as softening and nitrate removal for potable water production ion exchange resins (Tchobanoglous *et al*., 2003) and treatment of both bulk and micro pollutant organics from water and wastewater with activated carbon (Cooney, 1998). In more recent times, polymeric anion exchangers have been used to remove arsenic and phosphate (Awual and Jyo, 2011). The performance and selectivity of such resins is further enhanced through incorporation of metal nano-particles to produce hybrid anion exchange (HAIX) resins (Acelas *et al*., 2015a). Whilst any metal can be used (e.g. zirconium, aluminium, copper) the most common is iron where hydrous ferric oxide (HFO) nano particles are impregnated into a strong base anion exchange resin. The nanoparticle component provides a selective pathway for removal such that the process can work effectively even in highly contaminated source waters (Martin *et al*., 2017). To illustrate, estimation of the relative contribution of the base exchanger and the nanoparticles indicates that 90% of the removal is associated with nanoparticles (Martin *et al*., 2017). Similarly, research has also shown the benefits of the hybrid resins in extending operating cycles. For instance, comparison of HAIX against a conventional ion exchanger, IRA-900, treating a waste with an initial phosphorous concentration of 0.26 mg P L^{-1} demonstrated an order of magnitude increase in the bed life from 200 to 2000 bed volumes (Blaney *et al.*, 2007).

The key design variable of such systems is the EBCT which determines the size of the contactor and hence the capital cost and the capacity of the system which controls the operating cost. Larger EBCT, extend operating cycles but require

bigger vessels and resin inventories. Accordingly, a balance needs to be established so understanding the impact of EBCT across a range of conditions of initial P concentration, wastewater types and target discharge levels is crucial. Existing work on HAIX at short EBCT (2 minutes) has been completed using synthetic phosphorus solution whereas the work completed with real wastewater has been at longer EBCT (4, 10, 20 minutes). The shape of the breakthrough curve is also dependant on the bed depth, hence the media needs to be tested at a range of bed depths, until constant-pattern profiles develop (Cooney, 1998).

The aim of the chapter is to enhance the elucidation of the impacts of EBCT by exploring shorter EBCTs (0.5-10 minutes) over a broad range of initial P concentrations (0.3-7 mg P L^{-1}) that mimic potential applications on sewage works for both polishing on sites with existing P removal and full removal for sites with no other P removal process.

4.2 Materials and Methods

4.2.1 Experimental set up

Effluent wastewater for the HAIX column experiments was collected from two different WWTPs: Site 1 which was a rural works with population equivalence of 6500-8000 and an effluent P concentration between 3 - 7 mg P L^{-1} and site 2, a medium scale works with PE of 28,344 and an effluent P concentration of 0.3 - 1.3 mg P L^{-1}. The respective COD of each effluent was 30 - 45 mg L^{-1} and 20 - 30 mg L^{-1}, solids concentrations of 20 - 50 and 1 - 7 mg SS L^{-1} and pH between 6.51 - 7.86. At times, it was necessary to enrich the phosphorous concentration of the effluent from site 2 in which case the P concentration was supplement by addition of ammonium dihydrogen phosphate. The wastewater was collected in 25 L containers every day and used within 2 days.

The hybrid anion exchanger (HAIX) media was acquired from Layne Christensen Company (Texas, United States). HAIX is a strong-base anion exchange resin loaded with hydrous ferric nanoparticles. The size of the media varied between 0.18 and 1.0 mm with a mean size of 0.69 mm. The media was backwashed with

DI-water for 30 minutes to remove any fine ferric particles left over from manufacturing.

Two sets of columns were used through the trials. In the case of the EBCT tests, 38.1 g of media was placed in a 2.5 cm diameter glass econo-columns with the media reaching a bed height of 11 cm. Columns were fed with effluent wastewater in a down-flow configuration at empty bed contact times (EBCT) of 0.5, 1, 3, 5, 7 and 10 minutes using a Watson Marlow peristaltic pump. In the case of the bed depth experiments, 7.4 cm diameter, 70 cm tall Perspex columns were used and filled with different heights of media (7, 17, 27, and 37 cm) for each height the bed was operated at both 0.5 and 10 minute EBCTs treating the wastewater from site 1. A head of water was maintained above the media to minimise the risk of channelling in the columns. Each set of experiments was carried out in duplicate column setups.

4.2.2 Analytical Methods

Determination of phosphorus and COD was conducted using Spectroquant cell tests supplied by VWR International (Leicestershire, United Kingdom). The methods are analogous to EPA 365.2+3 (Thermo Fisher Scientific, 2003) and EPA 410.4 (Con-test Analytical Laboratory, 2012) respectively. Dissolved organic carbon analysis was completed using Shimadzu TOC-5000A (Milton Keynes, UK). The protein analysis was completed using the Lowry modified by Frolund method (Shen *et al*., 2013). A sample of 1.5 mL was mixed with a 2.1 mL of reagent A (consists of 143 mM NaOH, 270 mM Na_2CO_3, 57 mM $CuSO_4$ and 124 mM Na_2-Tartrate) and left at room temperature for 10 minutes. 0.3 mL of reagent B (Folin Ciocalteau and DI water in the ratio 2:1) was added to the mixture and left in the dark for 45 minutes. The absorbance of the sample was read at 750 nm. The carbohydrate analysis was completed using the Dubois method. A sample of 0.4 mL was mixed with 0.5 mL of 5% phenol and left at room temperature for 10 minutes. Two mL of sulphuric acid was added to the mixture and left in the dark for 30 minutes. The absorbance was read at 490 nm (DuBois *et al*., 1956). Glucose and bovine albumin serum were used for calibration for the carbohydrate and protein analysis respectively.

4.2.3 Data analysis

The media capacity was calculated from the breakthrough curve as the cumulative mass removed across the operating cycle:

$$Q = \frac{\sum(C_o - C)\ BV}{m} \qquad \textbf{Equation 5}$$

Where Q is media capacity (mg P g_{media}^{-1}), C_0 is Influent concentration (mg L^{-1}), C is effluent concentration (mg L^{-1}), BV is bed volumes treated (L), and m is mass of media in column (g). It is posited that the major impact of the EBCT is on the length mass transfer zone (LMTZ) which is calculated according to (Worch, 2012):

$$h_z = h\ \frac{t_s - t_b}{t_{st}} \qquad \textbf{Equation 6}$$

Where h_z is length of mass transfer zone (mm), h is length of bed (mm), ts is time to C/C_0 = 0.95 (calculated from breakthrough curve), t_b is time to C/C_0 = 0.05 (calculated from breakthrough curve), and t_{st} – stoichiometric time (C/C_0 = 0.5) (calculated from breakthrough curve). The data related to the impact of bed depth was analysed by applying a bed depth service time model (BDST) which assumes that the surface reaction between adsorbate and unused capacity of adsorbent control the rate of adsorption (Zulfadhly *et al.*, 2001). The linear relationship between service time and bed depth is (Mukhopadhyay *et al.*, 2008):

$$t = \frac{N_0}{CF/A}H - \frac{1}{K_b C_0} ln\left(\frac{C}{C_0} - 1\right) \qquad \textbf{Equation 7}$$

Where C_0 is the column influent concentration (mg L^{-1}), C is the column effluent concentration (mg L^{-1}), F is the volumetric flow rate (cm^3/h), N_0 is the adsorption capacity (mg L^{-1}), K_b is the rate constant (l/mg h), t is time (bed volumes) and H is bed depth (cm). Simplified form of the model is (HAN *et al.*, 2007):

$$t = mZ - c \qquad \textbf{Equation 8}$$

Where:

$$m = \frac{N_0}{C_o F/A} \; and \; c = \frac{1}{K_b C_0} ln\left(\frac{C_0}{C} - 1\right) \qquad \textbf{Equation 9}$$

The length of unused bed was calculated using equation 10, where t_b is time to C/C_0 = 0.05 (calculated from breakthrough curve), t_{st} – stoichiometric time (C/C_0 = 0.5) (calculated from breakthrough curve) and L is the length of the bed (Worch, 2012).

$$LUB = \left(1 - \frac{t_b}{t_{st}}\right) L \qquad \textbf{Equation 10}$$

4.3 Results and Discussions

4.3.1 Impact of empty bed contact time

Increasing the EBCT impacted the operation of the contactor through a sharpening of the mass transfer zone (MTZ), an increase in the bed life and an associated increase in operational capacity (Figure 4.1). To illustrate, for site 1 (high P load), the MTZ was observably (Figure 4.1) more vertical in the breakthrough curve once the EBCT has exceeded 5 minutes. Calculation of the height of the MTZ confirms this with heights of 111.6 mm and 100 mm at EBCTs of 30 seconds and 3 minutes compared to heights between 65.4 and 70.9 mm for EBCTs between 5 and 10 minutes (Table 4.1). For the shorter EBCTs, the wide MTZ and the lack of a stable initial period in the bed run, which would be observed as a flat horizontal line from the start of the run, indicates unfavourable conditions for adsorption commonly attributed to a poorly designed adsorber (Alhamed, 2009; Krech, 2013). In such circumstances, the target phosphate ions do not have sufficient time to interact with the surface and diffuse into the pores such that intra-particle diffusion is rate limiting (Chen *et al*., 2012; Sotelo *et al*., 2013). In contrast, at higher EBCT the ions have sufficient residence time at the surface of the media to effectively diffuse into the pores such that external mass transfer becomes limiting. Operationally this is seen as a long flat curve at the start followed by a sharp increase in P concentration over a relatively small number of bed volumes, as illustrated for EBCTs of 7 and 10 minutes (Figure 4.1).

Table 4.1 Impact of EBCT on operational parameters for sites 1 and 2.

EBCT	Site	Bed volumes to 0.1 mg P L^{-1}	Bed volumes to 0.5 mg P L^{-1}	Bed volumes to saturation	Capacity at 0.5 mg P L^{-1} (mg g_{media}^{-1})	Saturation capacity (mg g_{media}^{-1})	LMTZ (mm)	LUB (mm)	Reynolds number
0.5	1	30	195	875	1.29	3.69	116	73.6	3.61
	2	350	1660		1.19				
1	1	45	365	775	2.60	3.87	87.6	42.8	1.81
	2	660	2100		2.57				
3	1	238	375	900	3.46	4.45	100	40.7	0.6
	2	1565	2630		3.11				
5	1	390	600	1059	3.09	3.93	70.9	42.1	0.36
	2	1634	2340		3.01				
7	1	375	389	855	3.4	5.04	65.4	31.3	0.26
	2	1600	2500		2.69				
10	1	320	415	868	2.94	3.91	70.4	24.1	0.18
	2	2141	2275		2.86				

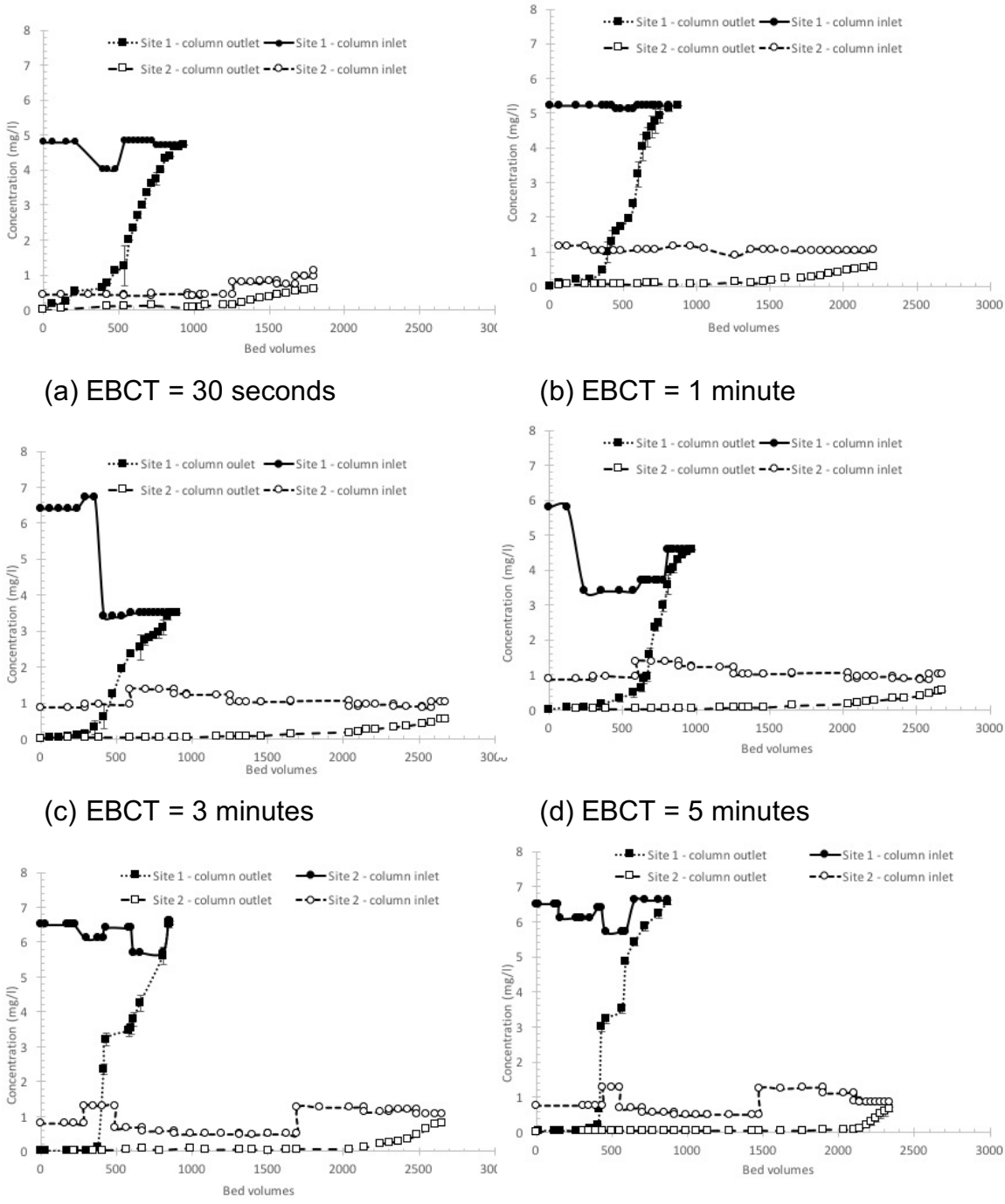

(a) EBCT = 30 seconds

(b) EBCT = 1 minute

(c) EBCT = 3 minutes

(d) EBCT = 5 minutes

(e) EBCT = 7 minutes

(f) EBCT = 10 minutes

Figure 4.1 Breakthrough curves for each EBCT (0.5 – 10 minutes) treating wastewater from sites 1 and 2.

The impact of the change in the height of the MTZ is seen with regards to the serviceable bed volumes prior to exceeding the target effluent concentration. In the case of a target concertation of 0.1 mg P L^{-1}, the serviceable bed life increased

from 30 BV at an EBCT of 30 seconds to a maximum of 390 BVs at an EBCT of 5 minutes. The absence of a linear relationship between EBCT and either height of the MTZ or the serviceable bed volumes is, in part, related to the variation in the influent concentration (Figure 4.1). For instance, in the case of the 5 minute EBCT, the influent P concentration started at 6 mg P L^{-1} for 120 BV before reducing to 3.5 mg P L^{-1} for a further 520 BV after which the influent concentration increased to 4.5 mg P L^{-1} (Figure 4.1d). In contrast, during the experiment with an EBCT of 10 minutes the influent P concentration remained between 5.7 and 6.6 mg P L^{-1} (Figure 4.1f). The current work extends the range of EBCTs that have been tested to treat high load P wastewater and demonstrates that even very short EBCTs are possible, albeit with short runtimes. More stable operation is achieved by extending the EBCT to 5 minutes which supports previous findings that between 4 and 10 minutes was required (Martin *et al*., 2017). Beyond such threshold values, the serviceable life is no longer directly influenced by EBCT and then becomes more about feed concentration and bed depth (Li *et al*., 2013).

In the case of site 2, the wastewater with the low initial P load, all the EBCTs where associated with a period of stable effluent concentration followed by a gradual increase in P concentration (Figure 4.1). The length of the stable period and the gradient of the slope both increased with EBCT. The latter is congruent with the decrease in the height of the MTZ observed for the high P load trials. For instance, serviceable bed life based on a target of 0.1 mg P L^{-1} extended from 350 BV and 660 BV at EBCTs of 30 seconds and 1 minutes to between 1565 and 1634 for EBCTs of between 3 and 7 minutes (Table 4.1). The longest serviceable bed life was observed for the 10 minutes EBCT at 2141 BVs, a 511 % increase in serviceable life compared to an EBCT of 30 seconds. This difference was reduced if a higher effluent P concentration target of 0.5 mg P L^{-1} was used whereby the difference in serviceable life is reduced to 37 % (Table 4.1). Interestingly, variation in the influent P concentration had no substantial impact in the residual P concentration achieved during the initial flat phase as observed across trials operated with EBCTs between 3 and 10 minutes indicating the robustness of the process to meeting very low residual P concentrations (Figure 4.1).

The difference in serviceable bed lives between sites 1 and 2 was a result of the different influent P concentration due to the faster exhaustion of the sorption sites (Maji *et al.*, 2007). This is evidenced by the similarity in overall operational capacity, especially at lower EBCTs (Figure 4.2). To illustrate, for site 1, the operational capacity at a breakthrough target of 0.5 mg P L^{-1}, increased from 1.29 mg P g_{media}^{-1} at 30 seconds EBCT to 3.46 mg P g_{media}^{-1} at an EBCT of 3 minutes reaching a maximum value of 3.94 mg P g_{media}^{-1} at an EBCT of 10 minutes (Figure 4.2). In comparison, for site 2, the operational capacity increased from 1.19 mg P g_{media}^{-1} at an EBCT of 30 seconds to a maximum value of 3.11 mg P g_{media}^{-1} at an EBCT of 3 minutes thereafter fluctuating just around 2.9 mg P g_{media}^{-1} for all subsequent EBCTs. Accordingly, the difference in capacity between the two wastewaters is greatest at the higher EBCTs at 27.5 % for a 10 minutes EBCT compared to 7.7 % for a 30 seconds EBCT. The observed differences as a function of EBCT are congruent with the respective change in the length of the MTZ for the two wastewaters. During the experiments, the trials with wastewater from site 2 did not reach saturation in reasonable times, prohibiting the calculation of the height of the MTZ. However, a surrogate of this can be considered by comparing the gradient of the breakthrough curves. At an EBCT of 0.5 minute, the slope of the breakthrough curve for site 1 is sharper than site 2, resulting in a smaller mass transfer zone such that intraparticle diffusion controls transfer for site 1, as compared to site 2 where external mass transfer is the major rate limiting component (Canteli *et al*., 2014; Chen *et al*., 2012). The much shallower gradients across all EBCTs reflect spreading of the MTZ and hence underutilisation of the available adsorption sites prior to a breakthrough. The impact of this is increased as the target concentration decreases due to the shallowness of the breakthrough curve. i.e. there are big BV differences between small changes in target concentration. To illustrate, in the case of site 2 the difference in serviceable bed volumes between a target of 0.1 and 0.3 mg P L^{-1} change from 1185 BV at an EBCT of 1 minute to 105 BV at an EBCT of 10 minutes. The equivalent respective change in bed volumes is 1080 BV for site 2 indicating the impact of having good mass transfer due to the higher

concentration gradient available to drive transport across the boundary layer surrounding the media (Tan *et al.*, 2008).

The other factor that influences operation is the Reynolds number which changed from 3.61 to 0.18 as the EBCT increased from 30 seconds to 10 minutes indicating that the flow pattern remained in the laminar regime throughout (Re <10) (Table 4.1). Previous studies have also seen a reduction in capacity as Re increases between 0.12 and 0.49 treating an influent concentration of 4 mg P L^{-1} in a 15 mm diameter column (Martin *et al.*, 2013). Over this range, capacity at saturation decreased from 3.1 to 2.3 mg P g_{media}^{-1}, a 26% decrease. The impact was increased as the target effluent P concentration was reduced with differences of 44, 52 and 62% for targets of 1, 0.5 and 0.1 mg P L^{-1}. An increase in Reynolds number is likely to have two impacts: a decrease in the boundary layer thickness and an increase in the degree of axial dispersion. The fact that the capacity decreases as Re goes up demonstrates that the impact of axial dispersion dominates. In the current case, a broader range of Reynolds numbers were explored generating a difference in capacity of 36 % at saturation and 204 % when meeting a target of 0.5 mg P L^{-1} for site 1.

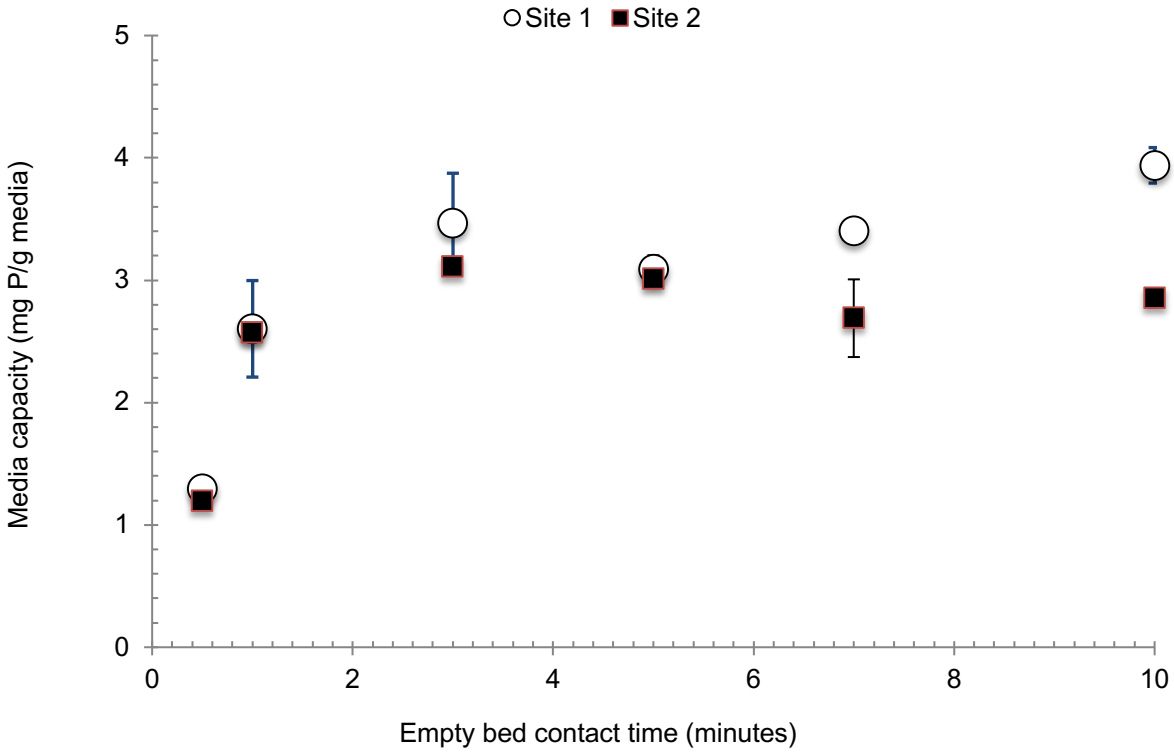

Figure 4.2 Impact of empty bed contact time on HAIX capacity at a breakthrough concentration of 0.5 mg P L^{-1} for sites 1 and 2.

The current data enriches the existing available data set concerning different wastewater strengths which has largely been based on either synthetics or batch studies. Comparison across the current study and the previous data provides confidence with capacities reported here. For instance, treatment of trace phosphorus with an influent concentration of 0.26 mg P L^{-1} at an EBCT of 2.2 minutes operated in a column of diameter 6 mm, resulted in an exhaustion capacity of 2.4 mg P g_{media}^{-1} at a pH of 7.6 reducing under more alkaline or acidic conditions due to the phosphate predominately existing in the divalent form which is known to be thermodynamically more favourable (Blaney *et al.,* 2007). Treatment of more highly P loaded water results in higher capacity with levels as high as 10 mg P g_{media}^{-1} reported for the treatment of urine in batch isotherm tests (P concentration between 700-800 mg P L^{-1}) (O'Neal and Boyer, 2013).

Capacity data generated from laboratory scale columns is known to underestimate operational capacity that will be realised at full scale (Martin *et al*., 2013). For instance, a study using a groundwater source enriched with

phosphorus to a starting concentration of 4 mg P L^{-1} demonstrated that the saturation capacity increased from 3.37 mg P g_{media}^{-1} to 6.27 mg P g_{media}^{-1} as the column diameter was increased from 15 mm to 500 mm (Martin *et al.*, 2013). Overall the variation of capacity as a function of scale followed a power law expression with an exponent of 1.2 when considering breakthrough at 0.1 mg P L^{-1}. This equates to a change in operational capacity, for a 0.1 mg P L^{-1} target of 3.7 mg P g_{media}^{-1} across the scale of reactors trialled. The impact is attributed to the influence of the wall which distorts the wave front and generates axial dispersion, blurring the mass transfer zone due to high bed porosity zones within the first three beads diameters from the wall (Cussler, 1997; Schmidtke and Smith, 1983). At the column size used in the current work, this accounts for 30 % of the total bead audit. In contrast, if a 500 mm diameter was used, only 1.6 % of the bead audit would be in this high bed porosity zone.

4.3.2 Impact of bed depth

Increasing the depth of the media for a fixed EBCT extended the serviceable bed life in an approximately linear fashion congruent with a bed depth service time model (Equation 7). For instance, at an EBCT of 30 seconds, the serviceable bed life to 1 mg P L^{-1} increased from 37 to 217 BVs as the depth of bed increased from 7 to 37 cm (Figure 4.3a). In comparison, at an EBCT of 10 minutes the equivalent change in serviceable life was from 120 to 188 BVs (Figure 4.3b). The greater change at low EBCT reflects the longer height of MTZ which was observed compared to the longer EBCT (Table 4.1). Importantly, at the shallowest bed depth, the mass transfer zone extends over the entire depth of media, resulting in a very short serviceable bed life. This is also reflected in the length of unused bed (Table 4.1) which defines the proportion of the bed not fully utilised under any given set of operating conditions and the corresponding use of available binding sites (Zulfadhly *et al.*, 2001). At the shorter EBCT, the proportion of the bed that is fully utilised increases from 0 % to 37 % across the different bed depths. In comparison, at 10 minutes EBCT, the proportion of the bed that is fully utilised increases from 0 to 93 %. This is observed in terms of the slope of the service time curves which are steeper for the shorter EBCT (Figure 4.3). This

occurs for all but the slope when operating to a 0.1 mg P L^{-1} target which reflects a degree of seepage due to the poor mass transfer characteristics (Martin *et al*., 2017). Similar trends have been observed in the uptake of copper on aspergillus niger biomass (Mukhopadhyay *et al.,* 2008), congo red on rise husk (Han *et al*., 2008) and nitrate on PAN-oxime-nano Fe_2O_3 (Jahangiri-rad *et al*., 2014). With increasing bed depth, the slope of the breakthrough curves decreases, resulting in a more broadened mass transfer zone (Han *et al*., 2009). A study on phosphate adsorption on nanosized FeOOH-modified anion resin yielded a similar pattern (Li *et al*., 2013).

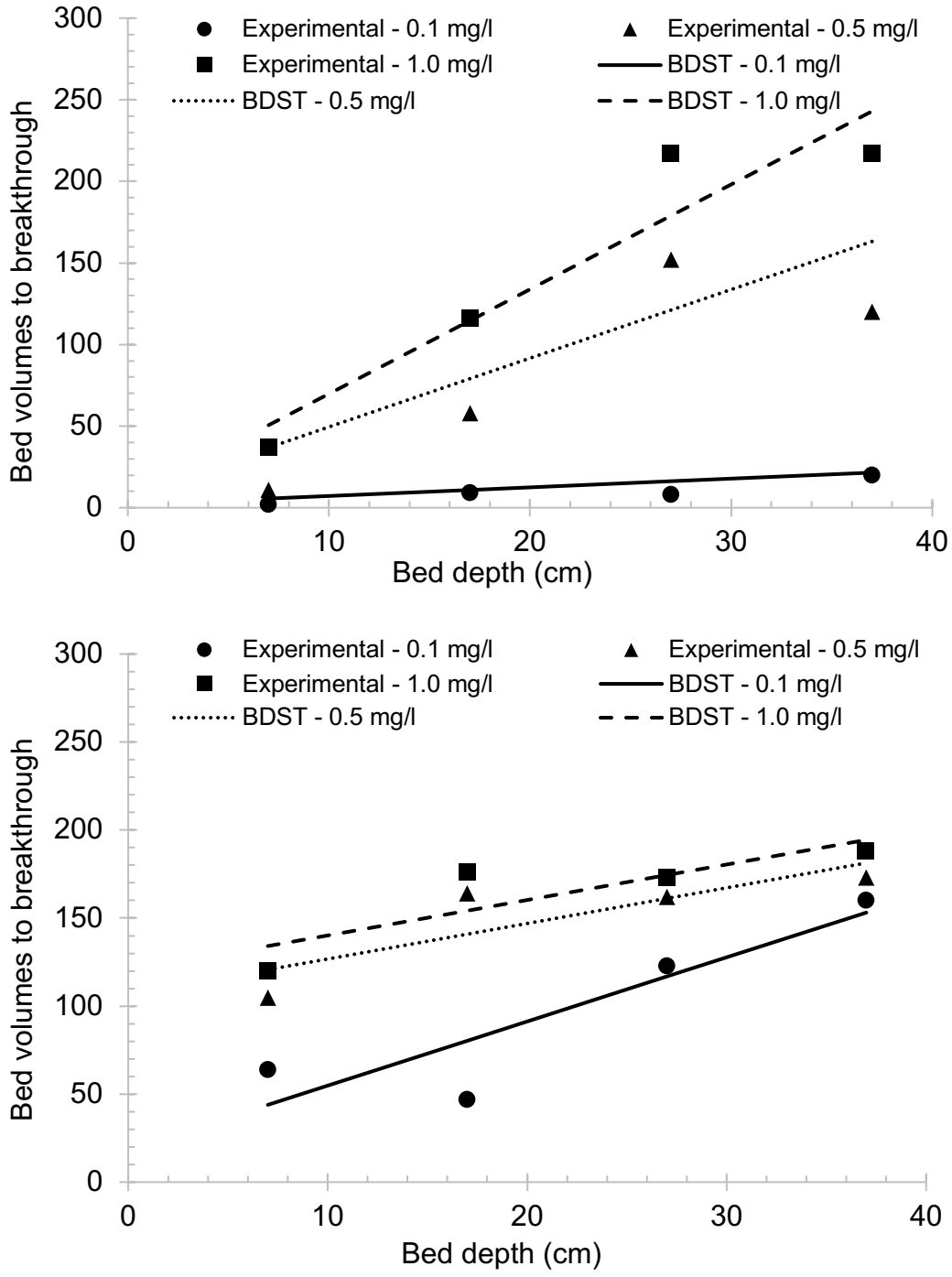

Figure 4.3 Impact of bed depth on service time of HAIX for site 1 operated at EBCTs of (a) 30 seconds and (b) 10 minutes.

4.3.2.1 Removal of other constituents

An additional benefit of using the hybrid resin is that other contaminates are removed simultaneously with the phosphorus but onto the polymeric framework.

For instance, in the case of site 1, removal of COD increased from 23 % at an EBCT of 30 seconds to a maximum value of 48 % at an EBCT of 10 minutes. However, the removal was effectively stable at EBCTs equal to and beyond 3 minutes (Figure 4.4). Similar data was observed for DOC with removals of 44 % for site 1 effluent and 45.5 % for site 2 effluent. However, the impact of EBCT was observed to be more gradual in the case of site 2 although removal was significantly better at short EBCTs (Figure 4.4b). The data is consistent with standard polymeric ion exchange resin (not embedded with nanoparticles) where equilibrium organic removal levels of around 50 % are normally expected at a contact time of 10 minutes (Bolto *et al.*, 2004). In comparison, ion exchange resin embedded with magnetite has been reported to remove between 30 to over 70 % of the COD from wastewater effluent depending on pre-treatment and initial concentration (Shon, Vigneswaran and Snyder, 2006; Wang *et al*., 2012). Impact of initial concentration was more evident at the shorter EBCT of 0.5 and 1 minute, with HAIX removing 18% and 17% more DOC respectively (Figure 4.4b). At the longer EBCT of 7 and 10 minutes, the initial DOC concentration had no impact, resulting in similar percentages removed for both sites. Hence, the high initial concentration does not result in HAIX achieving better organic removal efficiency as reported by for other ion exchange resin (Shon *et al.,* 2006).

Further elucidation of the organic removal was undertaken by analysing removal of carbohydrate and protein concentrations during the trials with wastewater from site 1 (Figure 4.4a). Protein removal increased steadily with EBCT from 14.4 % at an EBCT of 30 seconds to 56 % at an EBCT of 10 minutes. In contrast, the removal of carbohydrates was relatively flat remaining between 28 and 39 % irrespective of EBCT. The observed removal profile reflects the MW of the different components with the protein reported to contain a higher proportion of larger MW organics (Shon *et al.* 2006). It has been posited that the larger organic molecules take longer to be removed but form stronger bonds enabling preferential removal at longer EBCTs (Shon *et al.* 2006). Similar profiles with other organics such as chlorophenols have been attributed to the fact that intra-particle diffusion is rate limiting (Li and Sengupta, 2000) as was observed for the phosphorus at low EBCTs.

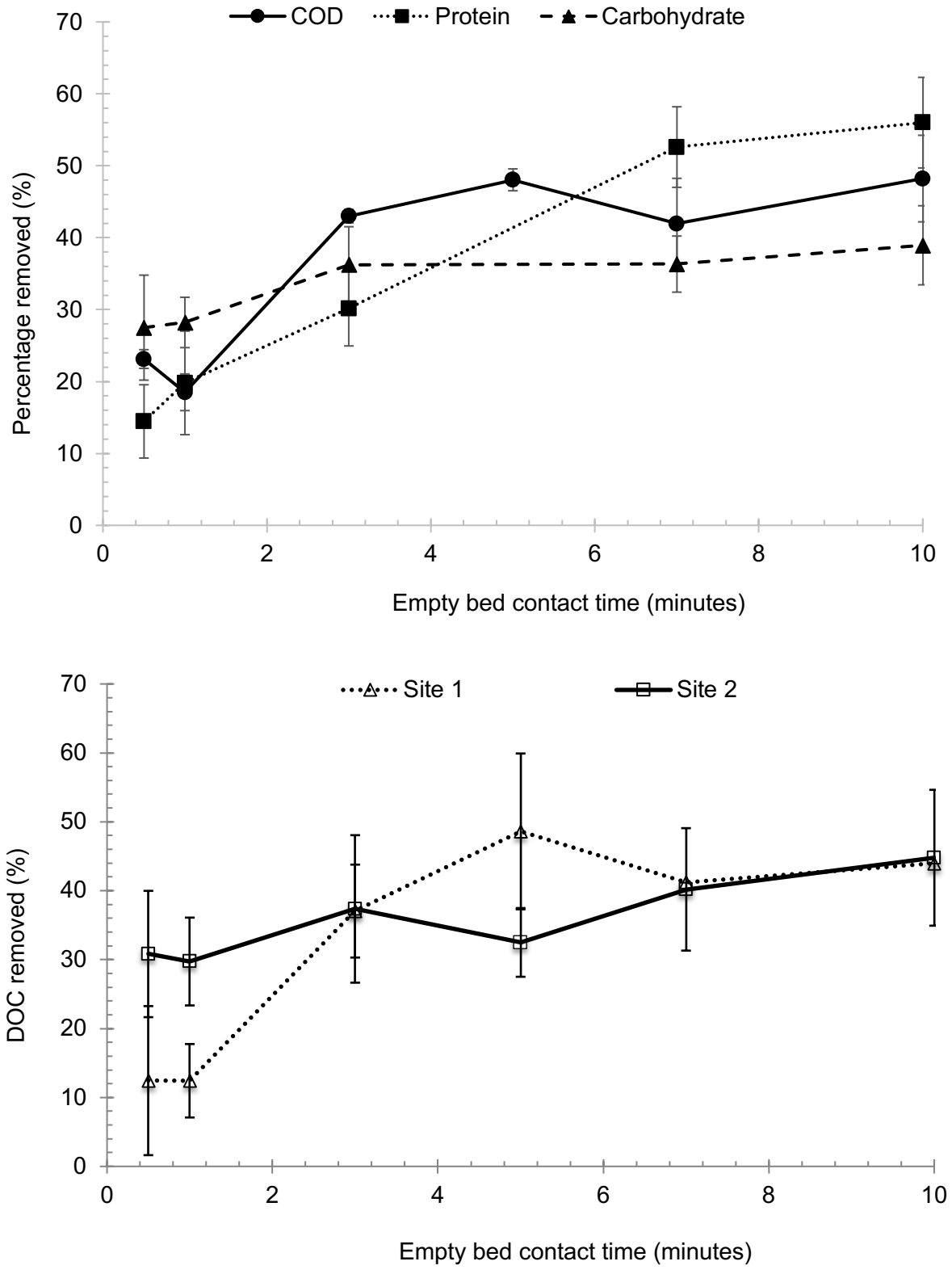

Figure 4.4 Impact of empty bed contact time on the removal of a) COD, proteins and carbohydrate from Site 1 and b) DOC by HAIX from site 1 and site 2.

4.4 Conclusions

The use of hybrid ion exchange resins is shown to be effective for phosphorus removal from wastewater as both the main phosphorus removal process (site 1) and as a tertiary polishing step (site 2). The system can deliver effective treatment even at very short empty bed contact times of 30 seconds where the process is known to be limited by the intraparticle diffusion rate (Chen *et al*., 2012) through the accumulation of other ions on to the base resin generating a reduction in the donnan membrane effect (Liu and Zhang, 2015). The impact is reduced by increasing the EBCT to 3 – 5 minutes but is not significantly reduced with larger EBCTs as the overall rate becomes external diffusion limited (Li *et al*., 2013). The overall net change in serviceable life between regenerations is 614 BV which is insufficient to justify additional capital expenditure associated with larger EBCTs (Chapter 5). Accordingly, it is recommended that EBCTs of around 5 minutes are likely to represent the optimum operating condition. In cases where the resin is removing bulk of the phosphorus from the wastewater, the optimum EBCT is again seen between 3 – 5 minutes with expected serviceable bed lives of around 300 BVs. The difference in bed life as a function of P load is congruent with a similar total number of adsorption sites becoming exhaustive, indicating that the overall mechanism of uptake has not changed (Maji *et al*., 2007).

Interestingly, the resin also removed COD at a level between 40-50% which enables the technology to offer solutions beyond just phosphorus to sites which require further reduction in both nutrients and organics. The removal is consistent with previous studies and consistent with the resin being intraparticle diffusion controlled (Li and Sengupta, 2000). Overall, the findings of the work indicate two application areas where the resin is most likely to offer a viable alternative to traditional approaches; small rural works and sites utilising anaerobic treatment of the main flow. A future aspiration should be to explore the nature of the organics that are removed to ascertain the potential of the technology for removal of hazardous chemicals.

4.5 Acknowledgements

The authors gratefully acknowledge financial support from the Engineering and

Physical Sciences Research Council (EPSRC) through their funding of the STREAM Industrial Doctorate Centre, and from the project sponsors Anglian Water, Severn Trent Water, Scottish Water, Thames Water, Yorkshire Water and Wessex Water for their financial and technical support throughout the project.

4.6 References

Acelas, N. Y., Martin, B. D., López, D. and Jefferson, B. (2015) 'Selective removal of phosphate from wastewater using hydrated metal oxides dispersed within anionic exchange media', *Chemosphere*, 119, pp. 1353–1360.

Alhamed, Y. A. (2009) 'Adsorption kinetics and performance of packed bed adsorber for phenol removal using activated carbon from dates' stones', *Journal of Hazardous Materials*, 170(2–3), pp. 763–770.

Awual, M. R., El-Safty, S. a. and Jyo, A. (2011) 'Removal of trace arsenic(V) and phosphate from water by a highly selective ligand exchange adsorbent', *Journal of Environmental Sciences*. The Research Centre for Eco-Environmental Sciences, Chinese Academy of Sciences, 23(12), pp. 1947–1954.

Awual, M. R. and Jyo, A. (2011) 'Assessing of phosphorus removal by polymeric anion exchangers', *Desalination*, 281(1), pp. 111–117.

Barca, C., Troesch, S., Meyer, D., Drissen, P., Andreìs, Y. and Chazarenc, F. (2013) 'Steel slag filters to upgrade phosphorus removal in constructed wetlands: Two years of field experiments', *Environmental Science and Technology*, 47(1), pp. 549–556.

Blaney, L. M., Cinar, S. and SenGupta, A. K. (2007) 'Hybrid anion exchanger for trace phosphate removal from water and wastewater', *Water Research*, 41(7), pp. 1603–1613.

Bolto, B., Dixon, D. and Eldridge, R. (2004) 'Ion exchange for the removal of natural organic matter', *Reactive and Functional Polymers*, 60(1–3), pp. 171–182.

Canteli, A. M. D., Carpiné, D., Scheer, A. D. P., Mafra, M. R. and Igarashi-Mafra, L. (2014) 'Fixed-bed column adsorption of the coffee aroma compound benzaldehyde from aqueous solution onto granular activated carbon from coconut husk', *LWT - Food Science and Technology*, 59.

Chen, L., Zhao, X., Pan, B., Zhang, W., Hua, M., Lv, L. and Zhang, W. (2015) 'Preferable removal of phosphate from water using hydrous zirconium oxide-based nanocomposite of high stability', *Journal of Hazardous Materials*, 284, pp. 35–42.

Chen, S., Yue, Q., Gao, B., Li, Q., Xu, X. and Fu, K. (2012) 'Adsorption of hexavalent chromium from aqueous solution by modified corn stalk: A fixed-bed column study', *Bioresource Technology*, 113, pp. 114–120.

Con-test Analytical Laboratory (2012) *The Determination of Chemical Oxygen Demand*. Available at: http://www.contestlabs.com/assets/method_library/COD.pdf (Accessed: 8 June 2015).

Cooney, D. O. (1998) *Adsorption Design for Wastewater Treatment*. Taylor & Francis (Environmental engineering).

Cussler, E. L. (1997) *Diffusion: Mass Transfer in Fluid Systems*. Cambridge University Press (Cambridge Series in Chemical Engineering), United Kingdom.

DuBois, M., Gilles, K. a., Hamilton, J. K., Rebers, P. a. and Smith, F. (1956) 'Colorimetric Method for Determination of Sugars and Related Substances', *Analytical Chemistry*, 28(3), pp. 350–356.

Gonçalves, A. L., Pires, J. C. M. and Simões, M. (2017) 'A review on the use of microalgal consortia for wastewater treatment', *Algal Research*, 24, pp. 403–415.

Han, R., Ding, D., Xu, Y., Zou, W., Wang, Y., Li, Y. and Zou, L. (2008) 'Use of rice husk for the adsorption of congo red from aqueous solution in column mode.', *Bioresource technology*, 99(8), pp. 2938–46.

HAN, R., WANG, Y., YU, W., ZOU, W., SHI, J. and LIU, H. (2007) 'Biosorption of methylene blue from aqueous solution by rice husk in a fixed-bed column', *Journal of Hazardous Materials*, 141(3), pp. 713–718.

Han, R., Wang, Y., Zhao, X., Wang, Y., Xie, F., Cheng, J. and Tang, M. (2009) 'Adsorption of methylene blue by phoenix tree leaf powder in a fixed-bed column: experiments and prediction of breakthrough curves', *Desalination*. Elsevier B.V., 245(1–3), pp. 284–297. doi: 10.1016/j.desal.2008.07.013.

Jahangiri-rad, M., Jamshidi, A., Rafiee, M. and Nabizadeh, R. (2014) 'Adsorption performance of packed bed column for nitrate removal using PAN-oxime-nano Fe2O3', *Journal of Environmental Health Science and Engineering*, 12(1), p. 90.

Krech, T. (2013) *Adsorptive exhaust treatment; kinetics and mass transfer zone*. Available at: http://www.jenoptik.com/Internet_EN_Adsorptive_Abluftreinigung_Kinetik_und_Massentransferzone (Accessed: 26 March 2015).

Li, N., Ren, J., Zhao, L. and Wang, Z. L. (2013) 'Fixed bed adsorption study on phosphate removal using nanosized FeOOH-modified anion resin', *Journal of Nanomaterials*, 2013, pp. 1–6. doi: 10.1155/2013/736275.

Li, P. and Sengupta, A. K. (2000) 'Intraparticle diffusion during selective ion exchange with a macroporous exchanger', *Reactive and Functional Polymers*, 44(3), pp. 273–287.

Lin, X., Huang, Q., Qi, G., Shi, S., Xiong, L. and Huang, C. (2017) 'Estimation of fixed-bed column parameters and mathematical modeling of breakthrough behaviors for adsorption of levulinic acid from aqueous solution using SY-01 resin', *Separation and Purification Technology*, 174, pp. 222–231.

Maji, S., Pal, A., Pal, T. and Adak, A. (2007) 'Modeling and fixed bed column adsorption of As(III) on laterite soil', *Separation and Purification Technology*, 56(3), pp. 284–290.

Martin, B. D., De Kock, L., Gallot, M., Guery, E., Stanowski, S., MacAdam, J., McAdam, E. J., Parsons, S. A. and Jefferson, B. (2017) 'Quantifying the

performance of a hybrid anion exchanger/adsorbent for phosphorus removal using mass spectrometry coupled with batch kinetic trials', *Environmental Technology*, In Press.

Martin, B. D., De Kock, L., Stephenson, T., Parsons, S. a. and Jefferson, B. (2013) 'The impact of contactor scale on a ferric nanoparticle adsorbent process for the removal of phosphorus from municipal wastewater', *Chemical Engineering Journal*, 215–216, pp. 209–215.

Mukhopadhyay, M., Noronha, S. B. and Suraishkumar, G. K. (2008) 'Copper biosorption in a column of pretreated Aspergillus niger biomass', *Chemical Engineering Journal*, 144(3), pp. 386–390.

Nur, T., Johir, M. A. H., Loganathan, P., Nguyen, T., Vigneswaran, S. and Kandasamy, J. (2014) 'Phosphate removal from water using an iron oxide impregnated strong base anion exchange resin', *Journal of Industrial and Engineering Chemistry*. The Korean Society of Industrial and Engineering Chemistry, 20(4), pp. 1301–1307.

O'Neal, J. A. and Boyer, T. H. (2013) 'Phosphate recovery using hybrid anion exchange: Applications to source-separated urine and combined wastewater streams', *Water Research*, 47(14), pp. 5003–5017.

Pan, B., Wu, J., Pan, B., Lv, L., Zhang, W., Xiao, L., Wang, X., Tao, X. and Zheng, S. (2009) 'Development of polymer-based nanosized hydrated ferric oxides (HFOs) for enhanced phosphate removal from waste effluents', *Water Research*, 43(17), pp. 4421–4429.

Pratt, C., Parsons, S. A., Soares, A. and Martin, B. D. (2012) 'Biologically and chemically mediated adsorption and precipitation of phosphorus from wastewater', *Current Opinion in Biotechnology*, 23(6), pp. 890–896.

de Rozari, P., Greenway, M. and El Hanandeh, A. (2016) 'Phosphorus removal from secondary sewage and septage using sand media amended with biochar in constructed wetland mesocosms', *Science of the Total Environment*, 569–570, pp. 123–133.

Schmidtke, N. W. and Smith, D. W. (1983) *Scale-up of Water and Wastewater Treatment Processes: From Papers Presented at the First International Workshop on Scale-up of Water and Wastewater Treatment Processes Held in Edmonton, Alberta, Canada in March 1983*. Butterworth Publishers (The Ann Arbor science book).

Shen, Y. X., Xiao, K., Liang, P., Ma, Y. W. and Huang, X. (2013) 'Improvement on the modified Lowry method against interference of divalent cations in soluble protein measurement.', *Applied microbiology and biotechnology*, 97(9), pp. 4167–4178.

Shon, H. K., Vigneswaran, S. and Snyder, S. a. (2006) 'Effluent Organic Matter (EfOM) in Wastewater: Constituents, Effects, and Treatment', *Critical Reviews in Environmental Science and Technology*, 36(4), pp. 327–374.

Sotelo, J. L., Ovejero, G., Rodríguez, A., Álvarez, S. and García, J. (2013) 'Analysis and modeling of fixed bed column operations on flumequine removal onto activated carbon: pH influence and desorption studies', *Chemical Engineering Journal*, 228, pp. 102–113.

Tan, I. a W., Ahmad, a. L. and Hameed, B. H. (2008) 'Adsorption of basic dye using activated carbon prepared from oil palm shell: batch and fixed bed studies', *Desalination*, 225(1–3), pp. 13–28.

Tchobanoglous, G., Burton, F. L., Stensel, H. D. and Eddy, M. & (2003) *Wastewater Engineering: Treatment and Reuse*. McGraw-Hill Education (McGraw-Hill higher education).

Thermo Fisher Scientific (2003) *ORTHOPHOSPHATE TEST KIT METHOD*.

Unuabonah, E. I., Olu-Owolabi, B. I., Fasuyi, E. I. and Adebowale, K. O. (2010) 'Modeling of fixed-bed column studies for the adsorption of cadmium onto novel polymer-clay composite adsorbent', *Journal of Hazardous Materials*, 179(1–3), pp. 415–423.

Wang, Q., Li, A., Wang, J. and Shuang, C. (2012) 'Selection of magnetic anion exchange resins for the removal of dissolved organic and inorganic matters',

Journal of Environmental Sciences (China). The Research Centre for Eco-Environmental Sciences, Chinese Academy of Sciences, 24(11), pp. 1891–1899.

Worch, E. (2012) *Adsorption Technology in Water Treatment: Fundamentals, Processes, and Modeling*. De Gruyter.

Zulfadhly, Z., Mashitah, M. D. and Bhatia, S. (2001) 'Heavy metals removal in ® xed-bed column by the macro fungus Pycnoporus sanguineus', *Environmental Pollution*, 112, pp. 463–470.

Chapter 5. Hybrid ion exchanger for tertiary phosphorus removal – an economic analysis to ascertain the potential and key development areas

Ahsan Muhammad, Ana Soares and Bruce Jefferson
Cranfield University, Bedfordshire, MK43 0AL, UK

Abstract

Existing phosphorus removal treatment are expected to find it challenging to consistently meet future phosphorus consents of 0.1 mg P L^{-1}. This has led to the investigation of novel solutions including immobilised or suspended algae and sorption medias. One such sorption media is the hybrid anion exchange media. The media has proven to be effective for treating full load of phosphorus as well as for phosphorus polishing and can consistently achieve effluent concentration below 0.1 mg P L^{-1}. This paper undertakes an economic assessment of the media in a fixed-bed and suspended system. The key economic parameters, CAPEX, OPEX and WLC were compared against conventional treatment of coagulant dosing followed by one-stage or two-stage filtration. The fixed bed system was found to be economically more viable compared to other solutions. The regen clean-up for a medium sized WWTW should be completed on site whereas for a small treatment works, a mobile regen clean-up system will be more economically beneficial.

Keywords: hybrid anion exchanger, HAIX, OPEX, CAPEX, WLC, fixed-bed, phosphorus removal

5.1 Introduction

The implementation of new legislation such as the Water Framework Directive is requiring sewage works to reduce phosphorus levels in their discharges to below 0.1 mg P L^{-1}. Accordingly, technology solutions that can achieve this are being developed and trialled (Vale, 2016). The majority of the commercially available solutions utilise additional coagulant dosing followed by clarification of the precipitated solids. These include cloth filters, depth filters, membranes and

ballasted sedimentation systems (Vale, 2016). Recent trials at demonstration scale across the UK have indicated that whilst single stage tertiary clarification post coagulant dosing is able to meet a 0.1 mg P L^{-1} standard it does not do so in a robust and resilient manner (Brookes and Barter, 2017; Smith *et al*., 2017). Consequently, two stage clarification systems are being considered which exert a high capital cost on the solution. In addition, the coagulant has to be dosed at a high molar ratio to ensure precipitation of the trace levels of phosphorus, thereby exerting a relatively high chemical demand. Accordingly, novel solutions are being considered such as the use of suspended or immobilised algae (Whitton *et al*., 2016), reactive media and sorption processes. One of the technically feasible solutions is to use a hybrid ion exchange resin which have been impregnated with iron nanoparticles (Chapter 2). The media enables selective removal of the phosphorous within the complex matrix of other constituents within wastewater. The efficacy of the system has been demonstrated at very low contact times of 30 seconds to 10 minutes (Chapter 4) indicating that the system may offer an attractive financial alternative to coagulation-based solutions.

Traditional ion exchange systems use small media particles in fixed beds operated at relatively short contact times 1.5-7.5 minutes to remove targeted pollutants from water (Woodard *et al*., 2017; Chowdhury *et al*., 2002). The system typically runs for relatively short periods of time, with regeneration required every day on site (Desilva and Galleti, 2005). The regeneration liquid is then disposed, typically down the sewer or by tankering. Ion exchange systems are relatively common in drinking water treatment for the removal of nitrate from groundwater and natural organic matter from organic rich source waters (Tchobanoglous *et al.,* 2004). Application to wastewater is limited due to issues associated with selectivity (Chapter 3), operation with solid containing waters blocking up the media beds and the management of the used regeneration liquids. Recent innovations related to the hybrid resin offer potential to resolve these issues suggesting that the process may be an appropriate alternative (McLeod *et al.,* 2017; Martin *et al*., 2017; De Kock 2015). Accordingly, the current study aims to explore the plausibility of using a fixed bed IEX system containing the hybrid resin

for the removal of phosphorus from a concentration of 1 mg P L^{-1} to below 0.1 mg P L^{-1}. The economic analysis will utilise an estimation of the capital and operating cost of the system compared to four benchmark alternatives to assess if there is any plausibility in the system being economically appropriate and then to establish the key components that require further development.

5.2 Business case scenarios

The study is based on the upgrading of a 2,000 PE and 20,000 PE WWTW with existing P removal achieving a consent of 1 mg P L^{-1} in order that the sites are able to reach a new consent of 0.1 mg P L^{-1}. The base case incorporates the use of secondary dosing of coagulant (Ferric) prior to a clarification processes (Figure 5.1). Three variations have been chosen including the use of a cloth filter followed by a depth filter (Scenario A), two depth filters in series (Scenario B) and a single stage depth filter (Scenario C) (Figure 5.1). These have been chosen as they represent the most commonly applied technologies for tertiary P removal. The two stage systems have been chosen to reflect on recent outcomes of a series of UK demonstration trials which reported that whilst less than 0.1 mg $P.L^{-1}$ can be achieved with dosing before a single stage cloth or depth filter, the robustness and resilience of the performance meant that two stage systems would probably be utilised (Brookes and Barter, 2017; Smith *et al*., 2017). This aligns to outcomes from existing process selection matrices that would indicate the need for two stage depth filtration due to concerns about excessive residual coagulant in the final water (Vale, 2017). The single stage filtration system is included to ascertain the impact of two stage filtration and to mirror commercially available solutions that are used elsewhere in the world.

The scenarios have been chosen to provide a conservative test to emphasise cost criticalities and enable stress testing of the impact of likely cost evolution of the innovative components so that the economic plausibility of the hybrid ion exchange process can be assessed. The findings are then discussed in relation to other factors and applications which potentially enhance the economic attractiveness of the process. The economic assessment is based on the use of the hybrid ion exchange resin in standard fixed bed contactors. The design is

based on standard approaches with two modifications to resolve known challenges: (1) a micro screen is added prior to the column to restrict solids load onto the beds as this is known to inhibit performance (Desilva, 2011) and (2) the system is modified to enable the regeneration liquid to be reused and recycled. This includes draining the beds between cycles and clean-up of the regeneration liquid by precipitation of the captured phosphorus via calcium hydroxide dosing. The precipitated solids are known to be predominately calcium phosphate (McLeod *et al*., 2017) and hence the process represents a resource recovery unit that aligns to the principles of the circular economy. The impact of such factors is considered through including the potential income that could be realised through selling the precipitated calcium phosphate. In addition, the hybrid resin is also used in a suspended ion exchange process. Such technology represents knowledge transfer from drinking water treatment through commercial systems such as MIEX ® or the SIX process (Cadee *et al*., 1998; O'Shea *et al*., 2008; Slunjski *et* al., 2000; Crittenden *et al*. 2012). The use of suspended ion exchange enables operation with higher solids loading and the use of larger individual contactors to reduce total infrastructure costs.

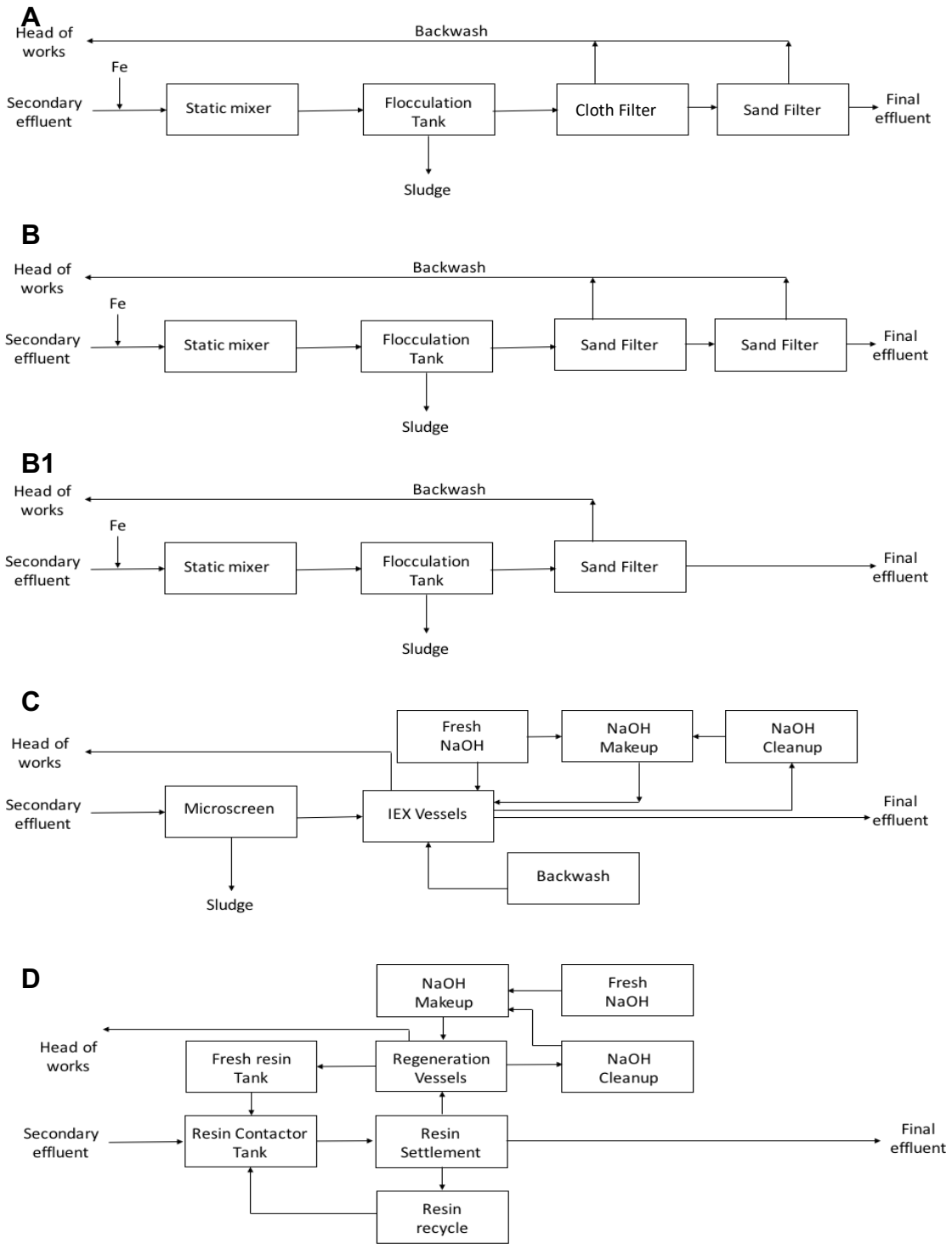

Figure 5.1 Flowsheets for tertiary phosphorus removal based on: (A) coagulation with two stage filtration [cloth filter followed by a depth filter], (B) coagulation with two stage depth filtration, (B1) coagulation with single stage depth filtration (C) fixed bed ion exchange and (D) suspended ion exchange.

5.3 Design parameters

The design of equipment for all scenarios is validated through information available within the thesis or existing literature with detailed design calculations available in supplementary information. Across all scenarios, it is assumed that there is (1) sufficient land available at no additional costs, (2) any additional sludge produced can be processed with the existing facilities (AD or tankering) and (3) the sites have all the required physical infrastructure (roads, chemical storage) and health and safety facilities associated with using chemicals (potable supply, health and safety showers etc..). All designs are based on existing operational systems with bed depths and washing frequency taken from manufacturers recommendations and/or operational practice (George Tchobanoglous *et* al., 2004; Parkson, 2010). Power requirements for electrical/mechanical equipment is based on a 50% motor efficiency.

All designs were based on full flow to treatment (FFT) based on three times dry weather flow (DWF) and a DWF flow of 150 L $head^{-1}$ day^{-1}.

5.3.1 Scenarios A, B and B1: Conventional solutions design philosophy

Scenarios A, B and B1 utilize secondary coagulant dosing followed by single or two stage clarification to remove precipitated solids. In all cases, ferric chloride was used at a molar dose ratio of 7.42 (Whitton, 2016). The chemical is dosed into the wastewater in a rapid mixing zone followed by flocculation to ensure sufficient precipitation. The flocculation system was sized based on standard practice with a retention time of 5 minutes operated with a mixer delivering a global G of 1200 s^{-1} (Crittenden *et al*., 2012; Tchobanoglous *et al*., 2004). The precipitated solids are then removed through application of a continuous mono media depth filter (e.g. Astrasand™, Dynasand™) or a cloth filter with a nominal pore size of 10 μm (e.g. a Meccana filter). The cloth for the cloth filter was assumed to require a deep clean, requiring the unit to be withdrawn from the housing and jet washed every 12 months.

Table 5.1 Key design parameters for scenario A, B and B1 for 2,000 and 20,000 PE.

Design Parameter	Unit	Value	Reference
Coagulant			
Fe:P	7.42	mol:mol	(Whitton, 2016)
$FeCl_3$ strength	36	% w/w	(Whitton, 2016)
Flocculation G	1200	s^{-1}	
Flocculation time	5	minutes	
Sand filter			
Hydraulic loading	12	$m^3 h^{-1} m^2$	(Parkson, 2010)
Air flow rate	54	$m^3 h^{-1} m^2$	(Crittenden *et al*., 2012)
Backwash	70	Litre sec^{-1}	(Crittenden *et al*., 2012)
Bed depth	1.35	m	Calculated
Media size	0.55	mm	(Tchobanoglous *et al*., 2004)
Backwash frequency	6	hours	
Cloth filter			
Hydraulic loading	11	$m^3 h^{-1} m^2$	(Five Star Filtration, 2014)
Area	0.6	m^2	Calculated
Backwash frequency	24	hours	(Five Star Filtration, 2014)
Backwash rate	1	Day^{-1}	(Five Star Filtration, 2014)

5.3.2 Scenarios C: Fixed bed vessels

The design for scenario C incorporated a pre-treatment drum filter, ion exchange contact tanks, a regeneration system and associated pumps (Figure 5.1). The whole system was designed at six different empty bed contact times for the two different PE (Table 5.2). The drum filter was based on an Andritz Vacuum Drum Filter unit with an aperture of 100 μm. The specifications and power requirements were based on suppliers information (Andritz, 2015). The ion exchange contact tanks were based on pressure vessels designed to cope with regeneration with sodium hydroxide. The maximum diameter of the ion exchange vessels was set at 3 m based on standard practice of transportation to small sites (Personal communication with Jason McLoughlin). The maximum bed depth allowed was 1 m to avoid excessive head loss resulting in an increase in pumping costs. In all cases a standby vessel was included to enable continuous treatment during

regeneration. The media is backwashed prior to regeneration using final effluent and the wash water sent to the head of the works.

Table 5.2. Key design parameters for fixed bed vessels for 2,000 and 20,000 PE.

Design Parameter	Unit	EBCT (minutes)						Notes and Reference
		0.5	1	3	5	7	10	
2, 000 PE								
FFT	$m^3 d^{-1}$				961			
Average flow	$m^3 d^{-1}$				401			
Media	m^3	0.33	0.67	2	3.33	4.67	6.67	(Woumfo *et* al., 2015)
No. of vessels		2	2	2	2	2	2	One duty and one stand-by.
Diameter	m	1	2	2	3	3	3	Optimal diameter between 0.5-3 m (Sinnott, 2005)
Bed depth	m	0.42	0.21	0.64	0.47	0.66	0.94	Calculated
20,000 PE								
FFT	$m^3 d^{-1}$				9610			
Average flow	$m^3 d^{-1}$				4010			
Media	m^3	3.33	6.67	20.0	33.4	46.7	66.7	(Woumfo *et* al., 2015)
No. of vessels		4	6	4	6	8	11	Assumption
Diameter	m	2	2	3	3	3	3	Optimal diameter between 0.5-3 m.(Sinnott, 2005)
Bed depth	m	0.35	0.42	0.94	0.94	0.94	0.94	Calculated

5.3.3 Scenarios D: Suspended ion exchange

The suspended ion exchange process was based on a 15-minute contact time at a media dose rate of 30 mL L^{-1} based on reported ranges for both variables (Table 5.3). The media and wastewater are combined in a mixing tank and then passed through the contact tank. Once through the contact tank the media is split with 95 % of the flow recycled to go back into the mixing tank and 5 % is sent to the regeneration vessels (Cadee *et al*., 1998). The media is then regenerated in the same way as for the fixed bed system. The use of a suspended media system precludes the need for pre-screening to remove solids.

Table 5.3 Key parameters and assumptions for suspended ion exchange for 2,000 and 20,000 PE.

Design Parameter	Unit	Population equivalent		Notes and Reference
		2,000	20,000	
Reaction tank				
Hydraulic retention time	min	15		Reported range: 10 - 30 minutes. (Slunjski *et* al., 2000)
Media dosage	ml litre^{-1}	30		Reported range: 10 - 30 ml. litre^{-1}.(Wert *et al*. 2005)
No. of mixing tanks		1	4	Assumed
Tank volume	m^3	15	30	Calculated
Media	L	720.7	7207	
Media recycled	%	90		*(O'Shea et al., 2008; Murray et al*., 2005)
	L min^{-1}	18	180	
Media regenerated	%	10		
	L.min^{-1}	2	20	
Impeller diameter	m	0.4	1.5	Reported range of impeller diameter/tank diameter = 0.3 - 0.5. (Sinnott, 2005)
Lamella settler				
Hydraulic retention time	minutes	20		(G Tchobanoglous *et al*., 2003)
Surface loading	m h^{-1}	17.5		Reported range: 10 - 25 m/h. (G Tchobanoglous *et al*., 2003)

5.3.4 Sodium hydroxide clean-up system

The ferric nano-particle component of the HAIX media can be selectively regenerated using sodium hydroxide. Previous work on the media has highlighted that unless sodium hydroxide is cleaned-up and reused, it is not economical to use the media for phosphorus removal (Martin, 2010). The clean-up system is made up of a mixing tank and a bag filtration system. Calcium hydroxide is dosed into the mixing tank where it reacts with the available phosphate to form calcium phosphate. The precipitated solids are then removed in a bag filter and the regeneration liquid return to the regeneration system and topped up with sodium

hydroxide as required. The regeneration system is assumed to remove 80% of the available phosphate which is then washed and available for sale.

The design of the system is based on previous findings (De Kock, 2015) whereby the regeneration liquid can be reused 10 times before requiring clean-up. The frequency and volume for regeneration and clean-up is summarised in Table 5.4. The time to regeneration (Table 5.4) was calculated by scaling up the capacities calculated in Chapter 4 for different EBCT using the model specified by Martin *et al*., (2012). The model only tested vessels up to a diameter of 1 m, hence, it was assumed that the media capacity did not increase significantly above vessel diameter of 1 m. The scale up capacities were then used to conduct a mass balance on the ion exchange system to determine the time to regeneration. The strategy for cleaning up regenerant from scenario D is similar to scenario C as it too utilizes pressure vessels, the only difference is the frequency of clean-up. Media replacement is based on 600 regeneration consistent with previously reported data (Hans *et al*., 2016).

Table 5.4 Operational parameters for sodium hydroxide clean up system for fixed bed system.

Design Parameter	Unit	EBCT (minutes)						Reference
		0.5	1	3	5	7	10	
General								
NaOH concentration	%	4						(Martin, 2010)
Empty bed contact time	minutes	20						(Martin, 2010)
Calcium required		Ca:P = 0.5						
Time to regeneration	days	2.85	6.66	20.0	36.1	50.6	72.2	(Chapter 4; Martin *et al*., 2013)
2,000 PE								
Time between regen clean up	days	29	67	200	361	506	722	Calculated
Clean-up tank size	m^3	1	2	7	10	15	20	Assumed
$CaPO_4$ precipitated per clean up	kg	15	35	103	187	262	374	Calculated
20,000 PE								
Time between regen clean up	days	86	60	60	72	51	72	Calculated
Clean-up tank size	m^3	11	20	20	20	25	25	Assumed
$CaPO_4$ precipitated per clean up	kg	443	310	310	374	785	785	Calculated

5.4 Economic evaluation

The capital (CAPEX) and operating (OPEX) costs were calculated in British Pound Sterling (£) and converted to 2017 using an inflation calculator with estimated costs obtained from cost curves, literature and water company data (Table 5.5). The costing has been limited to major plant items, excluding influent and effluent pipework. To ensure consistency of approach the cost estimates have been based on component parts as opposed to combined unit quotes. Some items were only available in aggregated form (including design, overheads etc..) and so where adjusted by applying a scaling ratio. The ratio was defined as the cost of a depth filter from an aggregated quote divided by the estimate by the

approach taken presently. The scaling ratio was 1/2 and this was applied to all aggregated cost estimates.

Table 5.5 Summary of cost estimates and energy consumption

Parameter	Value	Unit	Notes	Reference
Tanks	711	£.m^3		(Towler and Sinnott, 2013)
Mixer	1,962	£ kW^{-1}		(Towler and Sinnott, 2013)
Vessel	2,175 – 6,525	£.m^{-1}	For vessel diameter between 0.5 – 3 m	(Sinnott, 2005)
Pumps	7,824	£ sec L^{-1}		(Towler and Sinnott, 2013)
Screen	16,321	£ m^2		(Loh, Lyons and White, 2002)
Bag filter	7.52	£ bag^{-1}		(Cole-Parmer scientific experts, 2017)
Electricity	0.085	£ kWh^{-1}		(Whitton, 2016)
Labour	26.50	£ $hour^{-1}$		(Jenkins, 2017)
$FeCl_3$	290	£ ton^{-1}	Industrial bulk purchase	(Whitton, 2016)
Sand	175	£ ton^{-1}		(Personal communication Kate Silby)
HAIX media	13.5	£ $litre^{-1}$		LayneRT quotation
Sodium Hydroxide	275	£ ton^{-1}	Industrial bulk purchase	(Alibaba, 2017)
Lime	600	£ ton^{-1}	Industrial bulk purchase	(Mistralni, 2017)
Calcium phosphate	300	£ ton^{-1}	Industrial bulk purchase	(Alibaba, 2017)

5.4.1 Sensitivity analysis

Sensitivity analysis was completed on the key major component contributing to the CAPEX and OPEX for scenario C and D. This was done by changing one key parameter by increments of 10% from current costs while keeping all other costs fixed. The chosen components were dependant on what percentage they contribute to CAPEX and OPEX for the two different PEs.

5.4.2 Whole life cost estimate

The whole life cost is made up of initial capital cost and the operating cost for the life span of the plan. The whole life cost period has been taken as 25 years for all the analysed scenarios at a discount rate of 5%.

$$\text{Whole life cost (£)} = \text{CAPEX} + (\text{OPEX} \times 14) \qquad \textbf{Equation 11}$$

5.5 Results and Discussion

5.5.1 Capital cost estimates

In the case of the 2,000 PE works, the capital cost estimate for the four benchmark scenarios were £0.38M, £0.30M, £0.19M and £0.20M for scenarios A (cloth plus depth filter), B (two depth filters), B1 (single depth filter) and D (suspended IEX) respectively (Figure 5.2). In comparison, the CAPEX of the fixed bed IEX plant (scenario C) decreased from a high of £0.396M at an EBCT of 10 minutes to a low of £0.136M at an EBCT of 30 seconds. Consequently, the capital cost of the systems was lower than the other options at different critical EBCTs of 9.4 minutes, 6.3 minutes, 2.1 minutes and 4.9 minutes respectively. The difference between scenarios A-B1 is in the clarification process which represents the major cost item in all three scenarios. To illustrate, the depth filter constitutes 63 % of the total CAPEX in the single stage systems and this increases to 77 % and 88 % for the two-stage depth filter (scenario B) and the cloth filter followed depth filter (scenario A), respectively. The two stage systems are deemed necessary when meeting a 0.1 mg P L^{-1} consent (Smith *et al.*, 2017; Brookes and Barter 2017) enabling the EBCT that delivers CAPEX neutrality to extend by 360 % and 195 % for the use of a second depth filter with a cloth filter or a depth filter, respectively.

Component analysis of the capital cost of the fixed bed exchanger reveals the increasing significance of the media and vessels costs as the EBCT is increased (Figure 5.3). To illustrate, the media costs represent 6.6 % of the total costs at an EBCT of 30 seconds whereas at an EBCT of 10 minutes this has increased to 45.7 %. At the lower EBCTs the capital cost is dominated by the costs associated with the pumps, drum filters and regeneration liquid clean up. Technical analysis

of the system suggests that EBCTs of around 5 minutes are preferred to ensure good mass transfer wave fronts (Chapter 4). At this EBCT, the media and the vessels account for 33.2 and 9.1 % of the capital costs of the system which in total is about the same as the suspended ion exchanger.

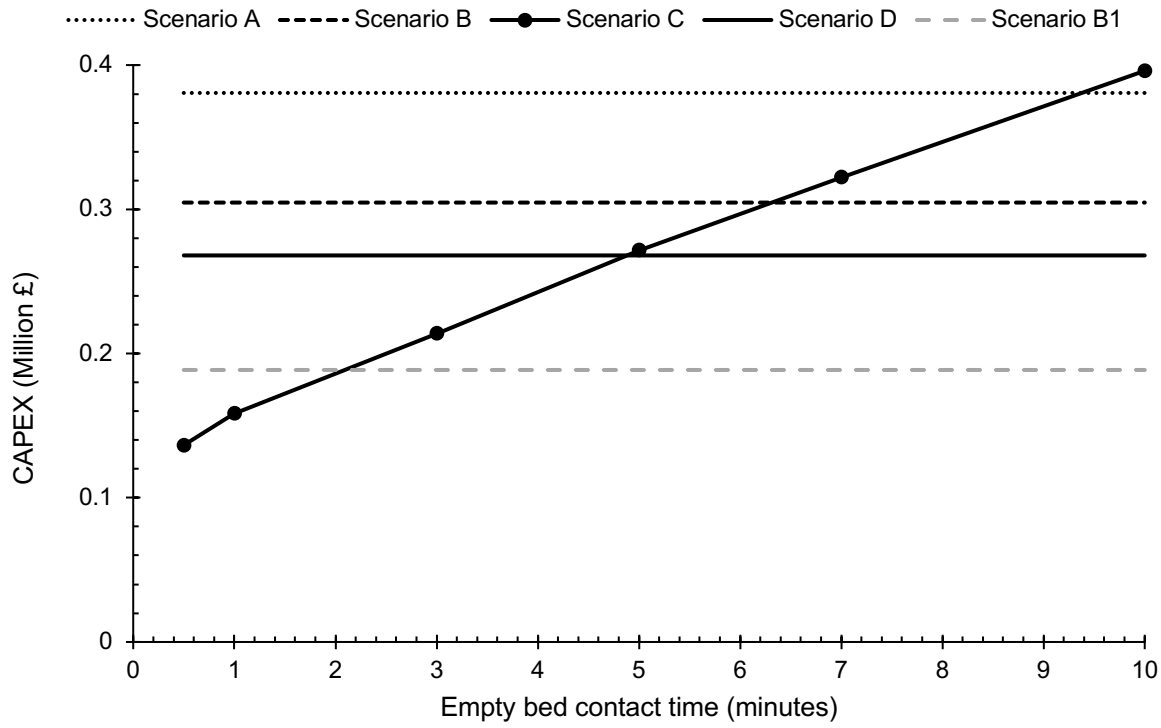

Figure 5.2 Capital cost for 2,000 PE for scenarios (A) coagulation with two stage filtration [cloth filter followed by a depth filter], (B) coagulation with two stage depth filtration, (B1) coagulation with single stage depth filtration (C) fixed bed ion exchange and (D) suspended ion exchange.

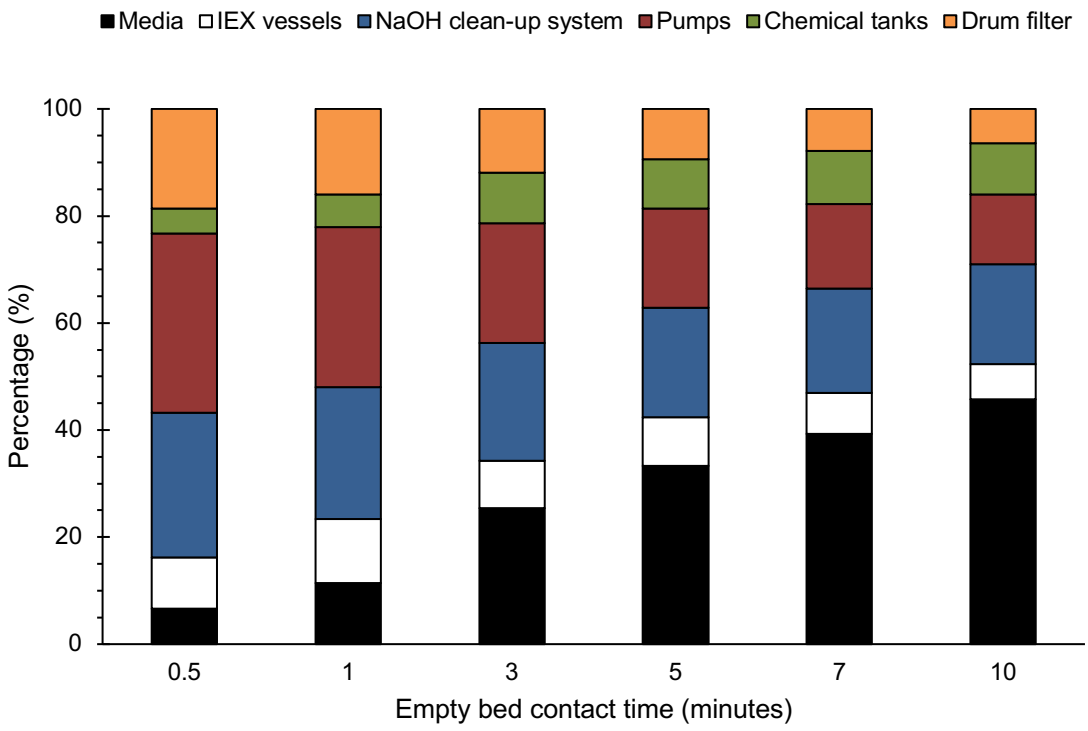

Figure 5.3 Contribution of major equipment to the CAPEX for Scenario C (fixed bed ion exchange system) for 2,000 PE for the different EBCTs

In comparison, for the 20,000 PE works, the capital costs of the base cases are relatively more favourable than for the fixed bed adsorber (Figure 5.4). For example, the capital costs of scenario A was £0.78M with a capital cost neutrality to the ion exchanger at an EBCT of 3 minutes. This represents 21 % of the critical EBCT for the 2,000 PE case. Similar, but less dramatic changes were seen for the single and dual depth filters (Scenarios B and B1) which had capital costs estimates of £0.9M and £0.6M respectively with corresponding critical EBCTs for cost neutrality of 3.8 and 1.4 minutes. The most expensive system was the suspended IEX (Scenario D) with a capital cost estimate of £1.0M and a critical EBCT for cost neutrality of 4.3 minutes.

Analysis of the cost components reveals a much greater significance with regards to the cost of the media and the associated reactor vessels (Figure 5.5). To illustrate, the media costs represents 13.5, 42.7 and 52% of the total capital cost at EBCTs of 30 seconds, 3 minutes and 10 minutes respectively. In addition, the vessel contributes another 28, 22 and 27 % of the total costs. The contribution

and actual costs varies in a non-linear manner with EBCT as both the vessel dimensions and number of vessel is changing. For instance, at an EBCT of 30 seconds, four 2 m diameter vessels are required. This increased to four 3 m diameter columns at an EBCT of 3 minutes and eleven 3 m diameter vessels at an EBCT of 10 minutes. This compares to the 2,000 PE works where two tank vessels are required, a duty and a standby for all EBCTs.

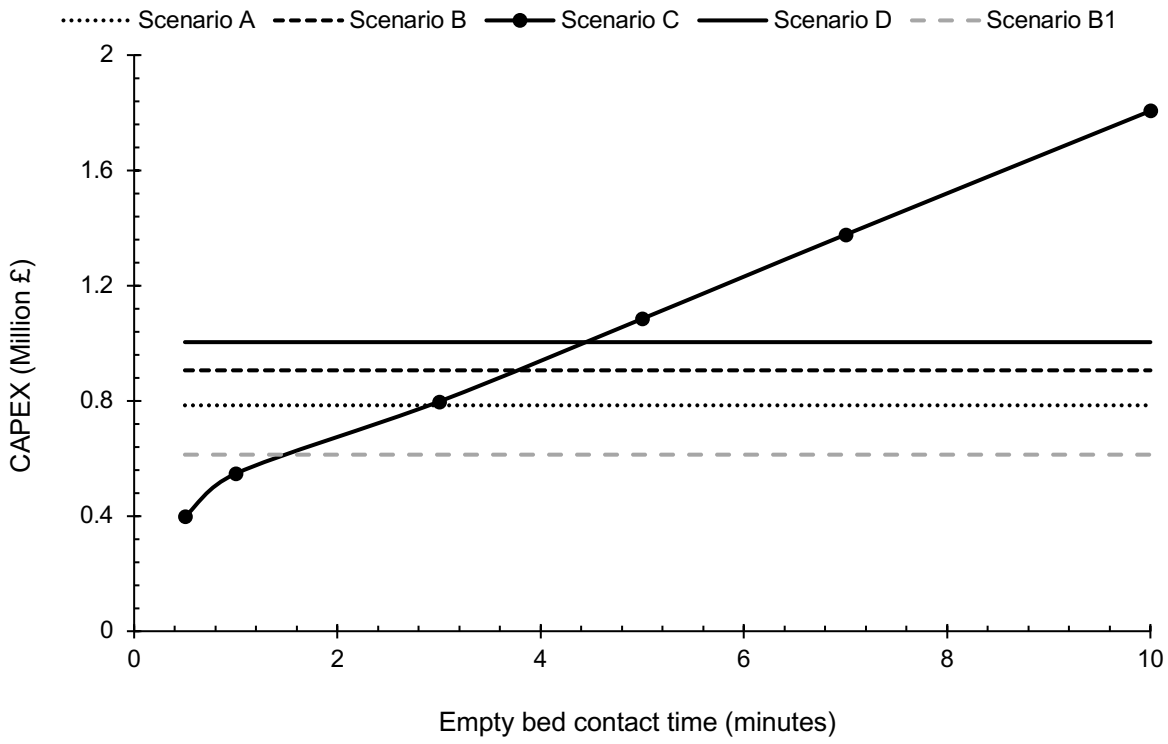

Figure 5.4 Capital cost for 20,000 PE for scenarios (A) coagulation with two stage filtration [cloth filter followed by a depth filter], (B) coagulation with two stage depth filtration, (B1) coagulation with single stage depth filtration (C) fixed bed ion exchange and (D) suspended ion exchange.

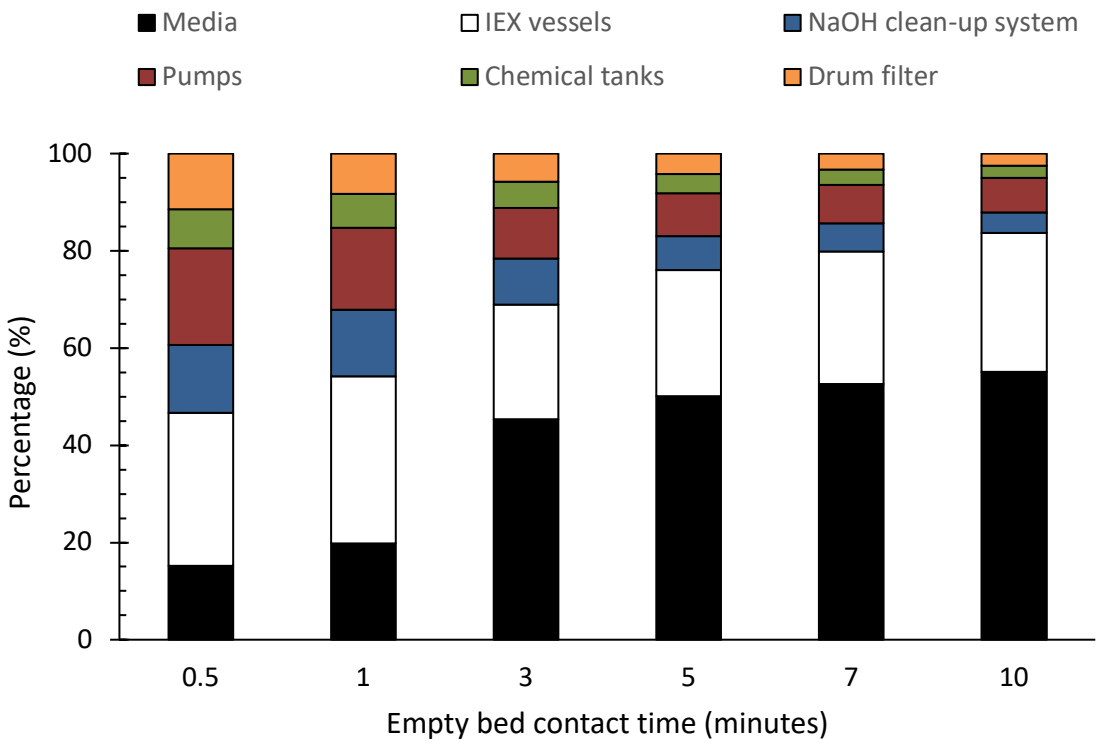

Figure 5.5 Contribution of major equipment to the CAPEX for Scenario C (fixed bed ion exchange system) for 20,000 PE for the different EBCTs.

5.5.2 Sensitivity analysis

The media is the most expensive component of the systems at high EBCTs for the small works and at EBCTs of 3 minutes or above for the 20,000 PE. The media is currently sourced from the United States where it is used for arsenic removal and production capacity is relatively low. Both aspects suggest the potential for cost reduction going forward, especially if the technology becomes an accepted option. Delivery of the media from United States to United Kingdom makes up about 30% of media's cost. Large scale production of the media too can also be expected to have a reasonable impact. A common analogy used in the impact of mass production is the F-150 truck manufactured by the Ford motor company. When producing 10,000 units, the cost of $30,000/unit reduced to 50% ($15,000/unit) once production had increased to 100,000 units (Walker, 2015). Further the innovative nature of the technology means that further development will likely reduce costs down through optimisation and experience (Neij, 2008) which can be cautiously assigned as a 10% reduction per decade. This will likely

come from better designs of the screens and the pumping systems to better use the modular nature of the tanks. Analogy can be found with membrane systems used in membrane bioreactors which have seen a progressive incremental decrease in energy demand through optimisation and innovation of the distribution and sparging systems. Overall, a cost reduction of the media of between 30-60% can be cautiously expected.

The impact of change in media costs depends on the operational EBCT due to its importance on deciding the relative cost by component made up of by the media. For instance, for the 2,000 PE works, a 50% reduction in media cost reduces the overall CAPEX from £0.136M to £0.132M at an EBCT of 30 seconds compared to from £0.39M to £0.305M at an EBCT of 10 minutes (Figure 5.6). The forecasted change is sufficient to extend the EBCT for cost neutrality to 7 minutes when comparing to the scheme that will consistently meet the standard (Scenarios A, B and D). Similarly, for the 20,000 PE works, the reduction in media costs generates a capital cost reduction of £0.03M, £0.27M and £0.5M for EBCTs of 30 seconds, 5 minutes and 10 minutes respectively. The impact is again to extend the critical EBCT but not by such a large extent. A 50% reduction in media cost would enable capital cost neutral operation against the dual depth filter and suspended systems at EBCTs between 5 and 7 minutes. However, comparison to the single stage filtration systems suggests that the reduction increases the critical EBCT to around 2 minutes.

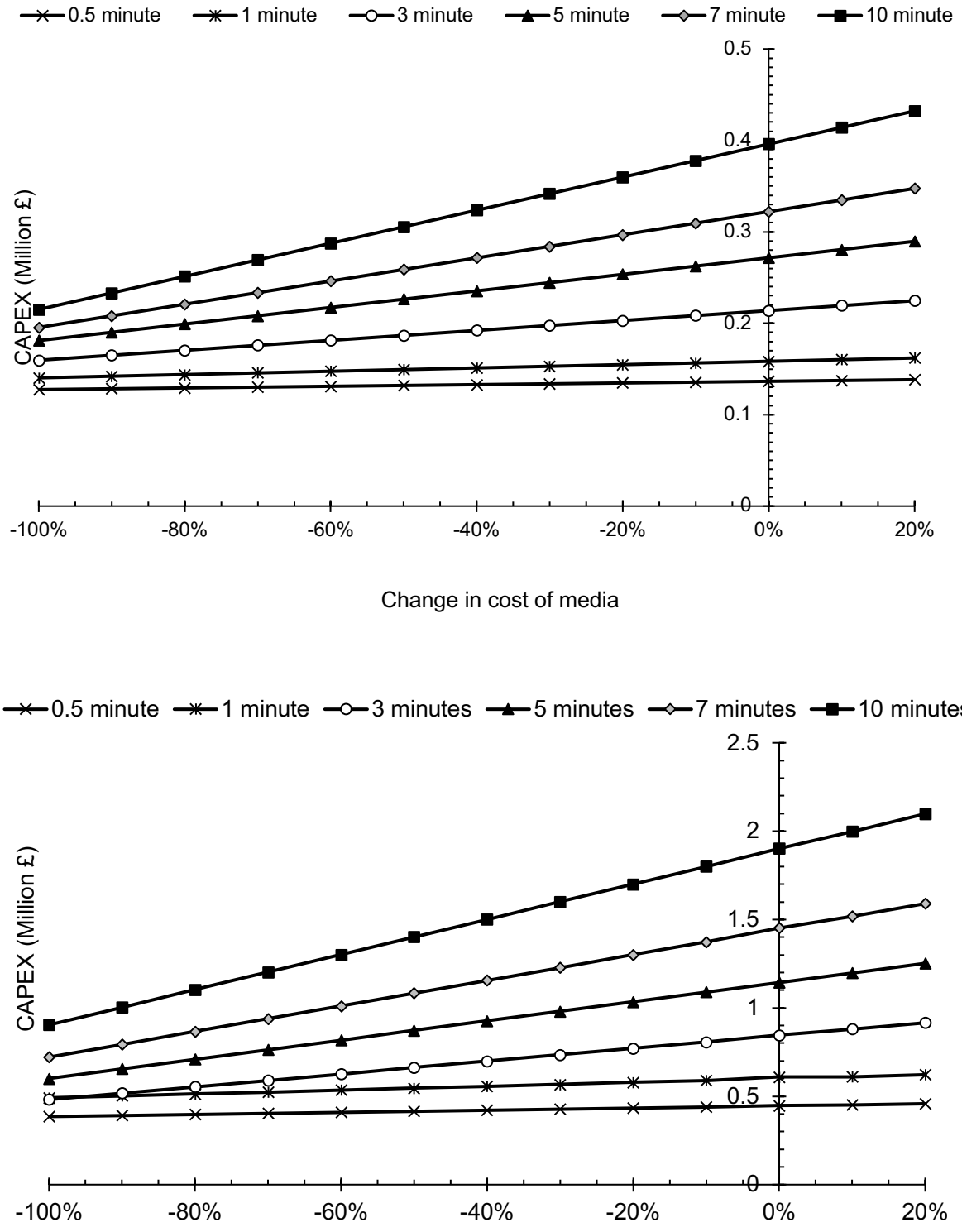

Figure 5.6 Change in CAPEX of scenario C (fixed bed ion exchange system) with reducing cost of HAIX media for (a) 2,000 PE and (b) 20,000 PE.

5.5.3 Operational cost estimates

The operating costs for the 2,000 PE works were £18,155, £18,752, £14, 526 and £16,905 per year for scenarios A, B, B1 and D respectively. In comparison, the operating cost of the fixed bed adsorber decreased as a function of EBCT from £7615 $year^{-1}$ at an EBCT of 30 seconds to £4476 $year^{-1}$ at an EBCT of 10 minutes (Figure 5.7). Analysis of the cost components reveals the major cost item to be labour through regular site visits / maintenance and the collection and management of the precipitated calcium phosphate. However, the higher OPEX at the very low EBCTs is generated by a requirement to replace the media after 4.5 years and 10.9 years at EBCTs of 30 seconds and 1 minute respectively. This is based on the criteria to replace the media every 600 regenerations (Hans *et al.*, 2016) which does not occur at EBCTs of 3 minutes and above. Comparison to use of IEX media elsewhere indicates a regeneration frequency of 6-7 years which would decrease OPEX for the low EBCTs but increase it for the higher ones. Overall, the OPEX of the fixed bed adsorber is substantially lower than that for the coagulation-based systems where the coagulant represents between 44 and 71 % of the total OPEX.

In comparison, for the 20,000 PE works, the electricity costs associated with the pumps and the drum filters become the most critical OPEX component constituting between 21 and 60 % of the total OPEX per year (Figure 5.7). The lower values represent the low EBCT where media replacement has a big impact providing 49 and 32% of the total OPEX at EBCTs of 30 seconds and 1 minute. Overall the OPEX varied between £24,434 $year^{-1}$ and £11,564 $year^{-1}$ as the EBCT increased from 30 seconds to 10 minutes. The equivalent OPEX for the bench mark cases were £153,563 $year^{-1}$ for the cloth filter and depth filter, £183,689 $year^{-1}$ for the dual stage depth filter and £145,579 $year^{-1}$ for the single stage filter. Accordingly, the OPEX of the fixed bed adsorber was at worst only 17 % of the OPEX of the alternative systems.

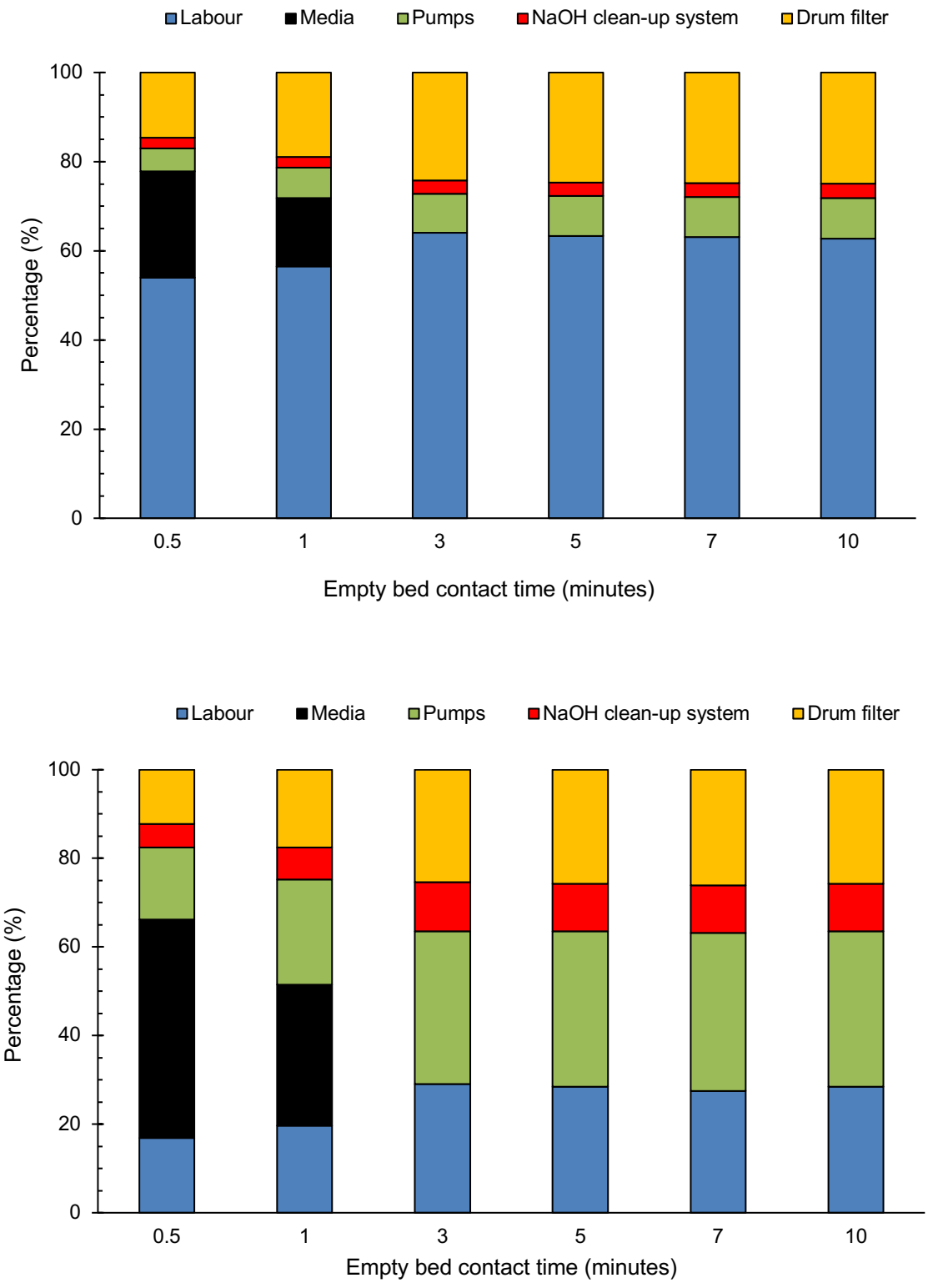

Figure 5.7 Contribution of major equipment to the OPEX for scenario C (fixed bed ion exchange system) for (1) 2,000 PE and (2) 20,000 PE works at empty bed contact time, A) 0.5, B) 1, C) 3, D) 5, E) 7 and F) 10 minutes.

5.5.4 Regeneration liquid clean up strategy

A major issue with using ion exchange systems is the management of the regeneration liquids (Martin, 2010). Previous work with the hybrid ion exchange resins used in the current study have shown the need to reuse and recycle the regeneration liquid. The inclusion of a regeneration system and a clean-up system for the regeneration process are significant aspects of the use of the technology that requires storage of potentially hazardous chemicals (sodium hydroxide at pH 14). The EBCT has an impact on both the service time between regenerations and the time before the regeneration liquid requires clean up (Table 5.5). For instance, service time between regenerations changes between 2.8, 6.6, 20, 36, 50 and 72 days for EBCTs of 0.5, 1, 3, 5, 7 and 10 minutes, respectively. Importantly at regeneration cycles of over 30 days, the use of a mobile unit transported to site becomes a possibility. This is especially true for the small works where a mobile unit could service several works in a local area. At the 2,000 PE scale, the impact of EBCT on the frequency of regeneration clean-up is very significant with cycle times of 29, 67, 200, 301, 506 and 722 days between clean ups. In such cases a mobile unit becomes more appropriate to avoid building permanent infrastructure for occasional activities. The concept was explored by comparing the capital cost of a permanent or a mobile regeneration liquid clean up system. The key difference was assumed to be that the mobile unit was contained within a 20 foot van (£17,995; Gumtree, 2017). Analysis of the comparison between mobile and permanent clean up facilities indicates that the cost of the mobile unit increased the total CAPEX from £64,746 if sized for the 0.5 minute EBCT to £101,972 for the 10 minute EBCT. This represented 137 % of the cost of the fixed unit at an EBCT of 10 minutes and 175% at an EBCT of 30 seconds. Consequently, the cost of the clean-up systems would break even if it served two sites. The other factor to consider is available potable water for the permanent installation as many small works do not currently have mains connections. To illustrate, if a water connection is already available, for 2,000 PE site, the clean-up system contributes between 27% - 19% to CAPEX. However, if a water connection is not available, it can cost up to £23,500 to install one

increasing the cost contribution of the clean-up systems to between 23% and 38%.

In the case of the 20,000 PE site, the volume of regeneration liquid required makes the use of a mobile unit for regeneration impractical. However, the clean-up system still provides an alternative option especially as it provides a method of collection of the precipitated material. Based on an assumption of 80 % recovery of the removed phosphorus every time the regeneration liquid is cleaned up the mass of produced calcium phosphate per clean up varies between 15 and 374 kg for the 2,000 PE works and between 310 and 785 kg for the 20,000 works.

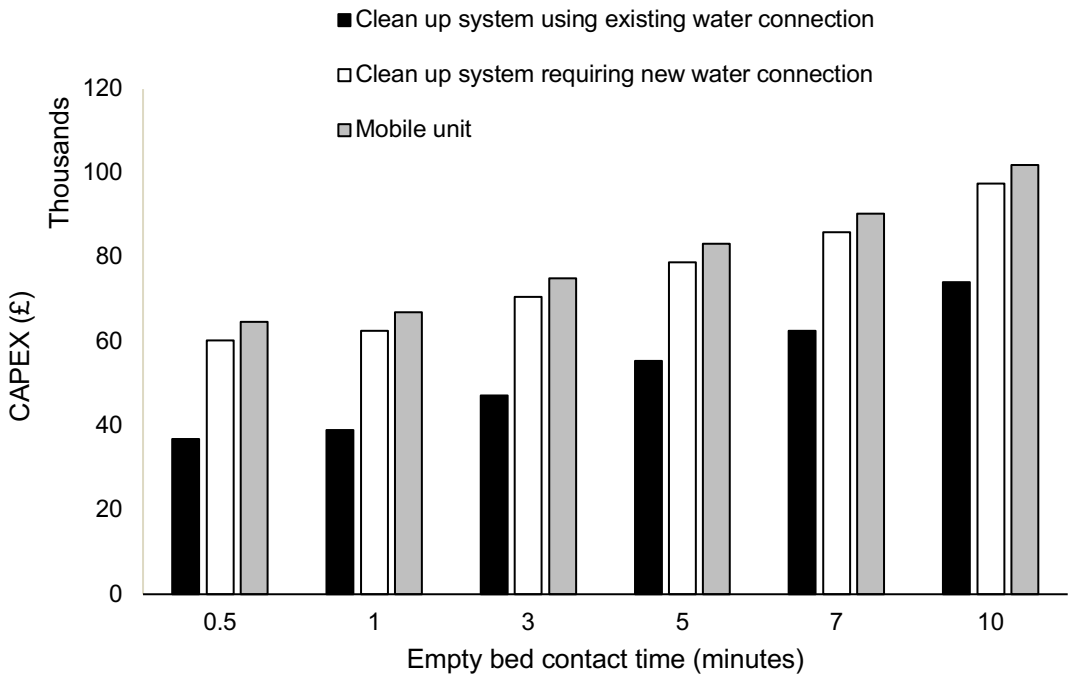

Figure 5.8 Different options for sodium hydroxide clean-up systems for 2,000 PE WWTW.

5.5.5 Whole life cost

Combining the capital and operating costs based on a 25-year life at a discount rate of 5 % resulted in whole life costs of £0.63M, £0.567M, £0.39M and £0.5 M for scenarios A, B, B1 and D respectively for the 2000 PE works. In comparison, the WLC of the fixed bed IEX plant varied with EBCT from £0.243M to £0.458M

as the EBCT increased from 30 seconds to 10 minutes. Accordingly, the hybrid ion exchange system configured as a fixed bed IEX system generated a lower WLC than all the alternative solutions that would consistently deliver against a 0.1 mg P L^{-1} target. At a 5 minute EBCT, the WLC of the fixed bed IEX system was 53%, 59% and 67% of the alternatives. Observed differences of 30% are generally considered to be significant in this type of analysis (Towler and Sinnott., 2013) so overall confidence can be assigned to there be a plausible economic basis for use of the technology for tertiary P removal from small sewage works. The equivalent level of difference with the single stage filtration systems occurs once the EBCT was reduced to 3 minutes. The total costs of the systems were seen to reduce with EBCT which reflects the significance of the CAPEX on the overall cost. To illustrate, CAPEX contributed 76% of the overall cost. This compares to the use of coagulant based systems where the CAPEX constituted between 48 and 52% of the WLC.

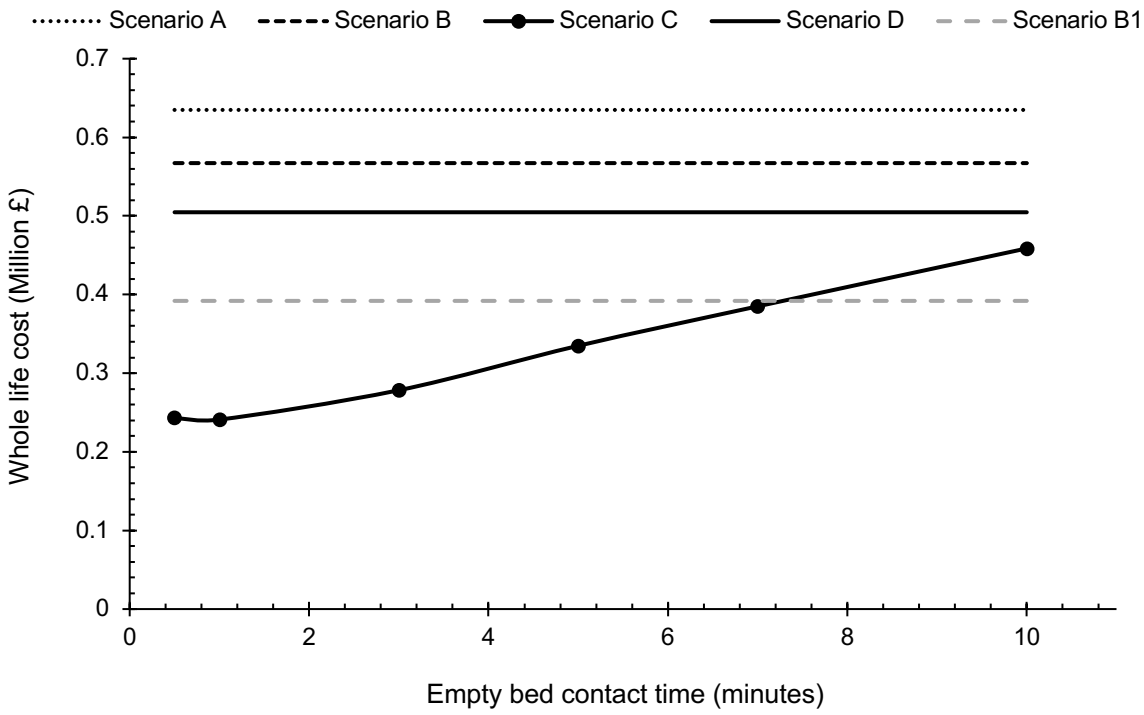

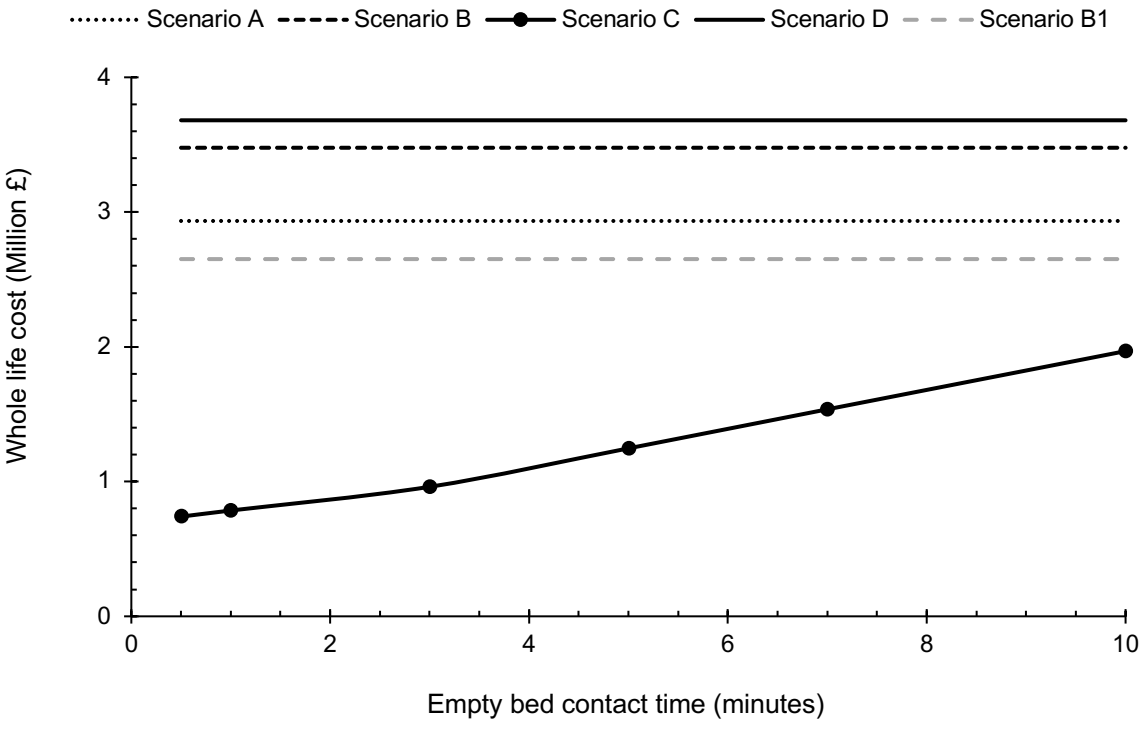

Figure 5.9 Whole life cost for scenarios (A) coagulation with two stage filtration [cloth filter followed by a depth filter], (B) coagulation with two stage depth filtration, (B1) coagulation with single stage depth filtration (C) fixed bed ion exchange and (D) suspended ion exchange at (a) 2,000 PE and (b) 20,000 PE.

Comparative analysis for the 20,000 PE works provides a similar outcome with the WLC of the fixed bed IEX system representing 44 %, 37 % and 34 % of scenarios A, B and D. Overall the fixed bed IEX system has a lower WLC at all EBCTs against all scenarios including the single stage filtration (B1). However, to have a 30 % difference the EBCT needed to be around 7 minutes. The difference reflects the greater contribution of OPEX for the coagulant based scenarios at the larger scale. For instance, coagulant constituted 74 % and 77 % of the OPEX for the two-stage and one stage depth filtration systems respectively.

The overall outcome from the economic analysis is that the use of the fixed bed IEX system appear economically plausible for tertiary P removal from 1 mg P L^{-1} down to below 0.1 mg P L^{-1}. The analysis above has not taken into account the potential for cost reduction in the novel component of the system and the potential optimisation that will occur once the system becomes operational. For instance, if the 50% reduction in media cost was applied. The WLC for the 2,000 PE site at an EBCT of 10 minutes would be reduced by £90,000 (21 %) down to £332, 293. The equivalent saving for the 20,000 PE site is £410,000 which can be considered to provide further confidence in the economic plausibility of the technology.

5.6 Conclusions

- The use of hybrid resin in fixed bed IEX systems appears economically plausible as a tertiary P removal process to enable effluent to be reduced from 1 mg P L^{-1} to less than 0.1 mg P L^{-1}.
- HAIX is more economical to operate at lower empty bed contact times due to the impact of the cost of the vessels and the media. Although the system is economically plausible at all the EBCT analysed for (0.5 to 10 minutes)
- The strategy for clean-up of sodium hydroxide is dependent on the size of the treatment works. For smaller sites, around 2,000 PE, a more economical strategy would be to have a mobile clean-up system that can be used for multiple sites. For medium size works, 20,000 PE, having an on-site clean up system would be more beneficial due to the practicality of the amount of sodium hydroxide that will need to be cleaned before reuse.

5.7 Acknowledgements

The authors gratefully acknowledge financial support from the Engineering and Physical Sciences Research Council (EPSRC) through their funding of the STREAM Industrial Doctorate Centre, and from the project sponsors Anglian Water, Severn Trent Water. Scottish Water, Thames Water, Yorkshire Water and Wessex Water for their financial and technical support throughout the project.

5.8 References

Alibaba (2017) *Weifang Zhongliang Chemical Co., Ltd*. Available at: https://www.alibaba.com/product-detail/Top-factory-directly-low-price-caustic_60492577957.html?spm=a2700.7724857.main07.33.cb5c502jlr6LZ&s=p (Accessed: 5 July 2017).

Andritz (2015) *YU vacuum drum filter High-capacity vacuum*. Available at: https://www.andritz.com/resource/blob/13392/f5090e11ad8fd07e50954455cbfdee20/se-yu-drum-filter-data.pdf (Accessed: 10 August 2017).

Twort, A. C., Ratnayaka, D. D., and Brandt, J. (2017) *Twort's Water Supply (7th Edition)*. Elsevier.

Brookes, A. and Barter, P. (2017) 'Chemical Investigations Programme 2 DynSand Oxy for combined Phosphorus and Ammonia removal: experiences from Anglian Water', in *The Big Phosphorous Conference*. Manchester.

Cadee, K., Leary, B. O., Smith, P., Slunjski, M. and Bourke, M. (1998) 'World's First Magnetic Ion Exchange (MIEX ®) 1 Water Treatment Plant to be Installed in Western Australia', p. 11.

Chowdhury, Z. K., Chinn, T. D., Black, B., Perry, S. A. L. and Foundation, A. R. (2002) *Implementation of Arsenic Treatment Systems: Design considerations, operation and maintenance*. AWWA Research Foundation and American Water Works Association (Implementation of Arsenic Treatment Systems Part 2: Design Considerations, Operation and Maintenance).

Cole-Parmer scientific experts (2017) *Hayward F3AB00002E double-length bags; 25 µm, 50/pack*. Available at: https://www.coleparmer.co.uk/i/hayward-

f3ab00002e-double-length-bags-25-m-50-pack/2999078 (Accessed: 10 August 2017).

Crittenden, J. C., M. W. H., Trussell, R. R., Hand, D. W. and Howe, K. J. (2012) MWH's Water Treatment: Principles and Design. Wiley.

De Kock, L.-A. (2015) *Hybrid ion exchanger supported metal hydroxides for the removal of phosphate from wastewater*. University of Johannesburg (PhD Thesis).

Desilva, F. (2011) Protecting ion exchange resins from suspended solids. Available at: https://www.wqpmag.com/protecting-ion-exchange-resins-suspended-solids (Accessed: 17 August 2017).

Desilva, F. and Galleti, C. (2005) *Resin Regeneration - More Than Meets The Eye*. Available at: https://www.wqpmag.com/resin-regeneration-more-meets-eye (Accessed: 17 August 2017).

Five Star Filtration (2014) 'Five Star Disk Filter'. Available at: http://www.5starfiltration.com/FSF-Disk_Filter_Brochure.pdf (Accessed: 5 August 2017).

Furuya, A., Calciano, G., Richard, D., Caliskaner, O. and Govea, P. (2005) 'Evaluation and Design of a Cloth Disk Filter To Meet Title 22 Reuse Criteria', *Proceedings of the Water Environment Federation*, 2005(9), pp. 6152–6164.

Gumtree (2017) *Ford Transit 3.5T 20ft 6m Curtain Side 20FT*. Available at: https://www.gumtree.com/p/vans/ford-transit-3.5t-20ft-6m-curtain-side-20ft-new-body-/1242842222 (Accessed: 10 July 2017).

Hans, R., Senanayake, G., Dharmasiri, L. C. S., Mathes, J. A. P. and Kim, D. J. (2016) 'A preliminary batch study of sorption kinetics of Cr(VI) ions from aqueous solutions by a magnetic ion exchange (MIEX®) resin and determination of film/pore diffusivity', *Hydrometallurgy*, 164, pp. 208–218.

Jenkins, N. (2017) *Vertical Flow Wetlands for Tertiary Wastewater Treatment*. Cranfield University (EngD Thesis).

Koreman, E. and Galjaard, G. (2016) ‘NOM-removal at SWTP Andijk (Netherlands) with a New Anion Exchange’ (Report).

Loh, H. P., Lyons, J. and White, C. W. (2002) *Process Equipment Cost Estimation Final Report*. Available at: https://www.osti.gov/scitech/servlets/purl/797810 (Accessed: 28 July 2017).

Martin, B. D. (2010) *Removal and Recovery of Phosphorus from Municipal Wastewaters using a Ferric Nanoparticle Adsorbent*. Cranfield University (PhD thesis).

Martin, B. D., De Kock, L., Gallot, M., Guery, E., Stanowski, S., MacAdam, J., McAdam, E. J., Parsons, S. A. and Jefferson, B. (2017) ‘Quantifying the performance of a hybrid anion exchanger/adsorbent for phosphorus removal using mass spectrometry coupled with batch kinetic trials’, *Environmental Technology*, In Press.

Martin, B. D., De Kock, L., Stephenson, T., Parsons, S. A. and Jefferson, B. (2013) ‘The impact of contactor scale on a ferric nanoparticle adsorbent process for the removal of phosphorus from municipal wastewater’, *Chemical Engineering Journal*, 215–216, pp. 209–215.

McLeod, A., Soares, A. and Jefferson, B. (2017) *Control of competitive precipitation for chemically efficient orthophosphate (PO4-P) removal and recovery by selective ion exchange,* (working paper).

Mistralni (2017) *Calcium Hydroxide - Hydrated Lime*. Available at: https://mistralni.co.uk/products/calcium-hydroxide-hydrated-lime (Accessed: 5 July 2017).

Murray, B., Pieterse, S., Raymer, D. and Swartz, C. (2005) *An Evaluation of Miex® Resin Technology for Potable Treatment of Highly Coloured Raw Waters Throughout the Cape Region of South Africa* (Report).

O’Shea, M. G., Dahlke, T., Staunton, S. P., Pope, G. M. and Holmquist, A. (2008) ‘Evaluation of a magnetic ion exchnage (MIEX ®) resin for decolorisation

applications within a raw sugar factory, *Australian Society of Sugar Cane Technologists*, 30, pp. 536–546.

Parkson (2010) 'DynaSand Continuous, Upflow, Grandular Media Filter'. Parkson.

Sinnott, R. K. (2005) *Coulson & Richardson's Chemical Engineering Design*, *ELSEVIER - Coulson & Richardson's Chemical Engineering series*.

Slunjski, M., Cadee, K. and Tattersall, J. (2000) 'MIEX resin water treatment process', *Proceedings of Aquatech*.

Smith, L., Moreta, E. A., Gardner, P. and O'Brien, L. (2017) 'Phosphorus removal at an ASP and Filter WOrks using MEcana Filter Technology - findings and experience from CIP P trials', in *The Big Phosphorous Conference*.

Tchobanoglous, G., Burton, F. L., Stensel, H. D. and Eddy, M. & (2003) *Wastewater Engineering: Treatment and Reuse*. McGraw-Hill Education (McGraw-Hill higher education).

Towler, G. P. and Sinnott, R. K. (2013) *Chemical engineering design : principles, practice, and economics of plant and process design*. Butterworth-Heinemann.

Vale, P. (2017) 'Applying a circular economy model to wastewater treatment', in *WWT Wastewater*. Birmingham.

Walker, N. (2015) *Reaping the benefits of economies of scale*. Available at: https://www.manufacturingchemist.com/technical/article_page/Reaping_the_benefits_of_economies_of_scale/104670 (Accessed: 5 July 2017).

Wert, E. C., Edwards-Brandt, J. C., Singer, P. C. and Budd, G. C. (2005) 'Evaluating magnetic ion exchange resin (MIEX ®) pretreatment to increase ozone disinfection and reduce bromate formation', *Ozone-Science & Engineering*, 27(5), pp. 371–379.

Whitton, R. L. (2016) *Algae Reactors for Wastewater Treatment*. Cranfield University (EngD Thesis).

Woodard, S., Berry, J. and Newman, B. (2017) ‘Ion exchange resin for PFAS removal and pilot test comparison to GAC’, *Remediation Journal*, 27(3), pp. 19–27.

Woumfo, E. D., Siéwé, J. M. and Njopwouo, D. (2015) ‘A fixed-bed column for phosphate removal from aqueous solutions using an andosol-bagasse mixture’, *Journal of Environmental Management*, 151, pp. 450–460.

Chapter 6. Implications of the work: Overall perspective on the appropriateness of HAIX media for wastewater treatment in the UK

The overall aim of the project was to understand and critically evaluate the technical and economic challenges with implementation of hybrid anion exchanger (HAIX) media for removing phosphorus from wastewater. Currently wastewater treatment sites can be divided into two categories: (a) sites with technologies currently designed to remove phosphorous (chemical or biological) in order to meet a consent of 2 mg P L^{-1} for 10,000-100,000 population equivalent and 1 mg P L^{-1} for population equivalent larger than 100,000 (Martin, 2010) and (b) site with no P consent, mainly small rural works and coastal discharges. The onset of the Water Framework Directive means that these consents are expected to be lowered, some to as low as 0.1 mg L^{-1}, and new consents are expected to be introduced on sites that were previously exempt (Vale, 2017). Accordingly, the work within this thesis has explored two potential applications of the HAIX technology through a combination of technical and economic analysis:

(1) As a tertiary P removal process reducing the concertation from 1 mg P L^{-1} to 0.1 mg L^{-1}

(2) As the main P removal process reducing the P concentration from 6-8 mg P L^{-1} to either 1 mg P L^{-1} or 0.1 mg P L^{-1}.

6.1 What can HAIX do?

The key observation from the experimental testing is that the HAIX media is able to effectively deliver both the full load and the polishing applications down to a 0.1 mg P L^{-1} standard (Chapter 4). The effluent concentration remained stable in the small column set up even when the feed concentration varied (Figure 4.1). The stability of performance against a variation in feed can be expected to increase as the scale of operation is increased and as such confidence can be assigned to the technology providing a robust and resilient solution to meet low P discharges. This provides contrast to recent reports of the resilience of coagulation dosing followed by single stage clarification (cloth or depth filter) which were reported to be able to meet the 0.1 mg P L^{-1} standard but not do so

resiliently (Brookes & Barter, 2017; Smith *et al*., 2017). Consequently, to meet the very low standards it is possible that two stage clarification processes will need to be adopted to ensure compliance with regards to either phosphorus or residual coagulant (Vale, 2017). Such concerns are significantly reduced when the target discharge consent is 0.3 mg P L^{-1} or above and hence the HAIX technology needs to be considered against both single and dual stage clarification systems.

In addition to the phosphorus removal, the HAIX media was observed to remove organics without it significantly impacting on the phosphorus removal capacity (Chapter 4). Overall, at or beyond an empty bed contact time (EBCT) of 3 minutes, COD removal varied between 42 and 51 % with the profile being most closely mirrored by the protein component (Figure 4.4). For the full load case the removal was reduced to around 20% for the 30 second and 1 minute EBCT and this coincided with an overall poorer mass transfer wave front indicating that higher EBCT should be employed in such applications. The stability of the organics removal was observed over nine cycles in the batch experiments (Figure 3.3) which is congruent with previous findings concerning organics removal when the media was used in conjunction with an anaerobic membrane bioreactor. In that case, the resin consistently removed 20-30 mg COD L^{-1} at an EBCT of 10 minutes which continued beyond the serviceable bed life of the media for phosphorus consistent with the suggestion that the organics are predominately occupying the polymer resin spaces as opposed to the embedded nanoparticles. Accordingly, the resin can be considered as a solution for works that require both phosphorus and organic polishing; this is a situation expected for a number of small rural sewage works. The added value potentially extends to the removal of micro-pollutants. However, no direct measurement was considered within the current work but polymer resins are known to remove organics, especially charged/hydrophobic molecules and as such some removal can be expected (Shon, Vigneswaran and Snyder, 2006).

The key variable for consideration has been identified as the EBCT which influences the mass transfer profile within the media bed impacting the

serviceable bed life between regenerations (Chapter 4) as well as both the capital and operating costs of the system (Chapter 5). In the case of serviceable bed life, this is most apparent in the case of the full load treatment (initial concentration between 5 and 8 mg P L^{-1}) where the serviceable bed life extended from 30 bed volumes at 30 seconds EBCT to 320 bed volumes at 10 minutes EBCT. This equates to requiring regeneration every 15 minutes or 53 hours. Significant difference was observed once the EBCT was 3 minutes or above where the serviceable bed life became 238 bed volumes or 11.9 hours. The service time was significantly extended when operating for a tertiary polish (initial concentration between 1 mg P L^{-1}) where the service time varied between 350 bed volumes to 2141 bed volumes equating to a time between 175 minutes to 357 hours (15 days). The above findings relate to small diameter column with small bed depths and so represents a worst-case scenario of operational performance. For instance, extending bed depth from 7 to 27 cm for the full load case was shown to extend service life from 37 to 217 bed volumes when meeting a target of 1 mg P L^{-1} at an EBCT of 30 seconds. The impact was reduced when considering lower target concentrations or longer EBCT but demonstrates the importance of bed depth when considering full scale systems. In such cases the bed depth is typically 1-2 m (Tchobanoglous *et al*., 2004) and so can be expected to provide significantly longer service times than observed here. Column diameter is also known to impact on operational capacity due to the reduction in axial dispersion as diameter increases. Previous research showed an increase in capacity from 3.37 mg P g_{media}^{-1} to 6.27 mg P g_{media}^{-1} as the column diameter was increased from 15 mm to 500 mm (Martin *et al*., 2013). Accordingly, operational capacities observed in the current work can be considered extremely conservative with at least a doubling in capacity likely when operating at full scale. The outcome of this is that a realistic expectation of operational capacity at full scale is estimated at 4.9 and 6.2 mg P g_{media}^{-1} for the full load and polishing applications at an EBCT of 5 minutes.

6.2 Proposed design guidelines for small and medium works

The main variable in specifying the system is the EBCT, in combination with the concentration being removed, due to its impact on cost, service run time and the time between regeneration liquid clean up (Chapter 5). The specific EBCT selected needs to be considered in relation to those factors and the potential manner in which the regeneration liquid will be cleaned up.

In the case of small rural works, the sites are often remote and unmanned, so the media and sodium hydroxide should last as long as possible before the media needs regeneration and sodium hydroxide needs clean-up. The majority of these applications are likely to require treatment of the full P load and in such cases, it is recommended to extend the EBCT to 10 minutes (Table 6.2). This would set a likely regeneration cycle time of 12 days and a regeneration clean up cycle of 36 days. This is sufficient to consider a mobile regeneration clean up system which could service multiple sites and provide a robust logistic model for the collection of the precipitated calcium phosphate (Chapter 5). However, if the sites only require polishing, a short EBCT could be utilised to reduce total cost without requiring excessive maintenance. In such case an EBCT of 0.5-3 minutes is recommended.

Comparatively, medium sized sites, around 20,000 PE, HAIX are more likely to be polishing the effluent and meeting phosphorus consent around 0.1 mg L^{-1}. Minimisation of the total costs without excessive maintenance can be achieved at very low EBCTs and accordingly it is recommended that an EBCT between 0.5 and 3 minutes is used at full flow to treatment as the WLC is relatively flat over this range (£0.7-1.01M).

Table 6.1 Recommended design parameters for fixed bed systems for small and medium site.

Design parameter	Value			Unit	Notes / Reference
	Small works		Medium works		
Initial phosphorus	6	1	1	mg L^{-1}	
Target effluent phosphorus	1	0.1	0.1	mg L^{-1}	
EBCT	10	0.5	0.5	minute	
No. of vessels	2	2	3	-	One vessel on stand-by.
Media	6.67	0.33	3.33	m^3	Calculated
Vessel diameter	3	1	2	m	(Sinnott, 2005)
Bed depth	0.94	0.42	0.35	m	
Time to regeneration	12	3	3	days	
Time to regenerant clean up	36	28	28	days	

6.3 Economic case for implementation of HAIX.

For HAIX to be applicable it has to be competitive with the most commonly used existing solutions to achieve low phosphorus concentrations. Current practice would suggest that coagulation followed by clarification represents such a benchmark. In the case of 0.1 mg P L^{-1} this may represent a two stage clarification system such as cloth filters or depth filters. At consents levels of 0.3 mg P L^{-1} this will reduce to single stage clarification units. Economic analysis of the systems revealed that the whole life cost for the medium scale works, over a 25-year life at a discount rate of 5 %, is lower than both two stage and single stage clarification systems at EBCTs of 10 minutes or lower (Figure 5.9). In the case of the small works, the HAIX systems had a higher WLC than the single stage system once the EBCT went above 7 minutes. Overall, the economic analysis established that the HAIX systems offers a plausible economic alternative to the conventional solutions. This extends across a range of potential target

phosphorus concentrations but will be most apparent once the target is below 0.3 mg P L^{-1}. Comparison to the coagulation processes revealed that both the CAPEX and OPEX of the HAIX process were lower, depending on EBCT (Figure 5.2,Figure 5.4). Importantly, the relative chemical costs of the coagulant based and HAIX process were £76,255 yr^{-1} and £6,737 yr^{-1} respectively, for 20,000 PE indicating the benefit of switching away from a focus on dosing single use chemicals.

EBCT has a significant impact of the WLC due to its impact on media volume, number and size of vessels, regeneration frequency and regeneration liquid clean up frequency. For instance, below 3 minutes EBCT it is likely that the media will need replacement whereas media life can be expected to extend at the longer EBCT due to the less frequent regenerations (Figure 5.9). However, the cost of media is sufficiently high that reducing the initial volume and replacing remains a more economically appropriate approach to adopt. Overall the WLC will always favour lower EBCT and so selection of the lowest EBCT that can provide the correct level of operability is a key area for future discovery.

One of the most important aspects of economical application of HAIX is to reuse the sodium hydroxide multiple times for regeneration. Sodium hydroxide can be used 10 times to regenerate the media before it is expected to require cleaning. This is achieved by precipitating the recovered phosphate from sodium hydroxide through addition of lime to form calcium phosphate. To carry out regeneration and clean-up, potable water is required for safety shower, dilution of chemicals, and backwashing the media. It is not uncommon for small sewage works to be unconnected to the potable mains which can exert a higher additional cost that may further support the idea of mobile regeneration liquid clean up (Figure 5.8).

Table 6.2 Capital and operating costs for different treatment scenarios for small and medium works including cost of sodium hydroxide clean-up system.

	Polishing (1 to 0.1 mg L^{-1})		Full load removal (6 to 1 mg L^{-1})		Full load removal (6 to 0.1 mg L^{-1})	
	2,000 PE	**20,000 PE**	**2,000 PE**	**20,000 PE**	**2,000 PE**	**20,000 PE**
EBCT (minutes)	0.5	0.5	10	10	10	10
BV_{cycle}	410	410	1,839	1,839	1,733	1,733
$COD_{reduced}$	52%	52%	56%	56%	56%	56%
Recovered calcium phosphate ($kg.year^{-1}$)	189	1,900	1,210	12,079	1,138	11,384
Value of product (£.$year^{-1}$)*	62	627	399	3986	375	3756
% of OPEX	0.8	2.6	4.3	16.2	4.1	15.4
CAPEX (£)	136,467	397,776	382,197	1,818,456	382,197	1,818,456
OPEX (£)	7,615	24,434	9,188	24,666	9,178	24,370
WLC (£)	243,078	739,856	510,834	2,163,788	509,696	2,159,643
Footprint (m^2)	79.2	130	145	255	145	255

*Based on £300/Tonne; 907kg/tonne.

6.4 Role of the circular economic thinking on the suitability of the HAIX process

Currently, most elements of a wastewater treatment works operate on a linear economic model where the chemicals are ‘used and thrown away’ and hence are not economically or environmentally sustainable. Globally, the water sector is starting to question this and explore the potential move towards more “Circular Economy” thinking where resources are used for as long as possible, before recovering, regenerating and reusing them.

The approach to phosphorus management in sewage is a core example of where a switch in thinking may be appropriate within a very short time frame. Phosphorus is a non-renewable resource, essential to human life with limited

remaining reserves (Cieślik and Konieczka, 2016). The reported mass of remaining raw material varies significantly but may be as short as 100-130 years. Action has already been taken with, for instance, the EU deciding to reduce the use of mined phosphate in favour of recycled phosphate from 2014. As such, phosphate rock has been added to the EU list of 20 critical raw materials. Further, this is influencing national policy where phosphate recovery is becoming increasingly required. For instance, in 2016, Switzerland made P-recovery obligatory from sewage sludge and animal waste ash (Thornton, 2017). In 2017, national policies in German government has put forward a legislation to make phosphorus recovery mandatory from sewage works with population equivalent greater than 50,000 (Thornton, 2017).

Common perceptions suggest that recovery imparts a high cost which cannot be recovered from the sale of the products. However, the current economic analysis demonstrates that the HAIX process is economically plausible whilst also providing a recovery route. Critically the economic analysis excluded the value of the recovered product such that the technology was assessed within the current economic framework and so does not require a switch to circular economy thinking to be considered economically appropriate. However, the approach does recover product and hence generates added value. The challenge is that the scale of production is low from a single small or medium sewage works with for instance 1,900 kg generated per year from the 20,000 PE works when HAIX is used for polishing and 12,079 kg per year if treating the full load. The product is used in the formation of fertilisers and phosphoric acid with an estimated bulk sale price between \$290-500.tonne^{-1} (£223-385.tonne^{-1}) (Alibaba, 2017). At this price, the value of the product will reduce the opex costs of running the plant by between 0.8-16.2% (Table 6.1). Consequently, monetary value alone will not be the driver to pursue recovery and reuse of phosphorus from wastewater (Stark, 2004). Indeed, there are remaining legislative barriers that must be overcome before recovered products can be used (Egle *et al*., 2016). However, with the rising cost of conventional phosphate fertilizers, desire for a more sustainable future and recovery legislations the need for technology that can recover as well as remove phosphorus are likely to increase.

6.5 Fixed bed v suspended media systems

The fixed bed adsorber systems require pre-screening of the effluent to remove solids and utilise relatively small contactors (diameters up to 3 m). Both represent challenges that require reflection. One potential solution that has been adopted in drinking water treatment is the use of suspended ion exchange systems which can handle higher solid loads and operate in relatively big single contactors. Illustrative systems include MIEX^{TM} and the SIX^{TM} process both used for organic removal (Cadee *et al*., 1998; Murray *et al*., 2005; O'Shea *et al*., 2008; Slunjski *et al*., 2000). To date no information exists on the efficacy of the approach for phosphorus removal but if standard operating conditions used in drinking water are applied a comparative assessment can be made (Chapter 5). In the economic analysis, the contact time was fixed at 15 minutes but if it is varied in similar manner to the EBCT of the fixed bed systems then direct comparison is possible (Figure 6.1). In such cases the WLC costs of the two approaches appear similar with a marginal lower WLC for the suspended systems once the contact time is reduced to below 3 minutes. Overall, the analysis indicates that the use of suspended systems may be appropriate and are worth of further investigation. One aspect that requires consideration is footprint as the area required for the suspended system for 20,000 PE is 400 m^2 compared to 100 m^2 for the fixed bed system which may limit retrofit opportunities.

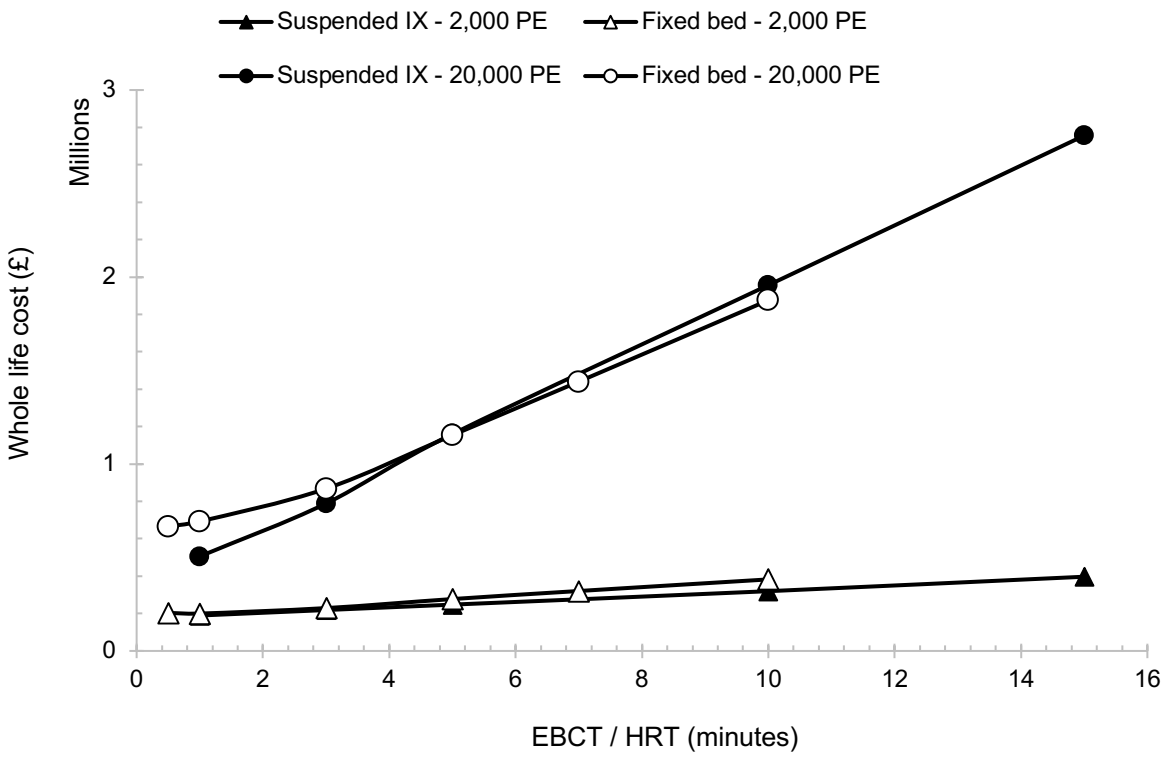

Figure 6.1 Impact of empty bed contact time and hydraulic retention time on whole life cost of fixed-bed and suspended system for 2,000 and 20,000 PE.

6.6 References

Brookes, A. and Barter, P. (2017) 'Chemical Investigations Programme 2 DynSand Oxy for combined Phosphorus and Ammonia removal: experimences from Anglian Water', in *The Big Phosphorous Conference*. Manchester.

Cadee, K., Leary, B. O., Smith, P., Slunjski, M. and Bourke, M. (1998) 'World ' s First Magnetic Ion Exchange (MIEX ®) 1 Water Treatment Plant to be Installed in Western Australia', p. 11.

Cieślik, B. and Konieczka, P. (2016) 'A review of phosphorus recovery methods at various steps of wastewater treatment and sewage sludge management. The concept of "no solid waste generation" and analytical methods', *Journal of Cleaner Production*, 142, pp. 1–13.

Egle, L., Rechberger, H., Krampe, J. and Zessner, M. (2016) 'Phosphorus recovery from municipal wastewater: An integrated comparative technological,

environmental and economic assessment of P recovery technologies', *Science of the Total Environment*, 571, pp. 522–542.

Martin, B. D. (2010) *Removal and Recovery of Phosphorus from Municipal Wastewaters using a Ferric Nanoparticle Adsorbent*. Cranfield University (PhD Thesis).

Murray, B., Pieterse, S., Raymer, D. and Swartz, C. (2005) *An Evaluation of Miex® Resin Technology for Potable Treatment of Highly Coloured Raw Waters Throughout the Cape Region of South Africa*.

O'Shea, M. G., Dahlke, T., Staunton, S. P., Pope, G. M. and Holmquist, A. (2008) 'EVALUATION OF A MAGNETIC ION EXCHANGE (MIEX ®) RESIN FOR DECOLORISATION APPLICATIONS WITHIN A RAW SUGAR FACTORY', *Australian Society of Sugar Cane Technologists*, 30, pp. 536–546.

Sinnott, R. K. (2005) *Coulson & Richardson's Chemical Engineering Design*, *ELSEVIER - Coulson & Richardson's Chemical Engineering series*.

Slunjski, M., Cadee, K. and Tattersall, J. (2000) 'MIEX resin water treatment process', *Proceedings of Aquatech*.

Smith, L., Moreta, E. A., Gardner, P. and O'Brien, L. (2017) 'Phosphorus removal at an ASP and Filter WOrks using MEcana Filter Technology - findings and experience from CIP P trials', in *The Big Phosphorous Conference*.

Stark, K. (2004) 'Phosphorus RecoverExperiences From European Countries', pp. 19–30.

Tchobanoglous, G., Burton, F. L. and Stensel, H. D. (2004) *Metcalf and Eddy: Wastewater engineering, treatment and reuse*. 4th edn. Asia: Mc Graw Hill.

Thornton, C. (2017) 'Policy developments in Europe', in *Big P Conference*. Manchester.

Vale, P. (2017) 'Applying a circular economy model to wastewater treatment', in *WWT Wastewater*. Birmingham.

Chapter 7. Conclusions

The overall conclusion of the research is that a short contact time reactor based on HAIX media is both technically and economically feasible as an alternative to remove phosphorus from wastewater. The process can operate effectively as either a polishing process to reduce phosphorous concentration from 1 to 0.1 mg P L^{-1} or as a treatment of the full load reducing the phosphorus concentration from 6-8 mg P L^{-1} down to either 1 or 0.1 mg L^{-1}. Specific conclusion are as follows:

- Metal oxide loaded sorbents were shown to be highly selective for phosphorus with zirconium (IV) and aluminium loaded sorbents showing the highest capacity. Other constituent in the water such as sulphate, nitrate and organics reduce the overall efficacy of the process through a combination of competition for adsorption sites and retardation of mass transfer of phosphate through the internal structure of the resin. However, the use of embedded nanoparticles coupled with selective regeneration enables the process to retain an appropriate level of effectiveness over prolonged operation.
- Modelling of the system is best accomplished through a combination of the intra-particle diffusion model and the pseudo-second-order model as they reflect the dual component impacts of the nanoparticle and the base resin on the overall uptake of phosphorus onto the nanoparticles.
- The use of the HAIX media is effective even at very low empty bed contact times of 0.5 and 1 minute. The mass transfer profile and the serviceable bed life improves at EBCT of 3 minutes and over, with an optimum operating EBCT suggested of 5 minutes from a technical stand point.
- The resin is effective at organic removal and will provide approximately a 40-50% reduction in COD at the operating EBCTs and thus provide added value for sites that require both nutrient and organic polishing.
- Economic analysis indicates that the technology provides an economically plausible alternative to current solutions to meet low phosphorus discharges. The solution is favourable across appropriate empty bed contact times and can be configured in either fixed bed or suspended media systems.

- The whole life cost of the systems is strongly influenced by the selection of empty bed contact time as it impacts on both the amount of media required and the frequency of regeneration. A key component to the economic suitability of the technology is related to the recovery of the regeneration fluid to enable reuse. This can be accomplished through either permanently installed systems or a mobile system to service multiple sites.
- The economic suitability of the process does not require inclusion of the sale of recovered products and hence is suitable within both a linear and circular economic framework. Accordingly, the recovery of calcium phosphate becomes an added value from using the technology rather than being a critical component in the economic case for use.

7.1 Recommendations for Further Work

Through the work conducted over the course of the doctorate, further areas of the work have been identified below:

- A large fixed bed pilot plant is required to validate the long-term performance of HAIX. The pilot plant should be operated for a full year at different WWTWs to understand if the background constituents such as water hardness have an impact on the performance of the media. This will also help determine how often the media will need to be changed as the current assumption of 600 regeneration cycles is based on standard ion exchange resins utilising brine for regeneration.
- A suspended ion-exchange pilot plant study will help determine if the performance is comparable to fixed-bed systems. The impact of HRT also needs to be assessed as that would determine the size of mixing tanks and hence the impellers. A pilot study would also establish the degree of saturation of the media that is leaving the mixing tanks so an appropriate regeneration strategy can be developed.
- A large scale regen clean-up system is required to understand the operational complexities. An appropriate filtration system to separate the precipitated calcium phosphate from sodium hydroxide needs to be

identified. This could influence the clean-up strategy and hence the operational costs.

- In fixed bed columns, phosphorus exhaustion was achieved but HAIX was still showing organic removal up to 50%. The HAIX mechanism which is primarily responsible for organic removal must be determined. It is likely to be the ion exchange mechanism as anion resins have been used for organic removal.
- The impact of regeneration and long-term use of HAIX on its ability to remove organics must be further investigated. If HAIX can provide consistent organic removal over multiple cycles, it expands the application opportunities of the technology.
- Conventional sorption media is not very effective at removing hazardous priority substances as they get out competed by humic and fulvic acids. HAIX with its dual mechanism could be more efficient and hence needs to be tested in single and multi-component systems for hazardous substances including pharmaceuticals, pesticides, hormones, among others.